

DÉCLARATION DE CANDIDATURE AU RECRUTEMENT SUR UN EMPLOI DE MAITRE DE CONFERENCES
(Campagne 2023)
(décret n° 84-431 du 6 juin 1984 modifié)

adressée au chef d'établissement de : UNIVERSITE TOULOUSE 3

Poste(s) : n°4815

Publié le : 23 février 2023 à 00:02

Section(s) C.N.U : 60 (Mécanique, génie mécanique, génie civil)

Profil : Le poste est axé autour de l'efficacité énergétique des bâtiments c'est-à-dire de la réduction des consommations d'énergie tout en se préoccupant du confort des occupants dans un espace habitable.

Localisation : Toulouse

Article 26-I-1

Je soussigné(e) M.

Nom de famille : M'SAOURI ELBAT

Nom d'usage : M'SAOURI EL BAT

Prénom : ADNANE

Date et lieu de naissance : 01/10/1993 - TANGIER

Nationalité : Hors Europ

N° de qualification : 22260374765

Fonctions et établissement actuel : Chercheur post-doctorant-

Date de création :

29/03/2023 à 14:03

Date de dernière modification :

07/04/2023 à 07:04

Titres universitaires français :

Doctorat ou diplôme équivalent au doctorat obtenu dans un établissement autre qu'un établissement public français pour lequel vous demandez une dispense de doctorat

Diplôme le plus récent : Doctorat

Titre : Développement d'un modèle pour l'étude de l'impact du microclimat urbain sur les performances énergétiques des bâtiments : cas des rues canyons et des cours intérieures

Date de soutenance : 17/12/2020

Lieu de la soutenance : UNIVERSITE ABDELMALEK ESSAADI, MAROC

Mention : Très honorable

Directeur : ABDESLAM DRAOUI

Composition du jury : ADIL HAFIDI ALAOUI

HASSAN EZBAKHE

KHALID EL HARROUNI

FREDERIC KUZNICK

EMMANUEL BOZONNET

ABDELMAJID EL BOUARDI

Liste des établissements et des unités de recherche d'exercice :

- Centre d'études et d'expertise sur les risques, l'environnement, la mobilité et l'aménagement, Nantes, France
- Faculté des Sciences et Techniques de Tanger, Maroc

Activités et responsabilités en matière d'enseignement :

Encadrement des PFE du cycle :

- Licence « Energies Renouvelables »
- Master « Génie Energétique »

Encadrement des TP de :

- Chauffe-Eau Solaire, Licence, filière «Energies Renouvelables».
- Thermique des Bâtiments, Cycle master en Sciences et Techniques, filières Génie Energétique et Génie Civil.
- Thermodynamique, 1ère année MIPC, MIP, BCG et DUT.
- Optique géométrique, 1ère année BCG

Thèmes et mots-clés de votre domaine de recherche :

- Energétique des bâtiments;
- Climat urbain;
- Microclimat urbain;
- Etude de l'interaction des microclimats urbains avec le bâti, et performance énergétique du bâtiment;
- Modélisation;
- Systèmes énergétiques des bâtiments.
- Transfert thermique
- Génie civil

Activités en matière d'administration et autres responsabilités :

- Ingénieur d'étude stagiaire au sein de l'équipe du projet Initiative Allemande pour les Technologies favorables au Climat, DKTI IV, GIZ Maroc.
- Chercheur scientifique et chef du projet maison Sunimplant - Compétition internationale des bâtiments à énergie positive "Solar Decathlon Africa 2019" (<https://www.solardecathlonafrica.com/fr/team-sunimplant/>).

Autres titres et diplômes :

- Master en Sciences et Techniques, Option : Génie Civil
- Licence en Sciences et Techniques Option : Génie Civil

Travaux, ouvrages, articles, réalisations :

Optimizing urban courtyard microclimate through a zonal approach for building energy performance. Energy, p. 126176. doi:10.1016/J.ENERGY.2022.126176.

Thermal impact of street canyon microclimate on building energy needs using TRNSYS : A case study of the city of Tangier in Morocco. Case Studies in Thermal Engineering, 24, 100834. doi:10.1016/j.csite.2020.100834.

Integration of a practical model to assess the local urban interactions in building energy simulation with a street canyon.
Journal of Building Performance Simulation, 13(6), 720-739. doi:10.1080/19401493.2020.1818829

Liste des pièces à fournir par le candidat :

Pièces obligatoires mentionnées selon le cas dans l'arrêté du 6 février 2023, fixant les dispositions permanentes applicables à l'ensemble des recrutements de professeurs des universités et de maîtres de conférences ou bien dans l'arrêté du 20 février 2012 relatif aux modalités de recrutement des professeurs du Muséum national d'Histoire Naturelle et des maitres de conférences du Muséum National d'Histoire Naturelle. Ces arrêtés sont accessibles depuis le portail GALAXIE (rubrique 'A consulter' dans la colonne droite).

Pièces administratives :

Pièce d'identité : S_2023_374765_1_ID.pdf

Présentation analytique : S_2023_374765_1_PA.pdf

Diplôme : S_2023_374765_1_DI.pdf

Rapport de soutenance : S_2023_374765_1_RS.pdf

Titres et travaux :

Document 1 : S_2023_374765_1_T1.pdf

Document 2 : S_2023_374765_1_T2.pdf

Document 3 : S_2023_374765_1_T3.pdf

Document 4 : Aucune pièce déposée

Document 5 : Aucune pièce déposée

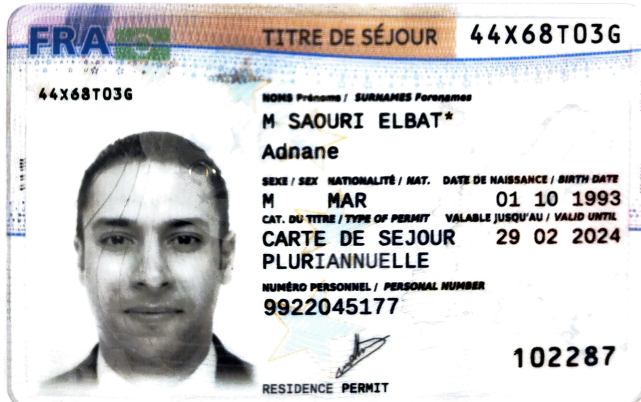
Document 6 : Aucune pièce déposée

Rapports déposés par les jurés :

Rapport 1 : Aucun rapport déposé

Rapport 2 : Rap2-M'SAOURI-Ghiaus.pdf

déclare faire acte de candidature sur l'emploi ci-dessus désigné



Dossier de candidature à la fonction de maître de conférences :
Poste 4815 à l’Université TOULOUSE 3
Section 60 62

Adnane M’SAOURI EL BAT
Mars 2023

Adnane M'SAOURI EL BAT
9 Boulevard Vincent Gâche
44200 Nantes, France
Email : a.msaourielbat@gmail.com
Portable : (+33) 6 18 72 05 65

Le 29 Mars 2023

Objet : Dossier de candidature à la fonction de maître de conférences

Monsieur, Madame,

Vous trouverez dans ce dossier les documents décrits ci-après :

- A.** Le curriculum Vitae.
- B.** La liste des publications.
- C.** Le bilan et projet d'activités de recherche.
- D.** Le bilan et projet d'activités d'enseignement.

Les trois articles à remettre en cas d'audition :

- M'Saouri El Bat, A., Romani, Z., Bozonnet, E., Draoui, A. & Allard, F. (2023). Optimizing urban courtyard microclimate through a zonal approach for building energy performance. *Energy*, p. 126176. <https://doi.org/10.1016/J.ENERGY.2022.126176>.
- M'Saouri El Bat, A., Romani, Z., Bozonnet, E., & Draoui, A. (2021). Thermal impact of street canyon microclimate on building energy needs using TRNSYS : A case study of the city of Tangier in Morocco. *Case Studies in Thermal Engineering*, 24, 100834. <https://doi.org/https://doi.org/10.1016/j.csite.2020.100834>.
- M'Saouri El Bat, A., Romani, Z., Bozonnet, E., & Draoui, A. (2020). Integration of a practical model to assess the local urban interactions in building energy simulation with a street canyon. *Journal of Building Performance Simulation*, 13(6), 720-739. <https://doi.org/10.1080/19401493.2020.1818829>.

Je vous prie de bien vouloir accepter l'expression de mes sentiments les meilleurs.

Adnane M'SAOURI EL BAT

A : CURRICULUM VITAE

Docteur en Energétique du Bâtiment

Adnane M'SAOURI EL BAT

Né le 01 Octobre 1993 à Tanger, Maroc

Téléphone : (+33) 6 18 72 05 65

Email : a.msaourielbat@gmail.com

RG : https://www.researchgate.net/profile/Adnane_Msaouri_El_Bat

Qualifications CNU : Section 60 N° 22260374765 et section 62 N° 22262374765 (campagne 2022).

Diplômes et titres universitaires

2017-2020 : **Doctorat en Energétique du Bâtiment**, Faculté des Sciences et Techniques de Tanger, Université Abdelmalek Essaâdi, Maroc.

Titre de la thèse : « *Développement d'un modèle pour l'étude de l'impact du microclimat urbain sur les performances énergétiques des bâtiments : cas des rues canyons et des cours intérieures* ». (Sous la direction de Pr. Abdeslam Draoui)

2014-2016 : **Master en Sciences et Techniques, Option : Génie Civil**, à la Faculté des Sciences et Techniques de Tanger Université Abdelmalek Essaâdi, Maroc.

2013-2014 : **Licence en Sciences et Techniques Option : Génie Civil** à la Faculté des Sciences et Techniques de Tanger, Université Abdelmalek Essaâdi, Maroc.

2011-2013 : **DEUST option MIPC** à la Faculté des Sciences et Techniques de Tanger, Université Abdelmalek Essaâdi, Maroc.

2010-2011 : **Baccalauréat Scientifique, option Sciences Physiques**, Lycée Moulay Rachid Tanger, Maroc.

Activités de recherche scientifique

Depuis Septembre 2022 **Chercheur postdoctoral** de projet « *ConforT thErmique – quAliTé de l'aIr & Vaque de chaleur (CREATIV)* » au sein de l'équipe Bâtiments Performants dans leur Environnement (BPE), Cerema Ouest, Nantes, France (Sous l'encadrement de : Sihem Guernouti, Marjorie Musy et Auline Rodler)

Août 2021 Juillet 2022 **Chercheur postdoctoral** de projet « *Evaluation des interactions climat urbain, systèmes des bâtiments* » au sein de l'équipe Bâtiments Performants dans leur Environnement (BPE), Cerema Ouest, Nantes, France (Sous l'encadrement de : Marjorie Musy, Sihem Guernouti et Auline Rodler)

Février 2018 Septembre 2019 **Chercheur scientifique et chef du projet** maison Sunimplant - Compétition internationale des bâtiments à énergie positive (<https://www.solardecathlonafrica.com/fr/team-sunimplant/>).

Sujet : Conception, modélisation et construction d'un bâtiment à énergie positive pour la compétition internationale **Solar Decathlon Africa 2019**.

✓ Les tâches réalisées :

- Conception de la maison « Sunimplant » ;
- Analyse énergétique et modélisation numérique des performances thermiques de « Sunimplant » ;
- Gestion de l'équipe Sunimplant ;
- Construction de la maison « Sunimplant ».

Octobre 2018 - Avril 2019 **Ingénieur d'étude stagiaire** au sein de l'équipe du projet Initiative Allemande pour les Technologies favorables au Climat – DTKI IV, GIZ Maroc.

✓ **Les tâches réalisées :**

- Contribution à l'évaluation économique et environnementale du potentiel énergétique dans la région du Nord du Maroc.
- Préparation des notes, des synthèses, des recherches bibliographiques ou autres documents.
- Appuyer le projet dans la consolidation des données et informations collectées en matière d'efficacité énergétique dans la région de Tanger, Tétouan Al Hoceima.
- Organisation des rencontres et activités du projet dans la région de Tanger, Tétouan Al Hoceima : réunions préparatoires, suivi des préparatifs (invitations, réservations, accueil, animation...).

Expériences professionnelles

Mars - septembre 2016 Stage de fin d'études du Master Sciences et Techniques Génie Civil, au sein du Cabinet d'Ingénierie et d'Expertise Rhoni, et de l'Equipe de recherche en Transferts Thermiques et Energétique (UAE/E14FST) sous le thème « Conception et Dimensionnement des Tunnels - Application au tunnel de Zaouait Ait Mellal ».

✓ **Les tâches réalisées :**

- Etude structurale du tunnel :
 - Choix de type de creusement.
 - Choix et conception du soutènement provisoire.
 - Conception et dimensionnement du revêtement définitif à l'aide du logiciel Plaxis.
- Etude de la sécurité incendie du tunnel :
 - Choix du système de ventilation.
 - Déterminations des besoins en air frais dans le tunnel.
 - Conception et dimensionnement de la ventilation à l'aide de FDS

Septembre - octobre 2015 Stage au sein du bureau d'études C.A.E.B (Conseil, Assistance, Etude en Bâtiment) sous le thème « Etude dynamique d'une structure en béton armé R+1 ».

Avril - Juin 2014 Stage de fin d'études du cycle Licence Sciences et Techniques « Génie Civil » au sein du Bureau d'Etudes C.A.E.B (Conseil, Assistance, Etudes en Bâtiment) intitulé « Etude d'une structure en béton armé (R+4) ».

✓ **Les tâches réalisées :**

- Établissement du plan de coffrage.
- Pré-dimensionnement et dimensionnement de tous les éléments du bâtiment.
- Étude parasismique selon le règlement **RPS 2000**.
- Calcul manuel des sollicitations sismiques en utilisant la méthode japonaise "**Muto**".

Expériences pédagogiques

- **Activités d'enseignement**

Encadrement des travaux pratiques de :

Année	Matières enseignées	Niveau	Etablissement	Statut	Type	Volume horaire
2020/2021	Thermique des Bâtiments	Master (M2)	Faculté des Sciences et Techniques de Tanger, Maroc.	Vacataire	TP	8
2019/2020	Thermique des Bâtiments	Master (M2)	Faculté des Sciences et Techniques de Tanger, Maroc.	Vacataire	TP	8
2019/2020	Chauffe-Eau Solaire	Licence (L3)	Faculté des Sciences et Techniques de Tanger, Maroc.	Vacataire	TP	8
2017/2018	Chauffe-Eau Solaire	Licence (L3)	Faculté des Sciences et Techniques de Tanger, Maroc.	Vacataire	TP	12
2017/2018	Thermodynamique	Licence (L1)	Faculté des Sciences et Techniques de Tanger, Maroc.	Vacataire	TP	20
2017/2018	Optique	Licence (L1)	Faculté des Sciences et Techniques de Tanger, Maroc.	Vacataire	TP	16
2017/2018	Thermodynamique	D.U.T (1 ^{ère} année)	Faculté des Sciences et Techniques de Tanger, Maroc.	Vacataire	TP	12
2016/2017	Thermodynamique	Licence (L1)	Faculté des Sciences et Techniques de Tanger, Maroc.	Vacataire	TP	34
2016/2017	Thermique des Bâtiments	Master (M2)	Faculté des Sciences et Techniques de Tanger, Maroc.	Vacataire	TP	16

- **Activités d'encadrement scientifique**

Participation à l'encadrement des sujets présentés dans le tableau suivant.

Date de début	Niveau	Nom de l'étudiant	Thème de recherche	Taux d'encadrement
A partir de Mai 2023	Stagiaire (Doctorat)	Manal ACH-CHKHAR	Développement d'un modèle de prédiction des écoulements de l'air en milieu urbain basé sur des méthodes d'ordre réduit (ROM) pour mieux estimer les échanges convectifs et les débits d'air dans les bâtiments <i>(Ce stage s'inscrit dans le cadre du projet CREATIV)</i>	25%

Date de début	Niveau	Nom de l'étudiant	Thème de recherche	Taux d'encadrement
Depuis Mars 2023	Master	Youssef AMHAOUD	Influence de la fraîcheur générée par un parc sur le comportement thermique du bâtiment dans son environnement urbain <i>(Ce stage s'inscrit dans le cadre du projet CoolParks)</i>	50%
Mars-Septembre 2022	Master	Fatima NAJOUI	Modélisation thermoacoustique des bâtiments en prenant en compte les effets du contexte urbain en période de vague de chaleur <i>(Ce stage s'inscrit dans le cadre du projet CREATIV)</i>	50%
Mars-Septembre 2022	Master	Safae OULMOUDEN	Influence de la fraîcheur générée par un parc sur le comportement thermique du bâtiment dans son environnement urbain <i>(Ce stage s'inscrit dans le cadre du projet CoolParks)</i>	50%
Février-Septembre 2021	Master	Manal ACH-CHKHAR	Modélisation d'un système de stockage de chaleur thermochimique pour le bâtiment <i>(Ce PFE en collaboration entre CETHIL (France) et ETTE de la FST de Tanger (Maroc))</i>	50%
Février-Juillet 2020	Master	Omar CHARIF	Modélisation et simulation du microclimat urbain : contribution à l'amélioration du confort extérieur d'un quartier à la ville de Tanger	50%
Avril-juillet 2020	Licence	Nada ALOUI et Nada ZQUIEK	Amélioration des performances énergétiques d'un bâtiment à l'aide de la simulation thermique dynamique de l'isolation thermique et du Plancher Solaire Direct (PSD)	50%
Avril-Juillet 2019	Licence	Mohammed ELGARTI	Propositions pour la réduction de la consommation d'énergie électrique au sein d'Eurostyle Systems de Tanger	50%

- **Participation à des jurys de diplôme**

- Participation en tant qu'**examinateur** à 3 jurys de soutenance de projet de fin d'étude du cycle Master en Sciences et Techniques « **Génie Energétique** », Faculté des Sciences et Techniques de Tanger, Maroc.
- Participation en tant qu'**examinateur** à 6 jurys de soutenance de projet de fin d'études du cycle Licence en Sciences et Techniques « Energies Renouvelables », à Faculté des Sciences et Techniques de Tanger, Maroc.

- **Activités d'évaluation scientifique**

- Membre du comité éditorial de « Journal of Civil, Construction and Environmental Engineering ».
- Relecture d'un article de « Journal of Building Performance Simulation ».
- Relecture d'un article de « Academia Letters »

- **Participation à des projets scientifiques**

Projet 1	<p>Projet « ConforT thErmique – quAliTé de l'aIr & Vaque de chaleur (CREATIV) »</p> <p>L'objectif du projet CREATIV est d'analyser, dans le contexte du changement climatique, les relations entre le confort thermique et la qualité de l'air intérieur plus particulièrement en période de vague de chaleur. Ce projet entend ainsi répondre à deux enjeux environnementaux majeurs, l'atténuation climatique et l'adaptation au changement climatique. Ce projet de recherche adopte une approche basée sur la modélisation et l'expérimentation in-situ. Ces deux aspects sont traités à la fois d'un point de vue physique mais aussi humain au moyen d'enquêtes auprès des occupants et d'une modélisation innovante de leur comportement.</p> <p>Ce projet mené dans le cadre de l'appel à projets bâtiments 2020 de l'Ademe. Il a démarré début 2021 pour une durée de 3 ans. Il est mené conjointement par le Cerema, l'université de Nantes, l'université d'Angers et le bureau d'étude Tribu.</p>
Projet 2	<p>Projet « Evaluation des interactions climat urbain, systèmes des bâtiments » au sein de l'équipe Bâtiments Performants dans leur Environnement (BPE), Cerema Ouest, Nantes, France.</p> <p>Ce projet s'inscrit dans le cadre d'une convention du Cerema avec Grdf et plus précisément dans l'action intitulée « Interactions entre rafraîchissement des espaces intérieurs et microclimat urbain ».</p> <p>Notez que ce projet a défini des actions précises et diverses à mener durant la période 2020-2022.</p>

Activités d'administration et d'animation de la recherche

- Participation à l'organisation de séminaire de l'équipe de recherche Équipe Bâtiments Performants dans leur Environnement (BPE) du Cerema.
- Participation à l'organisation de 2 séminaires de l'équipe de recherche en Transferts Thermiques et Energétique de la Faculté des Sciences et Techniques de Tanger, Maroc.
- Participation à l'organisation et animation des 1 et 2 sessions de formation « Règlement Thermique de Construction au Maroc » pour des architectes de Tanger et de Tétouan, Maroc.
- Participation à l'organisation et animation des 1 et 2 sessions de formation « Eco-conduite » pour l'unité scolaire de la Fondation Banque Populaire de Tanger, Maroc.
- Participation à l'organisation et animation du séminaire ouvert sur les outils de la recherche scientifique pour les doctorants du Centre des Etudes Doctorales « Sciences et Techniques de l'Ingénieur » de l'Université Abdelmalek Essaâdi, Maroc.

- Participation à l'organisation de la journée « porte ouverte » pour les doctorants du Centre des Etudes Doctorales « Sciences et Techniques de l'Ingénieur » de l'Université Abdelmalek Essaâdi, Maroc.
-

Rayonnement scientifique

- Membre fondateur et responsable de comité de formation du club des étudiants chercheurs du Centre des Etudes Doctorales « Sciences et Techniques de l'Ingénieur » de l'Université Abdelmalek Essaâdi, Maroc (2018-2019).
 - Membre fondateur et responsable de comité de suivi du club génie civil de la faculté de Faculté des Sciences et Techniques de Tanger – Maroc (2014-2016).
-

Domaines d'intérêts dans la recherche scientifique

- Microclimat urbain - Efficacité énergétique des bâtiments - Transfert thermique - Mécanique des fluides - Génie civil.
-

Outils

Logiciels techniques : Solene-Microclimat, TRNSYS, CODYBA, Envi-met, Sketchup, Salome, LabVIEW, FDS, Pyrosim, Plaxis AutoCAD, Robot, COVADIS, ABAQUS, TunRen.

Bureautique : Microsoft Office, Matlab, C++, Python, Minitab, Eviews.

Linguistiques :

Arabe : langue maternelle.

Français : niveau avancé.

Anglais: niveau pré-intermédiaire.

Divers

Voyages, Sports, Jeu des échecs, documentaires.

B : PUBLICATIONS SCIENTIFIQUES

Articles dans des revues à comité de lecture

Publiés :

- 1) **M'Saouri El Bat, A.**, Romani, Z., Bozonnet, E., Draoui, A. & Allard, F. (2023). Optimizing urban courtyard microclimate through a zonal approach for building energy performance. *Energy*, p. 126176. <https://doi.org/10.1016/J.ENERGY.2022.126176>.
- 2) **M'Saouri El Bat, A.**, Romani, Z., Bozonnet, E., & Draoui, A. (2021). Thermal impact of street canyon microclimate on building energy needs using TRNSYS : A case study of the city of Tangier in Morocco. *Case Studies in Thermal Engineering*, 24, 100834. <https://doi.org/https://doi.org/10.1016/j.csite.2020.100834>.
- 3) **M'Saouri El Bat, A.**, Romani, Z., Bozonnet, E., & Draoui, A. (2020). Integration of a practical model to assess the local urban interactions in building energy simulation with a street canyon. *Journal of Building Performance Simulation*, 13(6), 720-739. <https://doi.org/10.1080/19401493.2020.1818829>.

En phase finale de rédaction :

- **M'Saouri El Bat, A.**, Guernouti, S., Rodler, A., & Musy, M. "Interactions between indoor space cooling and urban microclimate – A review".
- **M'Saouri El Bat, A.**, Romani, Z., Guernouti, S., Rodler, A., Bozonnet, E., Musy, M. & Draoui, A.: "Assessment of the energy needs of a canyon type district with courtyards located in the city of Tangier".
- Idrissi Kaitouni, S., Wakil, M., Romani, Z., Brummer, M., **M'Saouri El Bat, A.**, Benhmidou, H., Ettoumi, Y., El Meghazli, O. & Brigui, J.: "Thermal behavior and BIPV production of a Net Zero Hemp-Concrete-based detached house under semi-arid climate: A real case study".

Communications Scientifiques dans des manifestations scientifiques à Comité de lecture

Communication avec actes dans un congrès international répertorié dans les BDI JCR, Scopus, ERIH, HCRES, DBLP

Publiées :

- 1) **M'Saouri El Bat, A.**, Romani, Z., Bozonnet, E., & Draoui, A. (2019). Impact of Urban Microclimate on the Energy Performance of Riad-Type Buildings. *Proc. Build. Simul.*, 3771–3778. [doi:10.26868/25222708.2019.211272](https://doi.org/10.26868/25222708.2019.211272).
- 2) **M'Saouri El Bat, A.**, Romani, Z., Bozonnet, E., & Draoui, A. (2021). Impact of Canyon and Courtyard Microclimate Interactions on Building Energy Performance. *2021 9th International Renewable and Sustainable Energy Conference (IRSEC)*, 1–6. <https://doi.org/10.1109/IRSEC53969.2021.9741102>.

-
- 3) Charif, O., M'Saouri El Bat, A., Romani, Z., & Draoui, A. (2021). Impact of Aspect Ratio and Green Surfaces on the outdoor Thermal Comfort of the Street Canyon under Mediterranean Climate. *2021 9th International Renewable and Sustainable Energy Conference (IRSEC)*, 1–6. <https://doi.org/10.1109/IRSEC53969.2021.9741167>

Acceptées pour la publication:

- 4) Ach-Chakhar, M., Guernouti, S., M'Saouri El Bat, A., Romani, Z., El Mankibi, M. & Draoui, A.: « **Assessment of the impact of urban density on building energy needs by considering the outdoor thermal microclimate** ». *11th international conference on indoor air quality, ventilation & energy conservation in buildings (IAQVEC 2023)*, Tokyo (Japon), 20-23 mai, 2023. (Accéptée)
- 5) M'Saouri El Bat, A., Romani, Z., Bozonnet, E., Draoui, A., Rodler, A., Guernouti, S. & Musy, M.: « **Sensitivity analysis of the energy needs of a building located in an urban canyon under Mediterranean climate** ». *Journée Internationales de Thermique 19^{ème} édition (JITH 2022)*, Tanger (Maroc), 15-17 Novembre, 2022. (Accéptée pour la publication dans lecture notes in mechanical engineering)
- 6) Ach-Chakhar, M., Guernouti, S., Romani, Z., M'Saouri El Bat, A., & Draoui, A.: « **Modeling shading and inter-building longwave radiative exchanges: Comparative study using BESTEST case** ». *Journée Internationales de Thermique 19^{ème} édition (JITH 2022)*, Tanger (Maroc), 15-17 Novembre, 2022. (Accéptée pour la publication dans lecture notes in mechanical engineering)
- 7) Charif, O., M'Saouri El Bat, A., Romani, Z., & Draoui, A.: « **Assessment of the Impact of a Green Wall on the Thermal Behavior of a Building in a Mediterranean Climate** ». *Journée Internationales de Thermique 19^{ème} édition (JITH 2022)*, Tanger (Maroc), 15-17 Novembre, 2022. (Accéptée pour la publication dans lecture notes in mechanical engineering)
- 8) Ach-Chakhar , M., M'Saouri El Bat, A., Michel, B.; Kuznik, F. & Draoui, A., « **Modélisation d'un système de stockage de chaleur thermochimique pour le bâtiment** ». *7th International Congress on Thermal Sciences (AMT'2022)*, Ouarzazate (Maroc), 22-24 Mars, 2022. (Acceptée pour la publication dans AIP Conference Proceedings)

Communication soumise :

- 9) Charif, O., M'Saouri El Bat, A., Romani, Z., & Draoui, A. (2021). Numerical and experimental Thermal study of a small-scale urban block with courtyard. ». *The 18th IBPSA International Conference and Exhibition (Building Simulation 2023)*, Shanghai (Chine), 4-6 September, 2023. (Résumé accepté, communication complète en cours de révision)

Communication avec actes dans un congrès international non répertorié dans les BDI JCR, Scopus, ERIH, HCRES, DBLP

- 10) M'Saouri El Bat, A., Rodler, A., Guernouti, S. & Musy, M. : « **Evaluation de l'impact du microclimat urbain sur les systèmes de refroidissement des bâtiments** ». *XVème Colloque International Franco-Québécois Ville et transition (CIFQ2022)*, Paris (France), 15-17 Juin, 2022.
- 11) M'Saouri El Bat, A., Romani, Z., Bozonnet, E. & Draoui, A. : « **Modélisation de microclimat urbain par un modèle zonal intégré dans un modèle de simulation énergétique des bâtiments** ». *Conférence Francophone de l'International Building Performance Simulation Association (conférence IBPSA France 2020)*, Reims (France), 12-13 Novembre, 2020.
-

-
- 12) M'Saouri El Bat, A., Romani, Z., Bozonnet, E. & Draoui, A. : « Etude de l'impact du microclimat urbain proche du bâti par une modélisation intégrée dans le logiciel TRNSYS ». *Conférence Francophone de l'International Building Performance Simulation Association (conférence IBPSA France 2018)*, Bordeaux (France), 15-16 mai, 2018.
- 13) M'Saouri El Bat, A., Romani, Z., Bozonnet, E. & Draoui, A. : « Développement d'un modèle simplifié pour l'évaluation de l'impact de phénomène de piégeage radiatif sur la demande énergétique des bâtiments ». *International Congress on Thermal Sciences (AMT'2018)*, Safi (Morocco), 18-19 Avril, 2018.

Communication avec actes dans un congrès national

- 14) M'Saouri El Bat, A., Guernouti, S., Rodler, A. & Musy, M. : « Évaluation des interactions bâtiment-microclimat à l'échelle du quartier par une approche intégrée à la simulation énergétique des bâtiments ». *31ème congrés français de thermique (SFT2023)*, Reims (France), 30 mai -2 juin, 2023.

Communication orale sans actes dans un congrès international ou national

- 15) M'Saouri El Bat, A., Romani, Z., Bozonnet, E. & Draoui, A. : « Développement d'une méthode pour la modélisation de l'impact du microclimat urbain d'une rue canyon ». *Journée Scientifique sur l'Efficacité Energétique des Bâtiments (JSEEB-2018)*, Casablanca (Maroc), 20 octobre, 2018.
-

Ouvrage scientifique ou chapitre

- 1) M'Saouri El Bat, A., Romani, Z., Bozonnet, E., & Draoui, A. (2021). Thermal impact of street canyon microclimate on the energy performance of courtyard under Mediterranean climate. *REHVA Journal*, 58 (1), 10-16.
-

Rapport de recherche

- 1) Livrable 1 : « Interactions entre rafraîchissement des espaces intérieurs et microclimat urbain », Projet : Convention Cerema-Grdf. (Rédacteur)
- 2) Livrable 2 : « Interactions entre rafraîchissement des espaces intérieurs et microclimat urbain », Projet : Convention Cerema-Grdf. (Rédacteur)

C : BILAN DE L'ACTIVITÉ DE RECHERCHE ET PROJET SCIENTIFIQUE EN RELATION AVEC LE POSTE PROPOSÉ

1) Déroulé et bilan de l'activité scientifique passée

▪ Travaux de thèse

Dans cette partie, les différents travaux de recherche effectués pendant ma thèse sont décrits. La thèse a été réalisée de 2017 à 2020 au sein de l'Equipe de recherche en Transferts Thermiques et Energétique à la Faculté des sciences et techniques de Tanger sous la direction de Professeur Abdeslam Draoui.

Le sujet de ma thèse n'a pas été choisi de manière arbitraire. J'ai toujours eu en tête la question de savoir comment concevoir des bâtiments énergétiquement efficaces dans des conditions très limitées, telles que le choix de l'emplacement du bâtiment, de sa surface et de son orientation.

Cette question fut ainsi l'objet de mon sujet de thèse qui porte sur le développement d'un modèle pour l'étude de l'impact du microclimat urbain sur les performances énergétiques des bâtiments : cas des rues canyons et des cours intérieures.

Partant de la problématique que les éléments bâties du tissu urbain, dans un environnement complexe tel qu'une zone urbaine, modifient fortement les conditions microclimatiques en perturbant la distribution des flux de vent et de chaleur entre les différentes surfaces. En effet, l'étude de l'impact du microclimat urbain sur les besoins énergétiques est devenue une nécessité pour une meilleure évaluation des performances énergétiques des bâtiments.

Face à la nécessité croissante de modéliser les interactions entre l'environnement bâti et le microclimat urbain et ses conséquences sur les performances énergétiques des bâtiments, les recherches menées dans le domaine de la simulation énergétique des bâtiments sont désormais davantage axées sur l'échelle du quartier ou de la ville que sur celle du bâtiment. Par conséquent, il est indispensable, pour modéliser un bâtiment dans un contexte urbain et pour prédire sa consommation énergétique, de simuler ces interactions avec d'autres bâtiments et avec le microclimat urbain, notamment dans le cas des rues canyon. En revanche, la complexité qui caractérise les environnements urbains rend la simulation énergétique des bâtiments à l'échelle urbaine très difficile.

Pour simplifier la modélisation de l'interaction entre le bâtiment et le microclimat, nous avons proposé dans le cadre de ma thèse une modélisation intégrée dans un outil de simulation thermique dynamique du bâtiment afin d'évaluer l'impact du microclimat urbain sur les besoins énergétiques des bâtiments.

L'importance de cette modélisation se reflète dans sa capacité à prendre en considération à la fois les effets des vents dominants, le piégeage radiatif, l'échange hygrothermique et le transfert de chaleur dans le sol selon trois directions sans passer par des calculs de type CFD coûteux en temps de calcul, tout en gardant une précision satisfaisante pour l'évaluation thermique et énergétique des bâtiments.

Dans un premier temps, nous avons réalisé un état de l'art sur le microclimat urbain et ses interactions énergétiques avec les bâtiments, en mettant l'accent sur les principales causes et sur le processus de formation des îlots de chaleur urbains, ainsi que l'effet du microclimat urbain sur le comportement énergétique du bâtiment. Cette étude bibliographique a montré que le problème majeur des modèles existants réside dans le temps de calcul et l'interopérabilité. Cette étude a été le socle pour le développement de nos modèles microclimatiques.

Nous avons ainsi intégré dans un outil de simulation énergétique des bâtiments (TRNSYS 18) un modèle pour évaluer les interactions entre le microclimat urbain et le bâtiment. Au préalable, nous avons développé un modèle thermoradiatif, permettant la modélisation du rayonnement solaire, du rayonnement thermique dans la rue canyon et du transfert de chaleur et d'humidité de l'enveloppe. De même, nous avons développé un modèle thermo-aéraulique selon deux approches différentes, nodale et zonale, qui permettent de prendre en considération le couplage des phénomènes hygrothermiques, aérauliques et radiatifs à l'échelle microclimatique dans le cas d'un quartier type canyon. La première approche nous a d'ailleurs permis de modéliser les écoulements d'air longitudinaux, transversaux et aux intersections des rues. A l'aide de la deuxième approche zonale, nous avons développé un modèle pour deux configurations, à savoir d'une rue canyon longue et d'un quartier.

La validation du modèle développé a été réalisée par une étude comparative avec des études expérimentales qui existent dans la littérature. Nous avons ainsi comparé les résultats de l'approche nodale avec ceux du modèle expérimental ClimaBat et les résultats de l'approche zonale avec ceux du dispositif expérimental EM2PAU. Le modèle nodal a ensuite été utilisé pour effectuer une étude paramétrique dans le cas de cette typologie de rue et pour quantifier l'impact sur les besoins énergétiques de chauffage et de refroidissement des bâtiments étudiés.

A l'instar du modèle précédent, un modèle zonal a été aussi développé et il porte sur la modélisation des cours intérieures dans le cas des bâtiments types « Riad ». Ce modèle a été comparé avec des simulations CFD par le logiciel ENVI-met. Les résultats obtenus sont très satisfaisants. Ensuite une étude a été réalisée sur l'impact de la forme des cours intérieures et des paramètres microclimatiques sur les besoins énergétiques de ces bâtiments.

Finalement, un quartier type Canyon avec des bâtiments comprenant des cours intérieures situé dans la ville de Tanger (Maroc) nous a servi de cas d'étude et a permis l'application de l'ensemble des modèles développés. Nous avons procédé à la modélisation de ce quartier avec des scénarios d'améliorations, en ajoutant une isolation extérieure et/ou un double vitrage, ainsi que l'augmentation de l'albédo des murs extérieurs. Les principaux résultats de ma thèse montrent clairement la nécessité de la prise en compte du microclimat urbain pour une meilleure estimation des performances énergétiques des bâtiments. Les modèles développés et intégrés dans le logiciel TRNSYS 18 présentent donc un compromis intéressant par rapport aux logiciels existants. Il a été aussi démontré qu'il y a une forte interaction entre la conception énergétique urbaine et l'enveloppe des bâtiments. Le choix des paramètres microclimatiques peut être déterminant sur le comportement hygro-thermo-aéraulique des bâtiments. Ces modèles développés restent à la portée des ingénieurs concepteurs et des chercheurs pour les implémenter facilement dans les outils de simulations thermiques dynamiques des bâtiments.

- **Travaux après la thèse : post-doctorat**

Mes travaux de recherche en qualité de post-doctorant s'inscrivent dans la parfaite continuité de ma thèse.

En effet, mon premier post-doc d'une durée d'un an a porté sur l'« Evaluation des interactions entre rafraîchissement des espaces intérieurs et microclimat urbain ». La dissipation de la chaleur des bâtiments climatisés contribue de manière significative à la dissipation de la chaleur anthropique et, par conséquent, à l'amplification du réchauffement urbain dans des conditions estivales.

Dans ce contexte, il est nécessaire d'évaluer non seulement l'impact du microclimat sur la performance énergétique des bâtiments et de leurs systèmes de refroidissement, mais aussi l'impact des rejets de ces systèmes sur le microclimat. En effet, le fait de négliger à la fois l'effet de l'îlot de chaleur urbain et la rétroaction des systèmes de climatisation sur le climat local

conduit à une estimation incorrecte des besoins énergétiques des bâtiments. Cela se traduit par des erreurs de dimensionnement des systèmes de climatisation utilisés dans les bâtiments.

Dans cette optique, l'objectif de mon post-doctorat est d'évaluer l'impact du microclimat urbain sur l'efficacité des systèmes de refroidissement et inversement, pour différentes configurations urbaines et usages de bâtiments.

A cette fin, un modèle calculant les rejets des systèmes de refroidissement a été développé et intégré dans le modèle microclimatique, « Solene-Microclimat ». Avant de développer le modèle permettant de calculer les rejets, nous avions rencontré un problème, les modèles de thermique de bâtiment dans Solene ne sont applicables qu'à un bâtiment de la scène urbaine alors que nous avions besoin, pour nos applications de connaître le besoin de froid de tous les bâtiments. Nous avons donc proposé un nouveau modèle de bâtiment, moins détaillé et applicable rapidement dans Solene-microclimat. Ce nouveau modèle thermique simplifié a été appliqué pour tous les bâtiments environnents le bâtiment plus précisément étudié. Pour évaluer la validité du sous-modèle développé, nous avons effectué une étude comparative entre les résultats issus de ce modèle et ceux d'un outil de simulation thermique dynamique (TRNSYS). Les résultats sont en accord avec une erreur relative moyenne d'environ 5%.

D'autre part, en intégrant les deux modèles (modèle simplifié de bâtiment et modèle de rejet de système de refroidissement) dans « Solene-Microclimat », nous avons réalisé une analyse de sensibilité pour différentes configurations d'une rue canyon. Celle-ci montre les effets du microclimat urbain sur les systèmes de refroidissement des bâtiments ; autrement dit, l'impact sur les besoins énergétiques et la dégradation du COP. Les résultats obtenus ont montré que la température de l'air à proximité de l'enveloppe du bâtiment augmente en présence d'un système de climatisation. Ils ont également montré qu'une hausse d'un degré de la température de l'air provoque une diminution de 3 % du COP alors que les besoins en énergie de refroidissement augmentent jusqu'à 11%. Pour la suite de notre étude, nous avons évalué l'impact des rejets thermiques des systèmes de climatisation à la fois sur le bâtiment et son microclimat pour 2 configurations réalistes différentes, un quartier récent et dense de la ville de Lyon, le quartier de la Buire et un quartier pavillonnaire à la périphérie de Lyon. Pour le cas du quartier de la Buire, nous avons simulé deux configurations d'équipement de climatisation : des climatiseurs individuels positionnés en façades et des groupes de refroidissement collectifs positionnés en toiture. Dans cette configuration urbaine, les résultats ont révélé que les rejets dans le cas où les unités extérieures sont positionnées en façade du bâtiment ont pour effet d'augmenter les besoins de 9% et la température moyenne de l'air à proximité de l'enveloppe de 1,75°C, tandis que le COP est dégradé de 10%. Dans le cas où les unités sont positionnées sur le toit, il a été constaté que les besoins ont été accrus de 5% et le COP dans ce cas est réduit de 17%. Pour la zone pavillonnaire, nous avons uniquement considéré les climatiseurs individuels en façade. Nous avons constaté que les besoins de refroidissement sont augmentés de 6% et le COP est dégradé de 2%.

Dans l'ensemble, la réduction de l'efficacité des systèmes de refroidissement due au microclimat urbain est un paramètre important lorsqu'il s'agit d'envisager les futurs investissements en infrastructures pour les quartiers urbains.

Finalement, la chaleur rejetée par un système de refroidissement du bâtiment résulte d'une relation complexe entre le bâtiment (son exposition au soleil, son niveau d'isolation...), le système lui-même et le microclimat, qui doivent tous être pris en compte, pour une bonne prédiction des besoins énergétiques, mais aussi pour une bonne évaluation des conditions microclimatiques et du confort extérieur. En plus, la position des unités extérieures influence sensiblement la performance des climatiseurs, raison pour laquelle ils doivent être pris en compte avec soin dans la conception architecturale.

Actuellement, je débute un second post-doctorat au sein de la même équipe que mon précédent poste, qui porte sur le « Développement d'un modèle couplé microclimatique, thermo-aéraulique intégrant les actions des occupants ». Cela fait partie d'une tâche dédiée à la « Modélisation intégrée » du projet CREATIV et qui a pour objectif le développement d'un modèle couplé microclimatique, thermo-aéraulique intégrant les actions des occupants. Le but étant de mieux prédire le confort thermique et la qualité de l'air intérieur dans les logements urbains en période de canicule.

Afin d'atteindre l'objectif de cette tâche, dans un premier temps, nous avons développé, en se basant sur mes travaux de thèse et en les améliorant, une approche d'une modélisation intégrée dans un outil de simulation énergétique des bâtiments couplé à un modèle basé sur une approche zonale pour le calcul des écoulements d'air à l'extérieur. Cette approche vise à évaluer les interactions entre le microclimat urbain et le bâtiment. Pour ce faire, un modèle thermoradiatif basé sur le facteur de Gebhart a été intégré dans un outil STD pour la modélisation du rayonnement solaire de courtes longueurs d'onde (CLO), du rayonnement thermique de grandes longueurs d'onde (GLO) dans le quartier. D'autre part, pour décrire de manière adéquate les champs de température et de vitesse du vent autour des bâtiments, un modèle zonal tridimensionnel d'écoulement du vent respectant la conservation de la masse a été développé sur la base de modèles empiriques existants dans la littérature.

Pour évaluer la fiabilité de la modélisation développée une comparaison avec des résultats expérimentaux a été effectuée. Les résultats numériques obtenus sont concordants avec ceux des expérimentations avec une erreur absolue moyenne sur la température surfacique des parois extérieures d'environ 1,3 °C et une erreur relative moyenne d'environ 7 %. L'utilisation de cette méthode montre son intérêt en terme du temps de calcul réduit par rapport à des calculs CFD tout en gardant une précision satisfaisante afin d'obtenir une meilleure précision par rapport à l'évaluation des performances énergétiques des bâtiments à l'échelle d'un quartier.

Dans une deuxième étape, nous développons une approche intermédiaire entre la zonale et la CFD en utilisant la Fast Fluid Dynamics (FFD) pour modéliser l'écoulement de l'air autour d'un bâtiment à l'échelle d'un quartier. Celle-ci peut fournir une simulation rapide et informative de l'écoulement de l'air, des coefficients de pression en façades avec des temps de calcul, selon la littérature, 30 à 50 fois plus rapide que ceux de la CFD. Cette dernière approche peut être directement couplée à CONTAM via les coefficients de pression pour évaluer l'influence de l'ouverture des fenêtres sur les ambiances thermiques et la qualité de l'air intérieur (QAI).

Dans ce travail, nous utilisons un outil classique de simulation thermique dynamique (STD) TRNSYS couplé à un outil aéraulique CONTAM. Ce dernier aura besoin de la température, de la pression, de la direction et de la vitesse du vent de l'air extérieur et renverra les flux d'air vers l'outil STD. Cette approche permet de différencier les performances des différents systèmes de ventilation et de traitement de l'air (purification/filtration) et de prendre en compte la dispersion des polluants.

Ainsi, par le couplage des approches zonales, FFD et thermo-radiatives avec le modèle thermo-aéraulique du bâtiment (TRNSYS - CONTAM) permettra de mieux prendre en compte les conditions climatiques locales et d'évaluer le confort ainsi que la pollution à l'intérieur du bâtiment tout en tenant compte de son environnement proche.

2) Projet scientifique pour le poste proposé

Mon projet de recherche est pleinement en phase avec les objectifs du poste proposé. Il s'inscrit dans la thématique de la thermique et l'énergétique du bâtiment du pôle1 « Matériaux Multiphasiques innovants » du LMDC. De plus, il permet de mettre à profit les compétences spécifiques que j'ai acquises pendant mes travaux de thèse sur l'énergétique des bâtiments ainsi que sur la modélisation du microclimat urbain et son interaction avec la performance énergétique des bâtiments, ainsi que celles acquises lors de mon post-doctorat sur l'évaluation des interactions entre le climat urbain et les systèmes des bâtiments. Par ailleurs, mes travaux de thèse et de post-doctorat suggèrent plusieurs pistes de recherche répondant directement aux objectifs dans lesquels Le « Laboratoire Matériaux et Durabilité des Constructions » souhaite s'investir. En outre, j'envisage de proposer de créer un nouveau thème de recherche qui traitera de l'interaction bâtiment-microclimat au sein de du même pôle.

A cette fin et pour répondre aux objectifs du poste, mon projet de recherche est composé des 5 volets ci-dessous.

Volet 1 : Développement d'une modélisation de la demande énergétique des bâtiments à l'échelle d'un quartier

Aujourd'hui, il est devenu indispensable ; pour vivre en ville ; de construire des bâtiments adaptables à leur environnement avec moins d'énergie consommée et qui répondent aux exigences collectives en matière de développement durable et de confort. Ainsi, le secteur du bâtiment demeure l'un des principaux contributeurs ayant un impact sur l'environnement en raison de sa consommation énergétique élevée, surtout que la grande majorité de cette énergie utilisée dans les bâtiments provient de ressources en combustibles fossiles non renouvelables. Dans ce cadre, l'estimation et l'optimisation des besoins énergétiques du bâtiment représentent le point clé pour maîtriser sa performance énergétique et donc de réduire son impact environnemental. Parallèlement, la prédition des besoins énergétiques doit être de plus en plus réaliste afin de garantir la performance énergétique et d'apporter des solutions techniques adéquates. En l'occurrence, la modélisation thermique des bâtiments doit tenir compte des conditions environnementales intérieures et extérieures d'une manière de plus en plus détaillée tout en veillant à maintenir des temps de calcul acceptables.

Afin de prévoir les besoins énergétiques et le confort thermique, la Simulation Thermique Dynamique des bâtiments (STD) a été initialement développée en utilisant des conditions météorologiques simplifiées. Ces outils de STD sont très utilisés et développés pour la conception des bâtiments tels que TRNSYS, EnergyPlus ou ESP-r, etc. Ils sont généralement basés sur des données météorologiques établies pour une année type et collectées par des stations météorologiques situées dans des zones rurales. En revanche, ces données météorologiques sont loin d'être représentatives de l'environnement extérieur d'un bâtiment situé en milieu urbain. En effet, les conditions climatiques sont les principaux déterminants de la demande énergétique des bâtiments puisqu'ils interagissent avec leur environnement extérieur immédiat. Plus précisément, le microclimat urbain résultant d'une interaction complexe entre les différents phénomènes physiques (la température de l'air, l'humidité, l'écoulement du vent et le rayonnement solaire) avec les éléments qui constituent la ville comme les aménagements urbains, les matériaux utilisés pour les constructions ainsi que l'activité humaine. Il est important de noter que l'interaction des phénomènes de transfert de chaleur et de masse dans un tissu urbain, avec les apports anthropiques, participent à

l'apparition des phénomènes microclimatiques particuliers dont l'îlot de chaleur urbain qui est le plus représentatif de ces phénomènes [1]–[7]. Dans cette optique, la connaissance et la prise en compte de l'impact du climat urbain sont essentielles pour améliorer la modélisation énergétique des bâtiments [8]–[12].

A ce titre, les ingénieurs, les architectes et les concepteurs doivent être capables de concevoir des bâtiments à haute efficacité énergétique tout en tenant compte du microclimat. Dans ce contexte, on trouve dans la littérature plusieurs modèles qui ont été développés parmi lesquels on peut citer les modèles noraux simplifiés [13]–[15], les modèles zonaux [16], [17] et le modèle SOLENE couplé à un modèle CFD [18]. Ces modèles sont généralement détaillés, cependant leur utilisation est complexe vu le temps de calcul élevé et les difficultés de couplage entre plusieurs logiciels (problème de l'interopérabilité). De plus, à l'heure actuelle, ces outils ne sont pas en mesure de modéliser avec précision le comportement thermique des bâtiments comme les outils de simulation thermique dynamique des bâtiments.

Pour contribuer à ces défis, je propose dans le cadre de ce projet de développer une modélisation intégrée dans le logiciel TRNSYS permettant, sans avoir recours à la CFD, d'évaluer l'impact du microclimat urbain sur la performance énergétique des bâtiments en utilisant un seul logiciel, et ce en se basant sur les modèles développés dans ma thèse. Cette modélisation permet de prendre en considération le couplage des phénomènes hygrothermiques, aérauliques et radiatifs à l'échelle microclimatique de l'environnement proche du bâtiment.

Pour évaluer la validité de cette approche, on pourra collaborer avec le laboratoire LaSie (Université de La Rochelle) pour exploiter le modèle expérimental ClimaBat, ainsi qu'avec le Cerema pour l'utilisation de ces outils de modélisation afin de les comparer avec le modèle qui sera développé. Dans le même sens, en termes de collaboration internationale, on pourra collaborer avec l'équipe de recherche en transferts thermiques et énergétiques de la Faculté des Sciences et Techniques de Tanger, Université Abdelmalek Essaâdi, Maroc.

Volet 2 : Evaluation de la qualité de l'environnement intérieur des bâtiments

Ces dernières années, la qualité de l'environnement intérieur a fait l'objet de nombreuses études en raison de l'augmentation des niveaux de pollution, qui entraîne des problèmes de santé importants. En effet, la question de la qualité de l'air intérieur est désormais importante, car le développement technologique des fenêtres thermiques et des bâtiments plus efficaces sur le plan énergétique conduit à des bâtiments plus étanches, ce qui peut augmenter considérablement la concentration de polluants et présenter des risques élevés pour la santé. En ce sens, les recherches se concentrent davantage sur l'évaluation des effets sur la santé humaine de l'exposition à différents niveaux de pollution [19]. D'ailleurs, la qualité de l'environnement intérieur varie selon les saisons et l'espace et est influencée par la saison, l'environnement extérieur, le type de système de chauffage et de climatisation et de ventilation et les caractéristiques du bâtiment (type de logement, période de construction, emplacement du logement, type de système de ventilation, matériau de construction).

En milieu urbain, la qualité de l'environnement intérieur (QEI) dans les bâtiments ventilés naturellement dépend fortement du microclimat urbain, notamment la vitesse du vent, la température de l'air, la concentration de polluants et le niveau de bruit [20]. Pour améliorer la qualité de l'environnement intérieur dans ces bâtiments, une bonne compréhension de l'état

actuel et des problèmes liés à la qualité de l'air et à son interaction avec le microclimat urbain est cruciale.

En effet, sur la base de la littérature existante, on peut retenir les suggestions suivantes :

- Un aménagement urbain adéquat et une conception soignée de l'enveloppe sont les principaux moyens d'améliorer la QEI dans les bâtiments à ventilation naturelle et de favoriser ainsi le recours à la ventilation naturelle.
- Pour les polluants et le bruit, les bâtiments à ventilation naturelle doivent être construits dans des zones à faible trafic et les fenêtres principales ne doivent pas donner sur des rues à fort trafic.
- La ventilation hybride utilisant une ventilation mécanique avec des filtres comme système d'appoint pour la ventilation naturelle est un système de ventilation prometteur dans les zones urbaines pour assurer un taux de ventilation minimum et éviter une pénétration excessive des polluants extérieurs.

D'autre part, en examinant la littérature existante, nous trouvons peu d'études qui traitent de ce sujet.

En tenant compte des limitations des études existantes et des problèmes actuels des bâtiments naturellement ventilés en milieu urbain, je propose dans ce qui suit, des pistes de travaux afin de mieux comprendre et d'améliorer la qualité de l'environnement intérieur dans les bâtiments en milieu urbain naturellement ventilés.

Les études quantitatives, notamment les mesures in situ, du microclimat et de la QEI dans les bâtiments urbains à ventilation naturelle restent très rares, et la plupart d'entre elles sont des mesures à court terme dans des conditions environnementales spécifiques. De plus, la comparaison entre ces études et l'analyse des facteurs influents n'est actuellement pas possible. Afin de mieux comprendre et d'améliorer la QEI dans les bâtiments urbains à ventilation naturelle, je propose d'entamer les points suivants dans le cadre des collaborations :

- Réaliser des mesures in situ à grande échelle, à long terme et à haute résolution pour un quartier ou une rue canyon permettant de recueillir des données microclimatiques, lesquelles constituent des informations fondamentales pour l'urbanisme, la conception de bâtiments et même les simulations.
- Étudier le procédé de pénétration dynamique des polluants particulaires et gazeux depuis l'environnement extérieur (Exemple : rue) jusqu'à l'environnement intérieur d'un bâtiment, afin de comprendre les mécanismes de pénétration et d'élaborer des recommandations relatives à la conception.
- Analyser les problèmes liés à la combinaison de la ventilation naturelle avec d'autres technologies de refroidissement actives et/ou passives dans les bâtiments urbains.
- Pour optimiser la conception de l'enveloppe du bâtiment en fonction du microclimat urbain, une étude des caractéristiques d'écoulement, de la pénétration des polluants et de l'atténuation du bruit est à effectuer.

Volet 3 : Développement d'un modèle pour la combinaison de revêtements froids avec des matériaux à changement de phase

Récemment, de nombreuses solutions ont été proposées pour lutter contre les effets négatifs du réchauffement climatique et de l'ICU sur les performances thermo-énergétiques des bâtiments

[21]. Parmi ces stratégies, on trouve : l'utilisation intensive d'espaces verts, l'application de matériaux hautement réfléchissants, la réduction de la chaleur anthropique, le contrôle solaire des espaces ouverts, l'utilisation de puits de chaleur environnementaux et l'augmentation de la circulation du vent dans la canopée [22].

Par ailleurs, les revêtements froids appliqués aux surfaces urbaines (c'est-à-dire les rues, les trottoirs, les places) et aux enveloppes des bâtiments (c'est-à-dire les toits et les façades) représentent l'une des solutions les plus efficaces pour réduire les besoins énergétiques de refroidissement des bâtiments tout en améliorant le confort thermique intérieur dans les conditions estivales extrêmes [23].

En effet, ces matériaux sont caractérisés par une forte capacité à réfléchir le rayonnement solaire et à émettre un rayonnement thermique. Ces deux propriétés contribuent à l'abaissement des températures de surface des revêtements extérieurs des bâtiments, diminuant la pénétration de la chaleur à travers l'enveloppe de ces derniers et réduisant leur charge de refroidissement [24], tandis que lorsqu'ils sont appliqués sur les trottoirs et autres surfaces urbaines, ils contribuent à réduire la température ambiante dans la mesure où l'intensité de la chaleur convective provenant d'une surface plus froide est plus faible [25].

En outre, pour diminuer davantage la température de surface des revêtements froids, trois options techniques principales sont disponibles : 1) augmenter la réflectivité solaire des matériaux, 2) augmenter leur capacité thermique, et 3) ajouter aux revêtements des matériaux à chaleur latente. Sachant cette dernière, les matériaux à changement de phase (MCP) représentent une autre stratégie appropriée pour atténuer l'impact négatif de la surchauffe environnementale [26]. En effet, ils sont capables de stocker l'énergie thermique sous forme de chaleur latente lorsqu'un changement de phase se produit [27]. Ainsi, en réduisant les fluctuations de température, ils peuvent réduire les pics thermiques lorsqu'ils sont intégrés aux composants de l'enveloppe du bâtiment [28].

Dans ce contexte, la combinaison des technologies précédemment citées, à savoir les matériaux froids et les MCP, a pour effet de maximiser le potentiel de refroidissement et les capacités d'économie d'énergie du bâtiment [29]. Cette combinaison permet de stocker la chaleur sous forme latente, en modérant les fluctuations des températures de surface, et de la restituer avec un décalage dans le temps ; et par conséquent de réaliser d'importantes économies d'énergie dans les bâtiments en maintenant un environnement intérieur thermiquement confortable. D'autre part, elle réduit le gain de chaleur solaire dans le bâtiment grâce à ses surfaces hautement réfléchissantes et, par conséquent, réduit le phénomène d'ICU.

Dans cette perspective, afin de mieux comprendre le potentiel de la combinaison des MCP avec des revêtements froids visant à réduire davantage la température de surface des zones urbaines et des bâtiments, ainsi que la consommation énergétique. A cette fin, je propose de développer et d'intégrer un modèle de MCP et de revêtements froids dans le modèle zonal de quartier que je développerai. En vue d'évaluer la fiabilité de ce modèle, on pourra mettre en place des dispositifs expérimentaux pour effectuer des mesures in-situ, tout en testant des matériaux innovants à ce propos. De plus, nous pourrons tester le potentiel de cette technologie à l'échelle réduite d'un modèle expérimental comme le ClimaBat de LaSie.

Volet 4 : Développement d'un modèle des systèmes photovoltaïques intégrés aux bâtiments (BIPV)

La production d'électricité solaire est l'un moyen qui permet de diminuer d'une manière forte notre dépendance vis-à-vis des combustibles fossiles mais aussi d'atténuer le réchauffement de la planète en réduisant les émissions de gaz à effet de serre [30].

Les systèmes photovoltaïques intégrés aux bâtiments (BIPV) constituent une technologie à fort potentiel pour augmenter la part des énergies renouvelables dans l'environnement bâti [31]. En effet, à la différence des panneaux photovoltaïques traditionnels installés à l'extérieur des bâtiments, un système BIPV fait partie intégrante de l'enveloppe du bâtiment et offre des avantages tels que l'ombrage et l'isolation thermique. Ainsi, ce système est l'une des technologies les plus appropriées pour répondre aux exigences de la norme européenne NZEB (Nearly Zero Energy Building) en matière de production d'énergie renouvelable sur site [32]. Toutefois, une exploitation efficace du BIPV dans l'environnement urbain nécessite une évaluation correcte de la demande énergétique du bâtiment et de la performance du système photovoltaïque.

Dans ce contexte, l'évaluation de la production d'énergie photovoltaïque, qui est souvent difficile en raison des nombreux facteurs influençant l'efficacité du système, est une autre question de recherche qui se pose [33]. En revanche, les modèles numériques des systèmes BIPV prenant en compte la consommation énergétique des bâtiments restent limités dans la littérature [34]. En effet, la plupart des modèles BIPV se focalisent uniquement sur les performances thermiques et électriques du système PV [35], et négligent l'interaction dynamique entre le système PV, les bâtiments et le climat local.

Dans cette optique, nous cherchons à aborder cette problématique en répondant aux questions de recherche suivantes :

1. Quel est l'impact du BIPV sur la consommation énergétique des bâtiments et le microclimat extérieur d'un quartier ?
2. Comment le milieu urbain influe-t-il sur les performances des systèmes BIPV installés dans les quartiers ?
3. Quels sont les paramètres qui conditionnent la performance des BIPV ?
4. Quels sont les impacts du BIPV (positifs et négatifs) sur l'environnement urbain ?

A cette fin, je propose de développer un sous-modèle d'enveloppe qui s'intègre au modèle de quartier à développer. Ce modèle présente une rétroaction dynamique entre les espaces intérieurs et extérieurs, permettant ainsi d'étudier l'impact du BIPV sur un environnement bâti totalement interactif, d'une part, et vise d'autre part à évaluer l'influence de la morphologie urbaine sur la production PV. Ce sous-modèle constituera un moyen d'avoir une vue d'ensemble des facteurs affectant la consommation énergétique des bâtiments et la production photovoltaïque, en quantifiant leurs conséquences, et en fournissant des lignes directrices pour la planification d'un quartier énergétiquement quasiment nul.

Pour aborder cette problématique, et afin de contribuer aux connaissances dans ce domaine, je propose de développer un modèle de système PV intégrable au modèle microclimatique zonal du quartier que je développerai. Pour valider le modèle, on pourra réaliser une maquette expérimentale à l'université.

Du point de vue des collaborations, nous pourrons bénéficier des expériences de l'équipe de recherche LOCIE de l'Université Savoie Mont Blanc dont le thème de recherche est systèmes et bâtiments intégrés dans la ville et les territoires "SITE". En termes de collaboration internationale, nous pourrons compter sur l'expertise de l'Institut de Recherche en Énergie Solaire et Énergies Nouvelles (IRESEN) au Maroc, et de sa plateforme de test de recherche "Green Energy Park" et la plateforme "Green & Smart Building Park".

Volet 5 : Réhabilitation énergétique des bâtiments existants

Dans un monde de plus en plus urbanisé, de nombreuses personnes considèrent les villes comme la clé d'un avenir où les ressources sont utilisées de manière efficace et durable. En vue de rendre les villes plus durables, une grande attention est souvent accordée à des stratégies ambitieuses d'économie d'énergie en rénovant les bâtiments existants et en construisant de nouvelles villes. Ce faisant, il est crucial d'être en mesure d'estimer les performances énergétiques réelles des bâtiments, afin de pouvoir définir des mesures d'économie d'énergie appropriées et raisonnables. Ces mesures visent à augmenter la performance énergétique des bâtiments existants lors de la rénovation énergétique, ou à intégrer des éléments dans la conception des nouveaux bâtiments afin qu'ils soient conformes aux politiques énergétiques visant un parc immobilier à énergie quasi nulle. Cependant, Les nouveaux bâtiments sont généralement basés sur une conception efficace et, pour cette raison, la rénovation de bâtiments existants peut être plus rentable que la construction de nouveaux bâtiments, dans la mesure où les bâtiments existants consomment une quantité importante d'énergie, en particulier pour le chauffage et la climatisation, et où ces bâtiments constituent un plus grand gisement d'économie d'énergie.

L'identification de la performance thermique réelle, et plus précisément les propriétés thermophysiques des éléments de bâtiments, est cruciale dans le cadre de la prise de décisions pour la rénovation énergétique et la mise en œuvre de mesures d'économie d'énergie concernant le choix de technologies constructives adaptées et performantes. Cependant, il peut être difficile d'identifier les propriétés thermiques des éléments de construction avec précision, et cela est particulièrement difficile dans les bâtiments historiques et patrimoniaux existants en raison de leur complexité et l'hétérogénéité des matériaux utilisés. En outre, plusieurs études ont été menées depuis les années 1990 [36] et ont montré la présence d'un écart entre les performances énergétiques mesurées et simulées[37]–[40], , dont les principales origines sont attribuées aux activités et au comportement des occupants, aux modifications apportées aux matériaux lors de la construction et au vieillissement ainsi qu'à la dégradation de l'enveloppe au cours du temps. D'autres études constatent également un écart entre les propriétés thermophysiques mesurées et calculées des éléments de construction[41]–[44].

Dans cette optique, je propose d'utiliser la technique de la thermographie infrarouge comme une méthode non destructive de mesure de la performance thermique des bâtiments où les images thermiques fournissent des informations détaillées sur la distribution de la température de surface interne ou externe. Cependant, ces images sont généralement enregistrées à des moments singuliers , alors que dans plusieurs cas, les anomalies ne peuvent être révélées qu'à des moments précis de la journée, éventuellement à différentes saisons de l'année. Et c'est pour cette raison que je propose un nouveau protocole pour la caractérisation et la modélisation des défauts d'enveloppe 3D à l'aide de la collecte de données aériennes de l'infrarouge thermique accélérées à l'aide de drones. A partir de ces images, nous pouvons déterminer la transmittance thermique (U) in-situ. Finalement, les véritables besoins énergétiques des bâtiments seront

estimés à l'aide d'une simulation thermique dynamique des bâtiments, où chaque élément de l'enveloppe reçoit une valeur U, afin de choisir les solutions appropriées pour une rénovation optimale des bâtiments étudiés.

Dans le cadre de l'application du protocole développé, je compte effectuer des collaborations avec les industries de l'infrarouge et des drones pour explorer les dernières technologies d'aujourd'hui dans ces domaines ainsi que des collaborations universitaires qui s'inscrivent dans un mouvement général d'échange scientifique.

D. BILAN ET PROJET D'ACTIVITES D'ENSEIGNEMENT

1) Bilan d'activités d'enseignement

Mon expérience dans l'enseignement supérieur et mes études m'ont fait acquérir des compétences qui m'ont permis d'enseigner dans différentes formations : Licence filière « Energies Renouvelables », D.U.T « Énergies Renouvelables et Efficacité Énergétique » et Master filières « Génie Énergétique » et « Génie Civil ». En effet, depuis ma première année de thèse à la faculté des Sciences et Techniques de Tanger au Maroc, j'ai effectué plus de 134 heures d'enseignement. Ces activités m'ont permis de m'adresser à un public d'étudiants, à travers de formes d'enseignement traditionnelle (travaux pratiques) ou plus innovantes (encadrement de projets de recherche), avec des approches théoriques et pratiques, sur des domaines variés (discipline de base et spécialisée). L'adaptabilité acquise au cours de mes expériences d'enseignement devrait me permettre de répondre sans délais aux besoins actuels du département de mécanique de la Faculté Sciences et Ingénierie de l'Université Toulouse 3. J'ai conscience que pour réaliser ses objectifs de formation, celui-ci doit permettre de développer chez le futur diplômé des capacités d'autonomie, de travail en équipe et d'esprit d'analyse tant du point de vue expérimental que dans l'exploitation des résultats de l'expérience. D'autre part, il doit lui apporter une large connaissance des différents domaines liés à la Thermique-Énergétique des bâtiments dans leurs aspects fondamentaux et expérimentaux.

Mon expérience d'enseignement ainsi que mes travaux de recherches qui s'inscrivent dans l'interaction bâtiment-systèmes-microclimat urbain de recherche m'ont permis de développer de très bonnes compétences dans différentes disciplines de la transferts thermique, énergétique des bâtiments ainsi que la mécanique des fluides : confort thermique, efficacité énergétique des bâtiments, Simulation Thermique Dynamique (STD), énergies renouvelables... Enfin, je mentionne que j'ai encadré 7 projets de fin d'étude traitant des sujets liés à l'énergétique des bâtiments.

2) Intégration pédagogique

Étant qualifié en sections 60 et 62 du CNU et ayant des compétences théoriques, numériques et pratiques, je peux couvrir une large variété d'enseignement proposés à l'Université Toulouse 3. En particulier, je peux enseigner en :

- Licence Génie de l'Habitat : Transferts thermiques, énergétique du bâtiment, analyse numérique et appliquée (Python).

- Master Génie de l'Habitat : bureau d'études autour des systèmes de CVC, Confort thermique, Énergies renouvelables, thermique du bâtiment, étude conception et optimisation des bâtiments, Simulation Thermique Dynamique (STD).

Parmi ces formations j'ai déjà des expériences d'enseignement en STD énergies renouvelables et transferts thermiques. Pour les autres, à travers ma formation initiale (Doctorat & Master) et mes travaux de recherche, je dispose d'une solide base théorique et d'une très bonne connaissance en énergétique du bâtiment et la Simulation Thermique Dynamique (TRNSYS).

L'apprentissage des étudiants est ma principale préoccupation et je suis prêt à appliquer de nouvelles approches pédagogiques combinées avec les nouvelles technologies pour qu'ils puissent apprendre de la meilleure façon possible. Cet aspect est très important dans le contexte actuel avec l'augmentation des cours à distance.

Avec l'ouverture internationale de l'université, mes connexions avec les universités marocaines FST de Tanger de l'Université Abdelmalek Essaâdi et Ecole Nationale d'Architecture de Tétouan, Faculté des Sciences de l'université Mohammed V et Université Mohammed VI Polytechnique peuvent permettre d'élargir le réseau de Université Toulouse 3 via notamment les mobilités d'étudiants. De plus, je peux suivre et encadrer des étudiants pendant leur stage et superviser leurs projets. Je peux également enseigner des matières où mes connaissances sont moins avancées, moyennant un peu plus de temps de préparation.

Aussi, je citerais ici quelques points dans lesquels je peux m'investir tout en restant conscient des nécessités liées au service :

- Mettre en place de nouvelles installations expérimentales pour les TP
- Gérer et à entretenir les montages de TP
- Créer de nouveaux contenus pédagogiques (polycopies de cours, séries de travaux dirigés, sujets d'exams, polycopiés de TP...).
- La planification des contenus des unités d'enseignement.
- Contribuer aux tâches administratives et collectives du département et des filières d'enseignement.
- Assurer la responsabilité d'unités d'enseignement.
- Assurer les encadrements et l'aide à la recherche de stage et la prise en charge des tâches administratives liées aux conventions des stages.

Références

- [1] J. Allegrini, V. Dorer, et J. Carmeliet, « Influence of the urban microclimate in street canyons on the energy demand for space cooling and heating of buildings », *Energy and Buildings*, vol. 55, p. 823-832, 2012, doi: 10.1016/j.enbuild.2012.10.013.
- [2] A. Yeziro, B. Dong, et F. Leite, « An applied artificial intelligence approach towards assessing building performance simulation tools », *Energy and Buildings*, vol. 40, no 4, p. 612-620, 2008, doi: 10.1016/j.enbuild.2007.04.014.
- [3] M. Santamouris, « Heat Island Research in Europe: The State of the Art », *Advances in Building Energy Research*, vol. 1, no 1, p. 123-150, 2007, doi: 10.1080/17512549.2007.9687272.
- [4] M. Kolokotroni, I. Giannitsaris, et R. Watkins, « The effect of the London urban heat island on building summer cooling demand and night ventilation strategies », *Solar Energy*, vol. 80, no 4, p. 383-392, 2006, doi: 10.1016/j.solener.2005.03.010.
- [5] F. Musco, Counteracting Urban Heat Island Effects in a Global Climate Change Scenario. 2016. doi: 10.1007/978-3-319-10425-6.
- [6] L. Gartland, Heat Islands: Understanding and mitigating heat in urban areas, vol. 9781849771. 2012. doi: 10.4324/9781849771559.
- [7] Y. Sun et G. Augenbroe, « Urban heat island effect on energy application studies of office buildings », *Energy and Buildings*, vol. 77, p. 171-179, 2014, doi: 10.1016/j.enbuild.2014.03.055.
- [8] J. Bouyer, C. Inard, et M. Musy, « Microclimatic coupling as a solution to improve building energy simulation in an urban context », *Energy and Buildings*, vol. 43, no 7, p. 1549-1559, 2011, doi: 10.1016/j.enbuild.2011.02.010.
- [9] P. Moonen, T. Defraeye, V. Dorer, B. Blocken, et J. Carmeliet, « Urban Physics: Effect of the micro-climate on comfort, health and energy demand », *Frontiers of Architectural Research*, vol. 1, no 3, p. 197-228, 2012, doi: 10.1016/j foar.2012.05.002.
- [10] E. Jamei, P. Rajagopalan, M. Seyedmahmoudian, et Y. Jamei, « Review on the impact of urban geometry and pedestrian level greening on outdoor thermal comfort », *Renewable and Sustainable Energy Reviews*, vol. 54, p. 1002-1017, 2016, doi: 10.1016/j.rser.2015.10.104.
- [11] G. Mills, « Urban climatology: History, status and prospects », *Urban Climate*, vol. 10, no P3, p. 479-489, 2014, doi: 10.1016/j.uclim.2014.06.004.
- [12] X. Yang, L. Zhao, M. Bruse, et Q. Meng, « An integrated simulation method for building energy performance assessment in urban environments », *Energy & Buildings*, vol. 54, p. 243-251, 2012, doi: 10.1016/j.enbuild.2012.07.042.
- [13] D. Robinson et al., « Citysim: Comprehensive micro-simulation of resource flows for sustainable urban planning », in IBPSA 2009 - International Building Performance Simulation Association 2009, 2009, p. 1083-1090.
- [14] V. Masson, « A physically-based scheme for the urban energy budget in atmospheric models », *Boundary-layer meteorology*, vol. 94, no 3, p. 357-397, 2000, doi: <https://doi.org/10.1023/A:1002463829265>.
- [15] A. Tsiringakis, G. Steeneveld, A. A. M. Holtslag, S. Kotthaus, et S. Grimmond, « On-and off-line evaluation of the single-layer urban canopy model in London summertime conditions », *Quarterly Journal of the Royal Meteorological Society*, vol. 145, no 721, p. 1474-1489, 2019, doi: <https://doi.org/10.1002/qj.3505>.
- [16] E. Bozonnet, R. Belarbi, et F. Allard, « Thermal Behaviour of buildings: modelling the impact of urban heat island », *Journal of Harbin Institute of Technology (New Series)*, vol. 14, no Sup., p. 19-22, janv. 2007.
- [17] A. Gros, E. Bozonnet, et C. Inard, « Cool materials impact at district scale - Coupling building energy and microclimate models », *Sustainable Cities and Society*, vol. 13, p. 254-266, 2014, doi: 10.1016/j.scs.2014.02.002.
- [18] M. Musy, L. Malys, B. Morille, et C. Inard, « The use of SOLENE-microclimat model to assess adaptation strategies at the district scale », *Urban Climate*, vol. 14, p. 213-223, 2015, doi: 10.1016/j.uclim.2015.07.004.
- [19] P. Spiru et P. L. Simona, « A review on interactions between energy performance of the buildings, outdoor air pollution and the indoor air quality », *Energy Procedia*, vol. 128, p. 179-186, sept. 2017, doi: 10.1016/j.egypro.2017.09.039.

- [20] Z. T. Ai et C. M. Mak, « From street canyon microclimate to indoor environmental quality in naturally ventilated urban buildings: Issues and possibilities for improvement », *Building and Environment*, vol. 94, p. 489-503, déc. 2015, doi: 10.1016/j.buildenv.2015.10.008.
- [21] M. Santamouris, A. Synnefa, et T. Karlessi, « Using advanced cool materials in the urban built environment to mitigate heat islands and improve thermal comfort conditions », *Solar Energy*, vol. 85, no 12, p. 3085-3102, déc. 2011, doi: 10.1016/j.solener.2010.12.023.
- [22] N. Gaitani, G. Mihalakakou, et M. Santamouris, « On the use of bioclimatic architecture principles in order to improve thermal comfort conditions in outdoor spaces », *Building and Environment*, vol. 42, no 1, p. 317-324, janv. 2007, doi: 10.1016/j.buildenv.2005.08.018.
- [23] T. Xu, J. Sathaye, H. Akbari, V. Garg, et S. Tetali, « Quantifying the direct benefits of cool roofs in an urban setting: Reduced cooling energy use and lowered greenhouse gas emissions », *Building and Environment*, vol. 48, p. 1-6, févr. 2012, doi: 10.1016/j.buildenv.2011.08.011.
- [24] A. Synnefa, M. Santamouris, et H. Akbari, « Estimating the effect of using cool coatings on energy loads and thermal comfort in residential buildings in various climatic conditions », *Energy and Buildings*, vol. 39, no 11, p. 1167-1174, nov. 2007, doi: 10.1016/j.enbuild.2007.01.004.
- [25] A. Synnefa, T. Karlessi, N. Gaitani, M. Santamouris, D. N. Assimakopoulos, et C. Papakatsikas, « Experimental testing of cool colored thin layer asphalt and estimation of its potential to improve the urban microclimate », *Building and Environment*, vol. 46, no 1, p. 38-44, janv. 2011, doi: 10.1016/j.buildenv.2010.06.014.
- [26] C. Barreneche, A. Solé, L. Miró, I. Martorell, A. I. Fernández, et L. F. Cabeza, « Study on differential scanning calorimetry analysis with two operation modes and organic and inorganic phase change material (PCM) », *Thermochimica Acta*, vol. 553, p. 23-26, févr. 2013, doi: 10.1016/j.tca.2012.11.027.
- [27] G. Zhou et Y. Xiang, « Experimental investigations on stable supercooling performance of sodium acetate trihydrate PCM for thermal storage », *Solar Energy*, vol. 155, p. 1261-1272, oct. 2017, doi: 10.1016/j.solener.2017.07.073.
- [28] A. Sarı, C. Alkan, et A. N. Özcan, « Synthesis and characterization of micro/nano capsules of PMMA/capric–stearic acid eutectic mixture for low temperature-thermal energy storage in buildings », *Energy and Buildings*, vol. 90, p. 106-113, mars 2015, doi: 10.1016/j.enbuild.2015.01.013.
- [29] M. Saffari, C. Piselli, A. de Gracia, A. L. Pisello, F. Cotana, et L. F. Cabeza, « Thermal stress reduction in cool roof membranes using phase change materials (PCM) », *Energy and Buildings*, vol. 158, p. 1097-1105, janv. 2018, doi: 10.1016/j.enbuild.2017.10.068.
- [30] D. El Helow, J. Drake, et L. Margolis, « Testing the Potential Synergy of Green Roof-Integrated Photovoltaics at the University of Toronto Green Roof Innovation Testing (GRIT) Laboratory », présenté à Proceedings 32nd RCI Convention and Tradeshow, 2017.
- [31] A. K. Shukla, K. Sudhakar, et P. Baredar, « Recent advancement in BIPV product technologies: A review », *Energy and Buildings*, vol. 140, p. 188-195, avr. 2017, doi: 10.1016/j.enbuild.2017.02.015.
- [32] B. P. Jelle et C. Breivik, « State-of-the-art building integrated photovoltaics », *Energy Procedia*, vol. 20, p. 68-77, 2012.
- [33] W. P. U. Wijeratne, R. J. Yang, E. Too, et R. Wakefield, « Design and development of distributed solar PV systems: Do the current tools work? », *Sustainable cities and society*, vol. 45, p. 553-578, 2019.
- [34] J. E. Gonçalves, T. van Hooff, et D. Saelens, « Simulating building integrated photovoltaic facades: Comparison to experimental data and evaluation of modelling complexity », *Applied Energy*, vol. 281, p. 116032, janv. 2021, doi: 10.1016/j.apenergy.2020.116032.
- [35] R. A. Agathokleous et S. A. Kalogirou, « Double skin facades (DSF) and building integrated photovoltaics (BIPV): A review of configurations and heat transfer characteristics », *Renewable Energy*, vol. 89, p. 743-756, avr. 2016, doi: 10.1016/j.renene.2015.12.043.
- [36] S. N. Flanders, « In-situ heat flux measurements in buildings; applications and interpretations of results », 1991.
- [37] M. Sunikka-Blank et R. Galvin, « Introducing the prebound effect: the gap between performance and actual energy consumption », *Building Research & Information*, vol. 40, no 3, p. 260-273, juin 2012, doi: 10.1080/09613218.2012.690952.

- [38] D. Majcen, L. Itard, et H. Visscher, « Actual and theoretical gas consumption in Dutch dwellings: What causes the differences? », Energy Policy, vol. 61, p. 460-471, oct. 2013, doi: 10.1016/J.ENPOL.2013.06.018.
- [39] D. Majcen, L. C. M. Itard, et H. Visscher, « Theoretical vs. actual energy consumption of labelled dwellings in the Netherlands: Discrepancies and policy implications », Energy Policy, vol. 54, p. 125-136, 2013, doi: <https://doi.org/10.1016/j.enpol.2012.11.008>.
- [40] G. Branco, B. Lachal, P. Gallinelli, et W. Weber, « Predicted versus observed heat consumption of a low energy multifamily complex in Switzerland based on long-term experimental data », Energy and Buildings, vol. 36, no 6, p. 543-555, 2004, doi: <https://doi.org/10.1016/j.enbuild.2004.01.028>.
- [41] R. Albatici, A. M. Tonelli, et M. Chiogna, « A comprehensive experimental approach for the validation of quantitative infrared thermography in the evaluation of building thermal transmittance », Applied Energy, vol. 141, p. 218-228, 2015, doi: 10.1016/j.apenergy.2014.12.035.
- [42] K. Gaspar, M. Casals, et M. Gangolells, « A comparison of standardized calculation methods for in situ measurements of façades U-value », Energy and Buildings, vol. 130, p. 592-599, oct. 2016, doi: 10.1016/j.enbuild.2016.08.072.
- [43] G. Desogus, S. Mura, et R. Ricciu, « Comparing different approaches to in situ measurement of building components thermal resistance », Energy and Buildings, vol. 43, no 10, p. 2613-2620, 2011, doi: 10.1016/j.enbuild.2011.05.025.
- [44] E. Lucchi, « Thermal transmittance of historical brick masonries: A comparison among standard data, analytical calculation procedures, and in situ heat flow meter measurements », Energy and Buildings, vol. 134, p. 171-184, 2017, doi: <https://doi.org/10.1016/j.enbuild.2016.10.045>.



شهادة الدكتوراه

Diplôme de Doctorat

بناء على القانون رقم 01.00 المتعلق بتنظيم التعليم العالي الصادر بتنفيذ الظهير الشريف رقم 1.00.199 من صفر 1421 (19 ماي 2000) و لاسيما المادة 3 منه؛ وعلى المرسوم رقم 2.04.89 الصادر في 18 من ربيع الآخر 1425 (7 يونيو 2004) بتحديد اختصاص المؤسسات الجامعية وأسلك الدراسات العليا وكذا الشهادات الوطنية المطابقة، كما وقع تغييره وتميمه، ولاسيما المادتين 8 و 9 منه؛ وعلى قرار وزير التربية الوطنية والتعليم العالي وتكون الأطر و البحث العلمي رقم 1371.07 الصادر في 22 رمضان 1429 (23 سبتمبر 2008) بالصادقة على دفتر الضوابط البيداغوجية الوطنية لسلك الدكتوراه. وبعد الاطلاع على محضر لجنة المناقشة بتاريخ 19 نونبر 2020

Nom et Prénom : **M'SAOURI EL BAT Adnane**

CNI N° : K487001

الطاقة الوطنية للتعريف:

رقم التسجيل: 1129687914

1993/10/01 : فی

المزداد(ة) بـ طنجة

A obtenu le **Doctorat en Sciences et Techniques**

Spécialité :

١٢٣

أحرز(ت) على الدكتوراه في العلوم والتكنولوجيات

مركز دراسات الدكتوراه: علوم وتقنيات المهندس

عنوان الأطروحة:

Titre de la thèse :

Energétique du Bâtiment

ent *as*

« Développement d'un modèle pour l'étude de l'impact du microclimat urbain sur les performances énergétiques des bâtiments : cas des rues canyons et des cours intérieures»

Mention : Très Honorable

حرر بطلان في 11-03-2021

أسماء أعضاء لجنة المذكرة وذريتهم العلمية

Président : Pr. EZBAKHE H.

Examiners : M^s. BOZONNET

Raporteuri : Prs. KUZNICKI, EL HARROUNI, KOMANTZ, BRAOUYA.

Rappel : AS : M. KOENIG, LE HAROUNI, LE BOUARDIA.

UAE 0023967

*تسلم هذه الشهادة في أصل واحد، ويمكن عند الحاجة استخراج نسخ والمصادقة عليها من طرف السلطات المختصة

**SOUTENANCE DE THESE DE
 DOCTORAT EN SCIENCES ET TECHNIQUES**

Discipline : Génie Civil
 Spécialité : Energétique du Bâtiment

CED : « Sciences et Techniques de l'Ingénieur »

Prénom et Nom de candidat : **M'SAOURI EL BAT ADNANE**

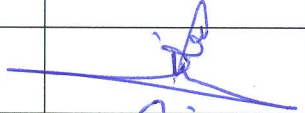
Date et lieu de naissance : **01/10/1993 à Tanger**

Date de 1^{ère} inscription : **2016-2017**

Date de transfert d'inscription :

Date de la soutenance : **17 décembre 2020**

Titre de la Thèse : « Développement d'un modèle pour l'étude de l'impact du microclimat urbain sur les performances énergétiques des bâtiments : cas des rues canyons et des cours intérieures ».

<i>Membres du jury</i>	<i>Signatures</i>
Pr. Hassan Ezbakhe, U.A.E. -Tétouan-,	<u>Président</u> 
Pr. Frédéric Kuznik, CETHIL -Lyon-, France	<u>Rapporteur</u> Par visioconférence
Pr. Khalid El Harrouni, E.N.A. -Rabat-,	<u>Rapporteur</u> Par visioconférence
Pr. Abdelmajid El Bouardi, F.S. Tétouan,	<u>Rapporteur</u> <i>Excusé</i>
Pr. Emmanuel Bozonnet, Univ. -La Rochelle-, France	<u>Examinateur</u> Par visioconférence
Pr. Adil Hafidi Alaoui, F.S.T. -Tanger-	<u>Examinateur</u> 
Pr. Ibtissam Jabrane, E.N.A. -Tétouan-,	<u>Invité</u> 
Pr. Zaid Romani, E.N.A. -Tétouan-,	<u>Co-Encadrant</u> 
Pr. Abdeslam Draoui, F.S.T. -Tanger-,	<u>Directeur de thèse</u> 

RESULTAT

MENTION



Admis

Ajourné

Honorable



Très Honorable

OBSERVATIONS

La thèse peut être déposée :



Telle qu'elle est

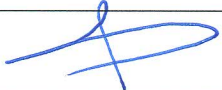
Après corrections proposées par le jury

Rapport :

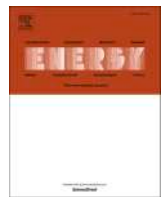
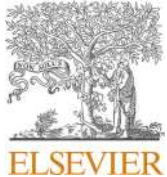
Monsieur Adnane M'SAOURI EL BAT a présenté l'essentiel de ses résultats de recherche d'une manière très claire pédagogique dans le temps qui lui a été réservé.

Il a su répondre aux différentes questions posées par les membres de jury ce qui montre sa maîtrise du sujet.

Les membres de jury considèrent le travail de recherche de Monsieur M'SAOURI EL BAT à l'unanimité, les membres de jury attribuent la titre de Docteur en Sciences et Techniques et le félicitent pour l'ensemble de son travail de recherche.

<u>Membres du jury</u>	<u>Signatures</u>
Pr. Hassan Ezbakhe, U.A.E. -Tétouan-, Président	
Pr. Frédéric Kuznik, CETHIL -Lyon-, France Rapporteur	Visioconférence
Pr. Khalid El Harrouni, E.N.A. -Rabat-, Rapporteur	Visioconférence
Pr. Abdelmajid El Bouardi, F.S. Tétouan, Rapporteur	Excusé
Pr. Emmanuel Bozonnet, Univ. -La Rochelle-, France Examinateur	Visioconférence
Pr. Adil Hafidi Alaoui, F.S.T. -Tanger- Examinateur	
Pr. Ibtissam Jabrane, E.N.A. -Tétouan-, Invité	
Pr. Zaid Romani, E.N.A. -Tétouan-, Co-Encadrant	
Pr. Abdeslam Draoui, F.S.T. -Tanger-, Directeur de thèse	

Fait à Tanger, le 17 décembre 2020



Optimizing urban courtyard form through the coupling of outdoor zonal approach and building energy modeling

Adnane M'Saouri El Bat^{a,*}, Zaid Romani^b, Emmanuel Bozonnet^c, Abdeslam Draoui^a, Francis Allard^c

^a Team of Heat Transfer & Energetic, Faculty of Sciences and Techniques of Tangier (UAE/U10FST), Abdelmalek Essaâdi University, Morocco

^b LaRAT, National School of Architecture of Tetouan, Morocco

^c LaSIE, La Rochelle University, France

ARTICLE INFO

Keywords:

Courtyard microclimate
Zonal model
Integrated modeling
TRNSYS
Multiple regression analysis
Morphology

ABSTRACT

Urban courtyards are well known for their potential thermal performances in vernacular urban morphology. Furthermore, in a more general approach considering various cities and locations, new building uses, and climate changes, a correct courtyard design requires an accurate understanding of the complex interactions between buildings and their surroundings. This study aims to develop tools and processes to optimize the design of these urban courtyards. A microclimate model is developed and integrated in a building simulation software (TRNSYS) to evaluate the thermal microclimatic conditions of courtyard building, and their heating and cooling energy demand. A specific zonal model is developed for the local courtyard microclimate, which is coupled with a previously developed thermoradiative model. Indoor conditions are modeled by the multizone building model of TRNSYS. This methodology is used to investigate the microclimatic influence of different courtyard morphology on their thermal behavior in three different climates (hot, temperate and cold). An extended study on the impact of courtyard aspect ratios has been carried out. In order to optimize the courtyard heating and cooling energy needs, a multiple regression analysis was further used to develop the fast prediction model and then select the non-dominated solutions using pareto efficiency. The results suggest optimal morphology in order to enhance the energy performance of the courtyard, from which square shape is more advantageous in cold climates (reduced heating energy needs by approximately 48%), while the deep and less wide shape is more advantageous for hot and arid climates (reduced the cooling energy needs by about 10%). For temperate climate, the shape guaranteeing minimum energy needs and, in all seasons, is the one with less width and medium depth (allowing a reduction in energy needs of about 58%).

1. Introduction

As urban population grows, main stakeholders faces new challenges considering building energy performance [1] which are directly or indirectly influenced by urban microclimate effects, and heat islands [2]. The building architecture and its design can ensure a better ratio between energy needs and the local microclimate modification. However, the relationship between building typology and its energy demand, resulting from a complex balance between climate, morphology, technology and use, also remains to be fully understood.

Courtyard architecture is one of the two major building models known in history whose characteristics depend on the surroundings and a region's culture [3]. More than 5000 years ago, courtyards were built

in the Middle East and China as a protective mechanism against both harsh weather and unfriendly neighbors [4]. Till now, the courtyard is used worldwide, and is a traditional component of construction in Asia, Middle East, South America and specifically in Mediterranean countries [5]. This building typology is generally considered as a microclimate modifier which improves its surrounding environment's comfort conditions [6]. A detailed history of the evolution of courtyards has been presented by Taleghani et al. [7].

In the literature, courtyard typology has been the subject of several studies in the last decade, which can be classified in two categories:

- studies examining only the thermal function of the courtyards [8–13];

* Corresponding author.

E-mail address: a.msaouri@uae.ac.ma (A. M'Saouri El Bat).

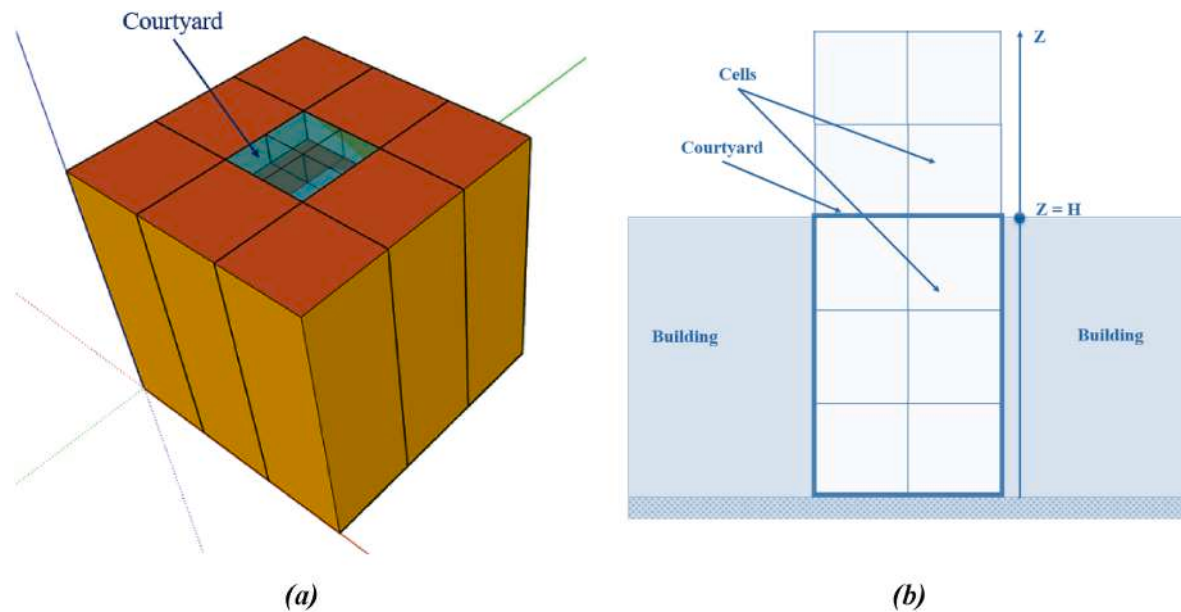


Fig. 1. Illustration of the courtyard mesh: (a) 3D view and (b) Plan view.

- and other studies that focus on microclimatic functions of courtyards [14–19].

Based on a recent review conducted by Zamani et al. [20], many papers have examined the microclimatic performance of courtyards, while very few authors investigate the coupled building and courtyard thermal performances. Most of these studies do not include an integrated approach for the simultaneous examination of indoor and outdoor thermal conditions. Actually, there is a lack of simulation tools developed for this complex interaction, since most of the existing simulation tools focus only on indoor conditions and building energy performance (e.g., the TRNSYS software which is used in the following study), or outdoor conditions often based on fluid dynamic simulations (CFD). For this specific courtyard study, a more integrated approach is considered to assess both the thermal performance of the courtyards, and the building energy performance.

At the design phase, several criteria must be considered for the optimization process of a courtyard building including the envelope cladding, the building envelope materials, the orientation and morphology of the courtyard [21]. The latter measure is the focus of the current research. In fact, the proportions of the courtyard has a significant impact on the received solar radiation and the shading areas created on the courtyard facades, thus strongly contributing to influence the building heating and cooling energy demand [7,22]. Generally, a courtyard building with inappropriate proportions or orientation will either receive too much solar radiation when it needs to be shaded, or will create too much shade when solar radiation is needed [9].

In this regard, the present study introduces a courtyard microclimate model to optimize the courtyard proportions in order to provide better indoor thermal conditions in different climates. In this model, the radiative model is based on the Gebhart factor [23] to calculate radiative exchanges and inter-reflections as well as the solar radiation distribution coefficients. A zonal model is developed to model the microclimatic phenomena generated by the courtyard, while a thermoradiative model developed and validated in a previous work [24–26] is used. The 3D courtyard geometry, the buoyancy and the external wind effects are considered. Air temperature, pressure and airflow in the courtyard are stimulated by interactively solving mass, pressure and energy balance equations. The originality of the proposed method is its capacity to model at the same time the microclimatic phenomena generated by the courtyard, and to integrate them in the building energy simulation tools

without going through the long CFD calculations often performed. To evaluate the quality of the developed method, a comparison between the obtained and the CFD results, more specifically those of ENVI-met [27], is presented. This new approach is then used to propose optimized courtyard morphologies, while their microclimate impact is analyzed through the building energy needs for three different climates (temperate, cold and hot arid).

2. Methodology

2.1. Developed numerical approach for the urban courtyard

In this research work, the TRNSYS 18 software was used for the energy simulation of buildings knowing that it does not include the modeling of the external environment. Indeed, we developed a new model adapted to TRNSYS 18 to be able to integrate the simulation of the courtyard microclimate. In this software, the transfer function method of Mitalas and Stephenson [28] is used to express heat conduction through the walls. However, there are two possibilities to model the heat transfer by convection. The first consists to set a constant value of the convective heat transfer coefficient and the second one is to use specific correlations from literature. In this study, the convective heat transfer coefficient value of building façades is assumed to be constant on the inside surfaces of the building (6.1 W/m²K for the ceiling, 1.6 W/m²K for the floor and 4.1 W/m²K for the vertical walls [29]). For the outside surfaces, the heat transfer coefficient by convection was evaluated using the Hagishima and Tanimoto correlation [30].

The modelling of ground heat transfers is based on Type 49 of TRNSYS. This component considers a three-dimensional finite differences model, which requires a mesh of the ground covered by the building (near-field) as well as the surrounding area of the building (far-field). Then, heat transfers are assessed between the ground floor or the road pavement areas (slab) and the building ground [25]. A more detailed description of this ground model is presented in Refs. [31,32]. The far-field temperature of the soil is fixed as a boundary condition at a 10 m-depth, and assessed from the Kusuda model [33].

Shortwave and longwave radiative exchanges are modeled differently for indoor and outdoor surfaces, i.e., buildings and courtyards. While the indoor radiative model of TRNSYS is used, a specific courtyard model was developed in a previous studies [24–26]. In this approach, the radiative model is based on the Gebhart factor [23] to calculate

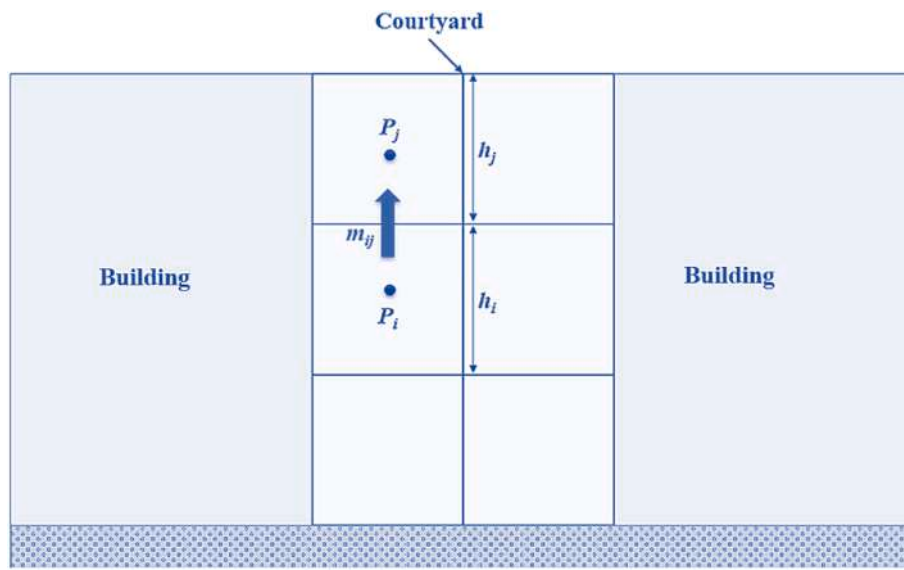


Fig. 2. Scheme representing the mass flow through the horizontal opening.

radiative exchanges and inter-reflections as well as the solar irradiance distribution coefficients. More details and experimental validations about this approach are reported in previous studies [24–26].

In order to model the microclimatic phenomena generated by the courtyard a zonal model is developed. The courtyard volume is meshed into interconnected sub-volumes called cells (Fig. 1). Each air cell is homogeneous, i.e., uniform state variables (temperature, density, pollutant concentration). The vertical division of the volume allows to account for the vertical temperature distribution within the courtyard. In each cell, the mass and energy balance equations as well as the fluid state equation (the ideal gas law) are used to calculate the air temperature and pressure variations (to obtain the mass flow rate).

To calculate the mass flow rate \dot{m}_{ij} between two adjacent cells i and j , it is necessary to determine the relationship between the mass flow rate and the pressure difference. For different conditions, the relationships can be expressed by different formulas. However, the TRNSYS 18 software does not allow to determine the airflow between cells and therefore it must be coupled with another program or software. In our case, we have coupled TRNSYS 18 with a code that we have developed using Python language. The originality of the method used lies in its capacity

to model the microclimatic phenomena generated by the courtyard, in order to take them into account in a dynamic thermal simulation software for building. The mathematical formulation of the equations introduced in the latter is detailed as follows, where the mass flow rates are calculated for horizontal and vertical opening respectively.

- For **horizontal openings** (airflow due to wind only):

The hydrostatic pressure (ΔP_{ij}) variation between two horizontally connected cells is expressed by Refs. [34–38]:

$$\Delta P_{ji} = P_j - P_i - \frac{1}{2}g(\rho_i h_i + \rho_j h_j) \quad (1)$$

where P , ρ et h are respectively the pressure, air density and overall height of the cell, j is the upper cell, i is the bottom one and g is the gravitational acceleration [m/s^2].

Thus, the mass flow rate across the horizontal opening can be expressed as (Fig. 2):

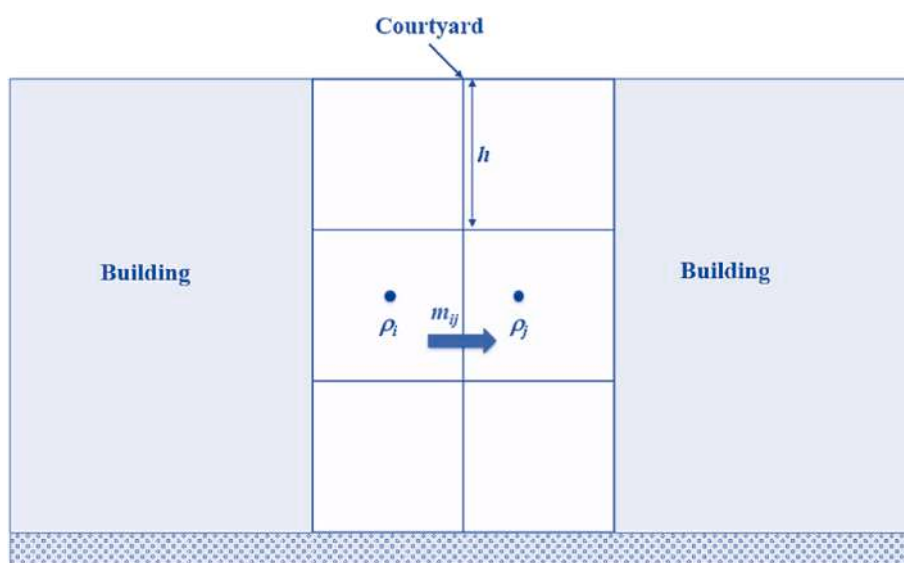


Fig. 3. Scheme representing the mass flow through the vertical opening.

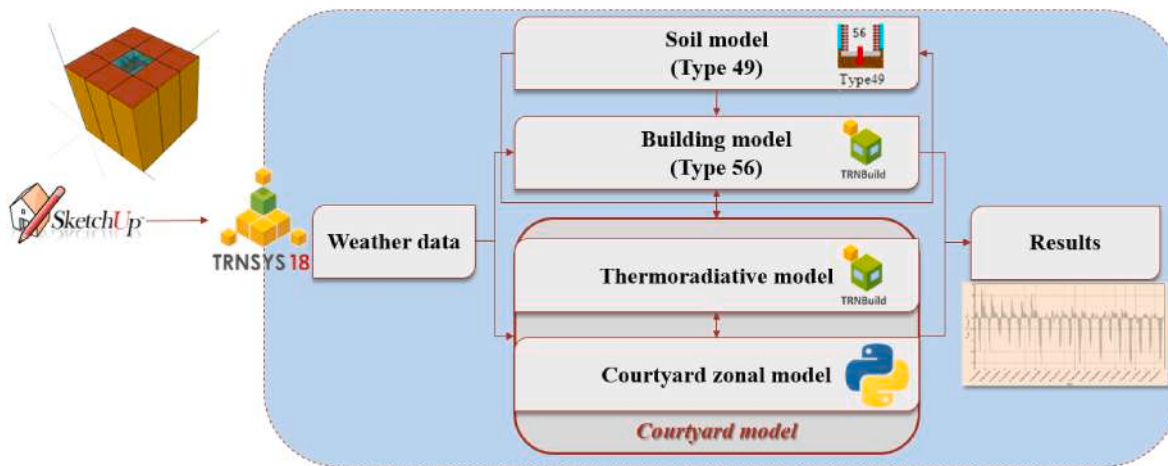


Fig. 4. Scheme of the developed zonal model.

- If $\Delta P_{ij} > 0$:

$$\begin{cases} \dot{m}_{ij} = 0 \\ \dot{m}_{ij} = \mu A \sqrt{2\rho_i |\Delta P_{ji}|} \end{cases} \quad (2)$$

- If $\Delta P_{ij} < 0$:

$$\begin{cases} \dot{m}_{ij} = \mu A \sqrt{2\rho_i |\Delta P_{ji}|} \\ \dot{m}_{ij} = 0 \end{cases} \quad (3)$$

where μ and A are respectively the discharge coefficient and the area of the opening [m^2]. The discharge coefficient depends on the opening Reynold number, wind incidence angle and direction of air flow, size and shape of the opening [39,40].

- For **vertical openings** (Airflow due to the stack effect):

For vertical openings between cells (Fig. 3), when there is temperature difference on both sides of the opening, this difference will result in an air density difference, with a positive pressure difference at the top of the opening and a negative pressure difference at the bottom (or vice-versa). There may be air flow as a function of the position of the neutral level. At neutral level, the air velocity is zero, which can be determined by using equation (4) below.

$$Z_n = \frac{\Delta P}{(\rho_i - \rho_j)g} \quad (4)$$

where Z_n is the neutral level [m] and ΔP is the pressure difference between cells [Pa].

The position of the neutral level depends on different conditions, so it can be distinguished in three situations (reference):

- 1) When $0 < Z_n < h$, the neutral level is within the opening. The mass flow rate at the opening can be determined by:

$$\dot{m}_{ij} = \frac{2}{3} \mu W \sqrt{2g\rho_i |\rho_i - \rho_j|} (h - Z_n)^{\frac{3}{2}} \quad (5)$$

$$\dot{m}_{ij} = \frac{2}{3} \mu W \sqrt{2g\rho_j |\rho_i - \rho_j|} (Z_n)^{\frac{3}{2}} \quad (6)$$

- 2) When $Z_n \leq 0$, the neutral level is under the opening. The mass flow rate can be determined by:

$$\dot{m}_{ij} = \frac{2}{3} \mu W \sqrt{2g\rho_i |\rho_i - \rho_j|} [(h - Z_n)^{\frac{3}{2}} - (Z_n)^{\frac{3}{2}}] \quad (7)$$

$$\dot{m}_{ij} = 0 \quad (8)$$

3) When $Z_n \geq h$, the neutral level is above the opening. The mass flow rate can be calculated by:

$$\dot{m}_{ij} = 0 \quad (9)$$

$$\dot{m}_{ij} = \frac{2}{3} \mu W \sqrt{2g\rho_j |\rho_i - \rho_j|} [(Z_n)^{\frac{3}{2}} - (Z_n - h)^{\frac{3}{2}}] \quad (10)$$

where h is the overall height of the vertical opening [m] et W is the width of the opening [m].

- Boundary conditions:

The wind speed and direction will affect the wind pressure around the simulation domain. For this reason, based on the Nicholson model [41], the following relations are obtained to calculate the components of the wind speed (u_i, u_j, u_k) beyond the courtyard ($z \geq H$).

$$u_i = \frac{u_i^*}{k} \ln \left(\frac{z + d + z_0}{Z_0} \right) \quad (11)$$

$$u_j = \frac{u_j^*}{k} \ln \left(\frac{z + d + z_0}{Z_0} \right) \quad (12)$$

$$u_k = \frac{u_k^*}{k} \ln \left(\frac{z + d + z_0}{z_0} \right) \quad (13)$$

where u^* is the friction velocity, $k = 0,4$ is von Karman's constant, d is the displacement length and z_0 is the roughness length of the urban canopy considered.

The flow rates found by the above equations must satisfy the principle of mass conservation (equation (14)) for each cell i . The summation in equation (14) is carried out over all cells adjacent to cell i :

$$\sum_{k=0}^n \dot{m}_{ij} = 0 \quad (14)$$

By replacing of the densities of each cell using the ideal gas law ($\rho_i = \frac{P_i}{RT_i}$), we obtain a system of N equations whose unknowns are the temperatures T_i and the pressures P_i . The solution of the system of these coupled nonlinear algebraic equations is obtained with the method of

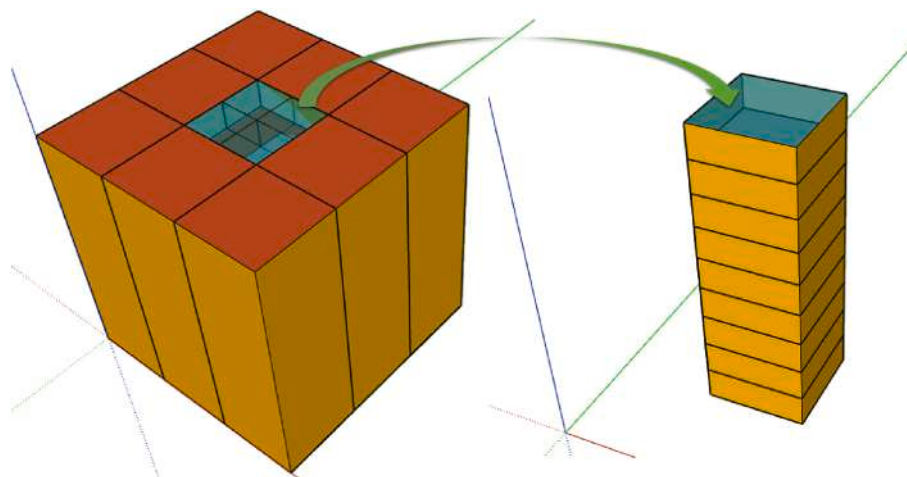


Fig. 5. TRNSYS 3D modeling of the courtyard building.

Newton-Raphson. During the simulation, multizone building model of TRNSYS (TRNBuild) takes the airflow rates calculated by Python and returns the air temperature of each zone. Fig. 4 below illustrates the different steps of these calculations.

2.2. ENVI-met software – a detailed reference model for the courtyard

In order to evaluate the accuracy of the developed zonal model and its applicability to a courtyard as well as its ability to correctly predict the temperatures of the air and the surfaces located in the courtyard, a comparison was made between the results obtained using this model and those obtained by the CFD simulations, precisely by the ENVI-met software [27].

ENVI-met is a three-dimensional model-based software for the simulation of surface-plant-air interactions, commonly used to simulate urban environments [42]. It includes a full 3D computational fluid dynamics model to solve the Reynolds-averaged non-hydrostatic Navier-Stokes equations for each grid in space and for each time step [42]. Typically, it has a horizontal resolution of 0.5–5 m and a time frame of 24–48 h with a time step of 1–5 s. This resolution allows for the analysis of small-scale interactions between individual buildings, surfaces, and plants [43]. About turbulence, is simulated in ENVI-met using a turbulence closure model of order 1.5 [42]. In addition, based on the work of Mellor and Yamada [44], two additional prognostic variables, the local turbulence (E) and its dissipation rate (ϵ) are added to the model.

The main input parameters required to perform ENVI-met simulations include meteorological data, features and properties of ground surfaces, vegetation and buildings, initial soil moisture and temperature profiles [45]. However, some limits exist when it comes to defining the initial conditions for the calculation. Most of all, the wind speed and direction must be constant during the simulation, and the same occurs with the cloudiness rate, unlike the air temperature and humidity which can be modified throughout the day [15]. A more detailed description of the microscale model ENVI-met is presented in Refs. [27,42].

2.3. Description of the case study: zonal and detailed meshing

To assess reliability and relevance of the developed model to simulate the thermal and the microclimate performance of the courtyards, a comparative study between the results obtained with this model and those obtained with the ENVI-met software was performed. To achieve this, a full-scale model of a courtyard building was simulated. This building, with a simple geometry, has a total area of 81 m² (9 m wide and 9 m long) and a height of 9 m, 11.2% of this area is occupied by a square-shaped courtyard (Fig. 5) which is vertically divided into nine

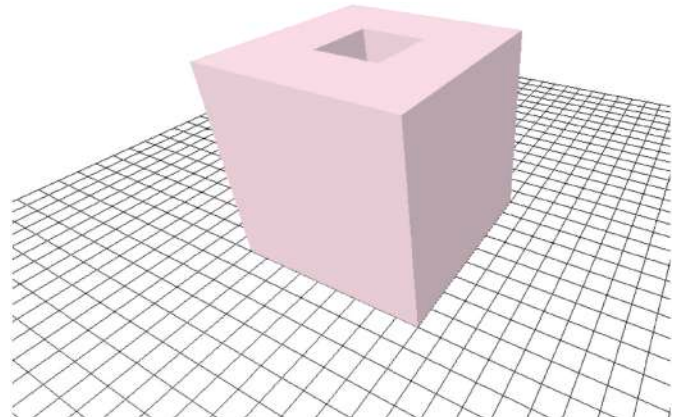


Fig. 6. Modeling of the courtyard building using ENVI-met.

Table 1
Thermophysical properties of building and soil materials.

Materials	Thickness [m]	α_s	ϵ	λ [W/m ² .K]	ρ [Kg/m ³]	C_p [J/Kg.K]
Concrete	0.2	0.36	0.9	2,36	2150	915
Roadway	0.1	0.64	0.9	2,36	2150	915

Table 2
Windows characteristics.

Envelope element	Material	U-value [W/m ² .K]	g-value	ϵ
Windows	Glass	1.4	0.6	0.84

zones (Fig. 5). Concerning the openings, the window surface represents 25% of the total surface of the walls constituting the courtyard. The number of zones has been chosen based on the one used for the modeling by the ENVI-met software (Fig. 6).

Table 1 presents the thermophysical properties of the building materials used in this study, while the features of the glazing used are shown in Table 2 below.

Where α_s is the solar absorption coefficient, ϵ is the thermal emissivity (longwaves), λ is the thermal conductivity, ρ is the density and C_p is the heat capacity.

The simulation was carried out for 24 h considering the weather conditions of the city Tangier in the north west of Morocco by using the

Table 3
Specifications of the simulated models related to the studied zone.

Hottest summer day (July 22)	
Wind speed [m/s] (avg)	1.83
Wind speed (North = 0) (avg)	111.04°
Air temperature (max/min)	37.2 °C/23.4 °C
Relative Humidity (max/min)	92%/38%
Size and grid adopted for ENVI-met [m]	X_grid = 50; Y_grid = 50; Z_grid = 30; dx = 1; dy = 1; dz = 1

TMY2 meteorological data file. It should be noted that TMY2 are databases containing hourly values of solar radiation and meteorological elements such as air temperature, humidity and wind velocity. Given the typical year (TMY) for this location with hot and humid summers, the hottest day (July 22) was selected for the study. Table 3 below shows the simulation parameters used for the case studied.

3. Comparison between courtyard air temperatures from the developed zonal model and the reference model

Fig. 7 illustrates the comparison between the daily evolution of mean courtyard air temperatures (mean cell temperature at each level) obtained by developed model (blue), and the reference ENVI-met, at different heights. We can see that the variations of courtyard air temperature simulated by the proposed model follow the same trend as those obtained by ENVI-met.

Based on the correlation analysis, it can be stated that the temperatures obtained by our model are consistent at each altitude with those calculated using ENVI-met. In this case, the mean absolute error is about

0.61 °C, the mean relative error is about 3.37% and the mean square error is about 0.64 °C. The regression coefficient R^2 is 0.99 (Fig. 8).

Similarly, to the air temperatures, a comparative study was conducted between the daily evolution of mean courtyard surface temperatures obtained by developed model, and the reference ENVI-met (Fig. 9). In this case, the mean absolute error is 0.79 °C and the mean relative error reaches 4.19% and the mean square error is about 1.09 °C. The regression coefficient R^2 is 0.99 (Fig. 10).

From this comparative study, the developed zonal model and ENVI-met provide very similar results, and consistent spatial and temporal courtyard air temperature evolutions. This numerical benchmark allows us to consider the use of this developed zonal model, given its increased calculation speed gain (reducing the calculation time by 80% compared to CFD), and its extended capabilities due to the coupled building model. It should be noted that, based on previous work [24,46], the negligence of microclimate generated by the courtyard has the effect of overestimating the building energy needs by 26%.

4. Parametric study of courtyard morphology

4.1. Presentation of the courtyard morphology variations

The courtyard morphologies have been defined by two ratios R_1 and R_2 (Fig. 11):

- $R_1 = P/H$, where P is the perimeter of the ground of the courtyard, and H the height of the building; this ratio varies from 1 to 10.
- $R_2 = W/L$, where W is the width of the courtyard, and L is the length; this ratio varies from 0.1 to 1.

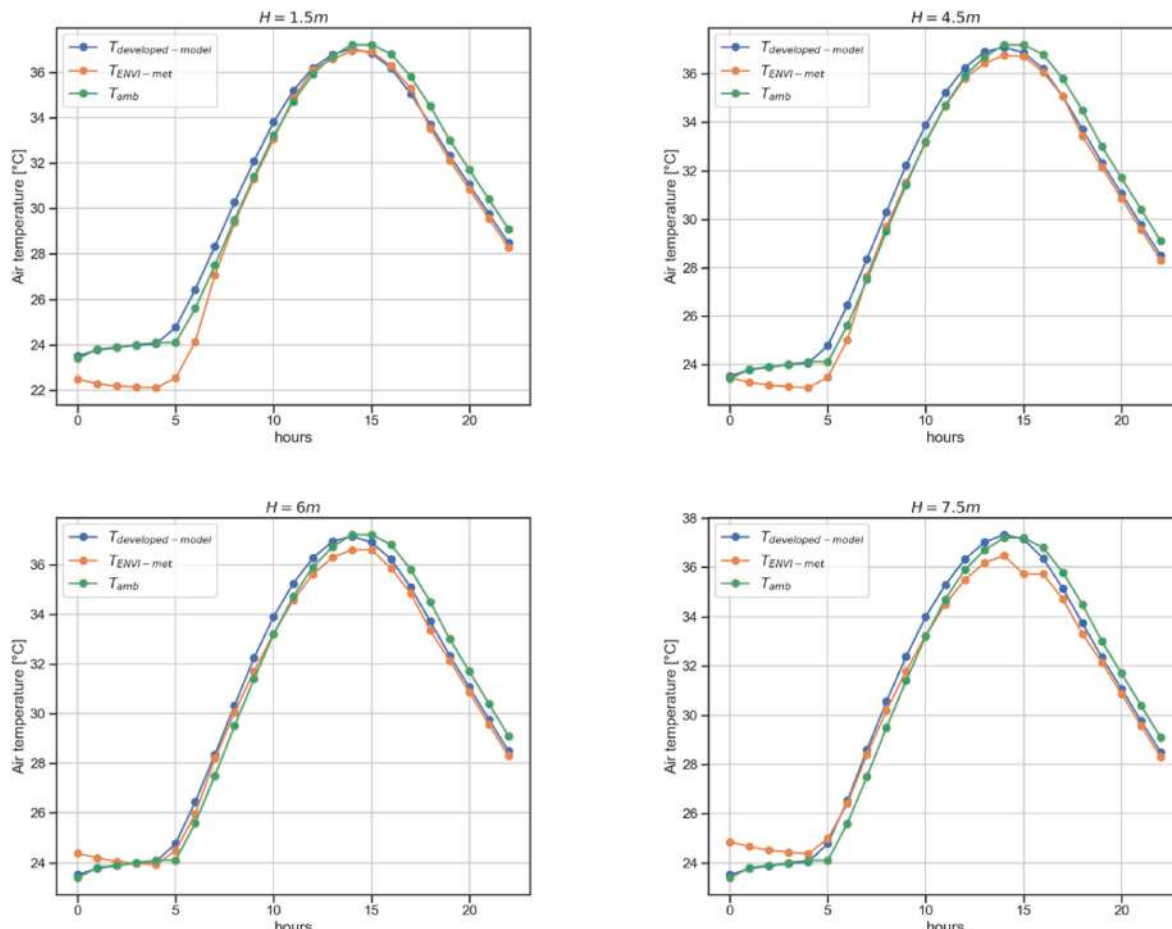


Fig. 7. Temporal variation of mean courtyard air temperature as a function of height.

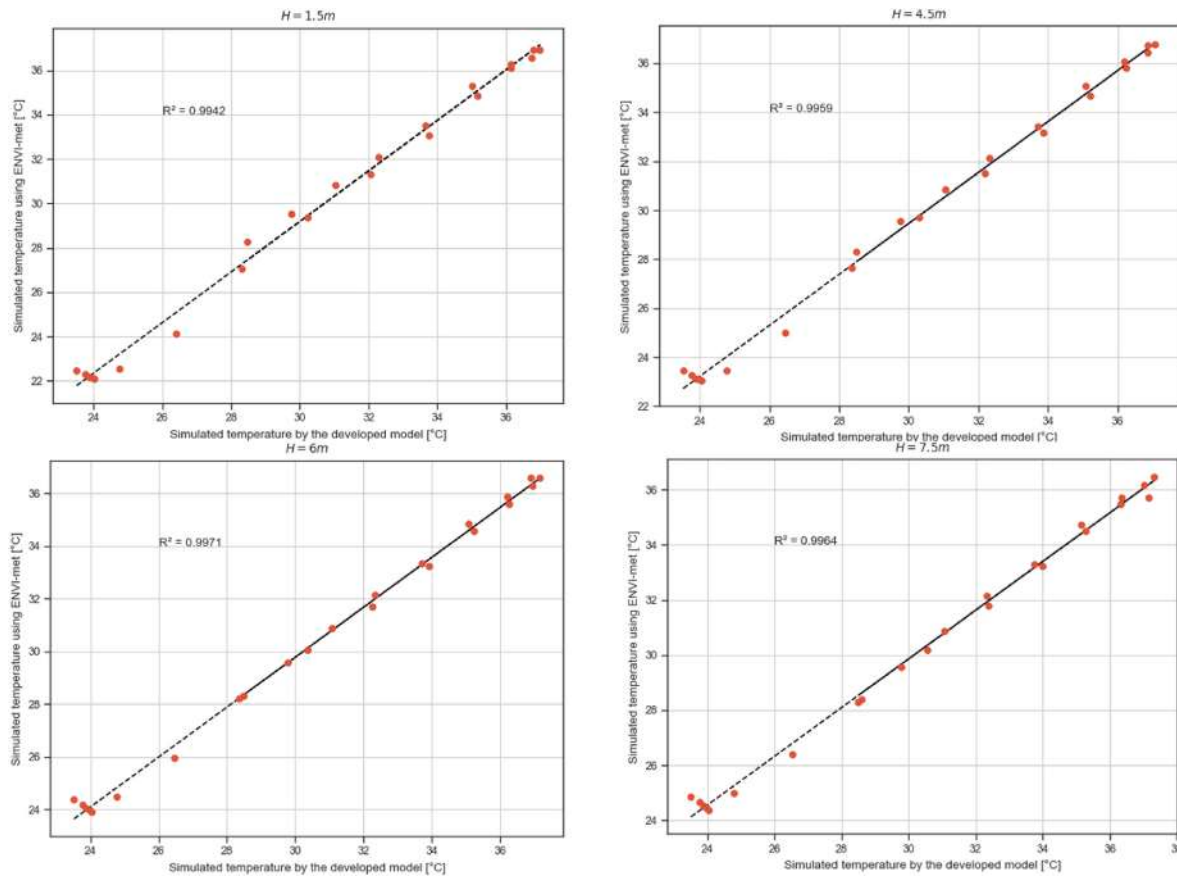


Fig. 8. Comparison of the air temperature simulated by the developed model and that simulated by ENVI-met.

The building's interior space, which forms the courtyard, is symmetrically distributed around the North-South and East-West axes of this courtyard.

In this study, the courtyard's minimum width was assumed to be 1 m. This implies that for an R_2 ratio equal to 0.1, the width of courtyard is 1 m and its length is 10 m. For an R_1 ratio equal to 1, the height of courtyard is 22 m. This courtyard, whose dimensions and proportions are identical to those previously defined ($W = 1$ m, $L = 10$ m, and $H = 22$ m), was considered as the reference configuration with a total living area of 500 m². The window surface, it represents 25% of the total surface of the walls constituting the courtyard.

As the courtyard walls are more directly affected by these ratio variations, the wall surface was taken as a reference for comparing the thermal behavior of the different courtyards. All shapes studied have the same surface area of walls and glazing as the reference shape, regardless of the shape's proportions. Additionally, the external façades and the roofs are totally opaque, i.e., the thermal performance of the building is only influenced by the windows inside the courtyard (Fig. 12).

Table 4 gives the features of the opaque and transparent element of the courtyard buildings envelope studied.

Where λ is the thermal conductivity, C_p is the heat capacity and ρ is the density.

The following Table 5 shows the glazing characteristics used.

During the modelling, the internal gains due to the lighting system, electrical appliances, users and occupancy schedules are set according to residential use, as described in reference [47]. The gains shown in Table 6 are related to the total floor area. The presence of users is considered for 24 h per day. The usage schedule for the electrical appliances is set "on" from 8:00 a.m. to 12:00 p.m., while the usage schedule for the lights is set "on" from 5:00 p.m. to 12:00 a.m.

As shown in Fig.13, courtyards are distributed in many regions of the

world, in different climates and in different civilizations. Therefore, to further this study and to better understand the impact of the climatic conditions on the different regions where the courtyard is located, three climate conditions were chosen: temperate climate, cold climate and hot arid climate. This choice is justified by Köppen's classification which shows that the regions where the courtyard is located are characterized by the selected climates.

In this view, the temperate climate is represented by the city of Tangier (North West Morocco), the cold climate is represented by the city of Kunming (China) and the hot arid climate is represented by the city of Riyadh (Saudi Arabia); which are illustrated in Figures , Figs. 14, 15 and 16 respectively. These data are from the software Meteonorm [48] and they are used as input for the building energy simulation.

4.2. Effect of courtyard proportions on heating and cooling energy needs

The effect of varying the ratios R_1 and R_2 on the heating and cooling energy needs is shown in Figures , Figs. 17, 18 and 19. It is noticeable that with the increase of the ratio R_2 , and independently of the climates considered, at the approach of the square shaped courtyard, the cooling demand increases progressively for all values of the ratio R_1 (Fig. 17-a and Fig. 18-a). Also, it can be noted that the cooling demand increases proportionally to the depth of the courtyard in both cold and temperate climates, whereas it is the opposite in hot arid climate (Fig. 19-a).

In the case where the ration R_1 is equals to 1 or 2, we remark that the increase of the ratio R_2 has almost any effect on the heating energy needs. However, the heating demand increases significantly with the increase of R_1 , especially when its value increases from 1 to 4 (Fig. 17-b, Fig. 18-b and Fig. 19-b). Thus, independently of R_2 value, any increase of R_1 beyond 4 has insignificant influence on the heating energy needs. Moreover, as R_2 increases, the heating energy needs decreases up to a

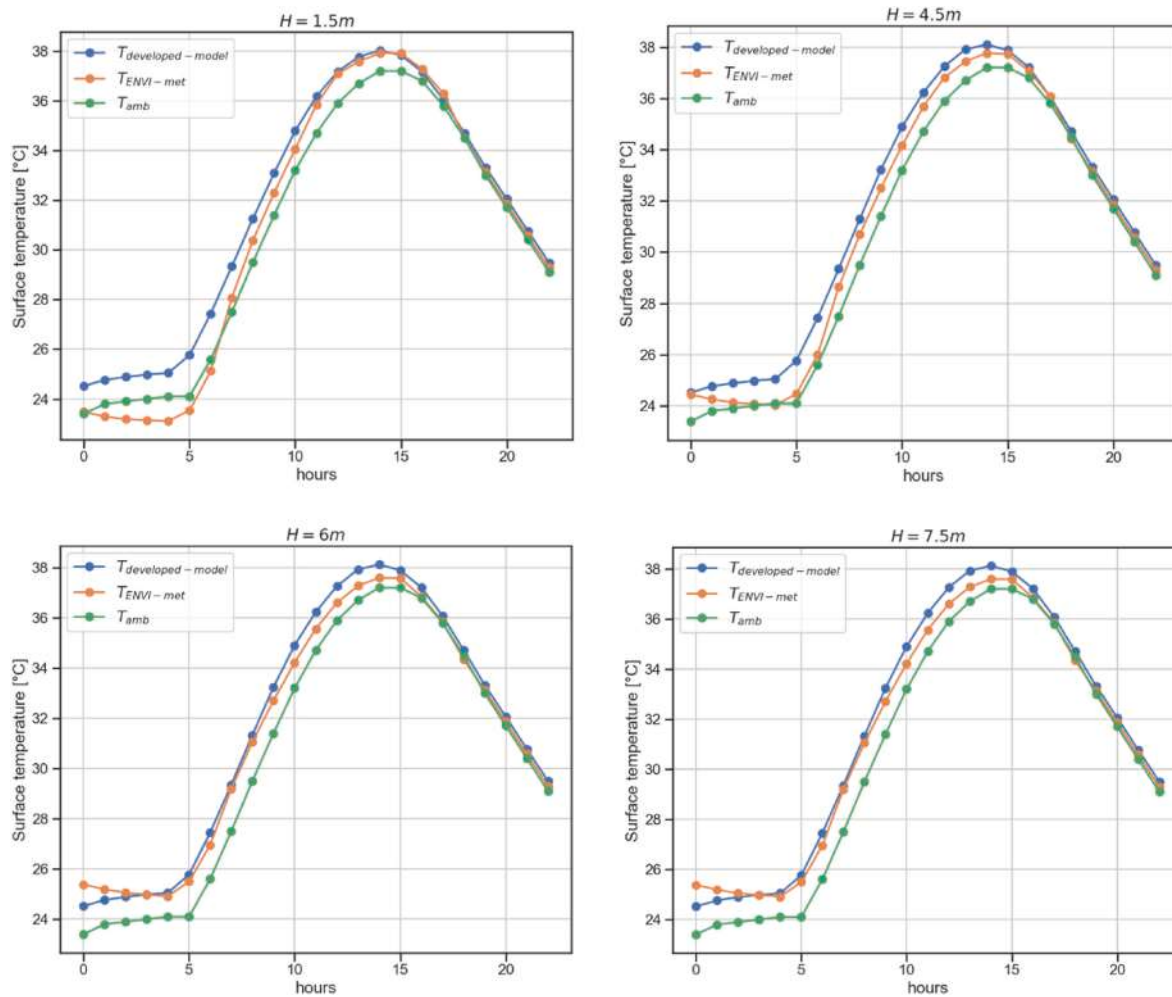


Fig. 9. Temporal variation of mean courtyard surface temperature as a function of height.

value of $R_1 = 5$, where any increase in this case has an insignificant influence on the heating energy needs of courtyard building.

Increasing the ratio R_1 from 1 to 10 results in an average increase in cooling energy needs for a temperate climate of $43 \text{ kWh/m}^2\text{year}$, regardless of the R_2 value, for a cold climate of $19 \text{ kWh/m}^2\text{year}$, and a decrease of $55 \text{ kWh/m}^2\text{year}$ for a hot arid climate. The average increase in cooling energy needs due to a change in R_2 from 0.1 to 1, for any R_1 value, is about $15 \text{ kWh/m}^2\text{year}$ for a temperate climate, $1.2 \text{ kWh/m}^2\text{year}$ for a cold climate, and $23 \text{ kWh/m}^2\text{Year}$ for a hot arid climate.

As to the cooling energy needs, the average decrease in heating energy needs, which can result from a change of R_1 from 1 to 10, independent of the R_2 value, is about $61 \text{ kWh/m}^2\text{year}$ in the case of a temperate climate, $97 \text{ kWh/m}^2\text{year}$ in the case of a cold climate and $22 \text{ kWh/m}^2\text{year}$ in the case of a hot arid climate. Alternatively, raising R_2 from 0.1 to 1, only reduces the heating energy needs, independently of the R_1 value, by $12 \text{ kWh/m}^2\text{year}$ in the case of a temperate climate, by $15 \text{ kWh/m}^2\text{year}$ in the case of a cold climate and by $5 \text{ kWh/m}^2\text{Year}$ in the case of a hot arid climate.

Based on this analysis, reaching an optimal proportion choice while keeping a well-balanced between courtyard building heating and cooling energy needs may be difficult. Indeed, the deep and elongated courtyard building constitutes the most efficient solution to reduce the cooling energy needs in both cold and temperate climates, while the courtyard building with R_1 ratio higher than 4 are rather recommended as a solution to reduce the heating energy needs during the winter season for all climates considered in this study. Furthermore, a change in the courtyard lengthening has only a modest effect on heating energy

needs. This highlights the possibility of adapting the depth of building courtyard, especially since the lengthening of the courtyard has a small influence on the heating energy needs.

4.3. Abacus to assess the impact of the courtyard's proportions

In order to determine the optimal courtyard proportions relative to the minimum heating and cooling energy needs in all seasons, the annual energy needs for the various configurations studied and for the different climates considered is presented in the abacus following (Figs. 20, 21 and 22).

In this context, the maximum energy needs for the temperate climate is found when R_1 is equal to 1 (Fig. 20). However, a decrease in energy needs is more pronounced when R_1 ranges from 1 to 5, while it is gradually increased when R_1 reaches 10. In summary, the maximum energy need is reached with R_1 equal to 1 and R_2 equal to 0.1 (deep form). That is due to the reduced quantity of irradiation received in winter by this form, which leads to a low heat gain and consequently to higher heating energy needs. Effectively, the solar radiation received by the surfaces composing the courtyard building significantly affects the resulting heat gains and, consequently, the energy requirements for cooling and heating. However, the minimum energy need corresponds to a R_1 value comprised between 3 and 6.

For the cold climate case, Fig. 21, for any value of R_1 , the total energy needs decrease as the courtyard shape gets closer to the square (increase of R_2). This decrease in energy demand is more marked when R_1 has a value greater than 5. Generally, the maximum energy need is obtained

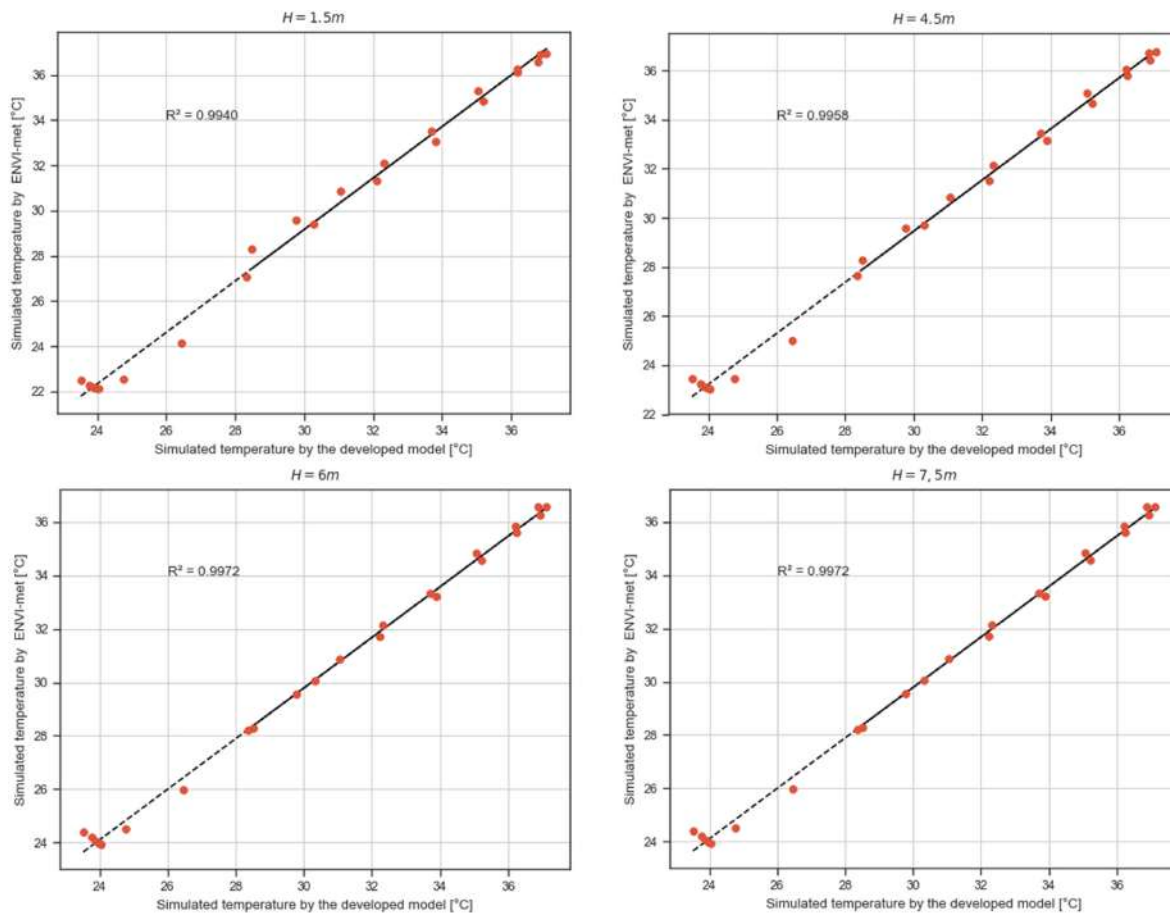


Fig. 10. Comparison of the surface temperature simulated by the developed model and that simulated by ENVI-met.

when R_2 is equal to 0.1 (deep form). It is because the solar radiation received by the surfaces composing the courtyard building considerably affects the resulting heat gains and, consequently, the cooling and heating energy requirements. As opposed to this, the minimum energy demand corresponds to a value of R_2 equal to 1 (square shape). This is due to the quantity of irradiation received, which results in the reduction of heat loss in winter and thus the heating energy needs.

When considering the case of the hot arid climate, Fig. 22, the optimal solutions, i.e. those where the total energy needs are minimal, correspond to the values of R_1 greater than 3 with R_2 being between 0.1 and 0.2. In contrast, the maximum needs correspond to a R_1 lower than 3 independently of R_2 .

Based on these results, it should be noted that in practice the suggestion of a R_1 and R_2 ratio that allows for an optimal shading area on the walls during the summer while obtaining an optimal sunlight area in the winter is difficult, as these ratios cannot always be achieved in real situations [11]. From this, a perspective was deduced, which aims to determine a range of courtyard proportions that minimize the total energy needs. As a result, it is possible to approach a more optimal courtyard design for each climate considered in this work. In this way, it becomes possible to design a courtyard with a large range of proportions without significantly affecting its annual energy needs. However, optimizing courtyard proportions to provide better indoor thermal conditions in different climates remains a necessity to guide engineers, architects and designers in designing courtyards with high energy efficiency while maintaining optimal comfort levels during summer and winter. Indeed, an optimization of the R_1 and R_2 ratios is necessary to obtain the optimal energy performance of the courtyards.

5. Optimization of courtyard morphology

5.1. Multiple regression model for fast prediction of courtyard heating and cooling energy needs

5.1.1. Multiple regression analysis

In order to optimize the courtyard morphology and then get the minimum of heating and cooling energy needs, we used multiple regression analysis to run a fast parametric study and pareto front. This method, is widely used to estimate the relationships among different sets of variables allowing to determine both interpolation and extrapolation trends [49]. It could be an easier and more practical solution to various problems compared to neural networks [50]. The objective of this approach is to find an appropriate mathematical model to approximate the response Y (heating and cooling energy needs) through a set of independent variables X_i (R_1 and R_2 ratios used as inputs in the function) and to determine the best fitting coefficients of the model from the given data. In this study, the developed regression model for predicting the heating and cooling has the following form:

$$Y = f(R, \beta) \quad (15)$$

where:

Y is the predicted heating or cooling energy needs;

$R = (R_1, R_2)$ is the input parameters;

$\beta = (\beta_1, \beta_2, \dots, \beta_n)$ is the corresponding regression coefficient.

To this end, regression models were developed to predict courtyard heating and cooling energy needs, which are expressed in the following equations for each climate.

For temperate and hot arid climate:

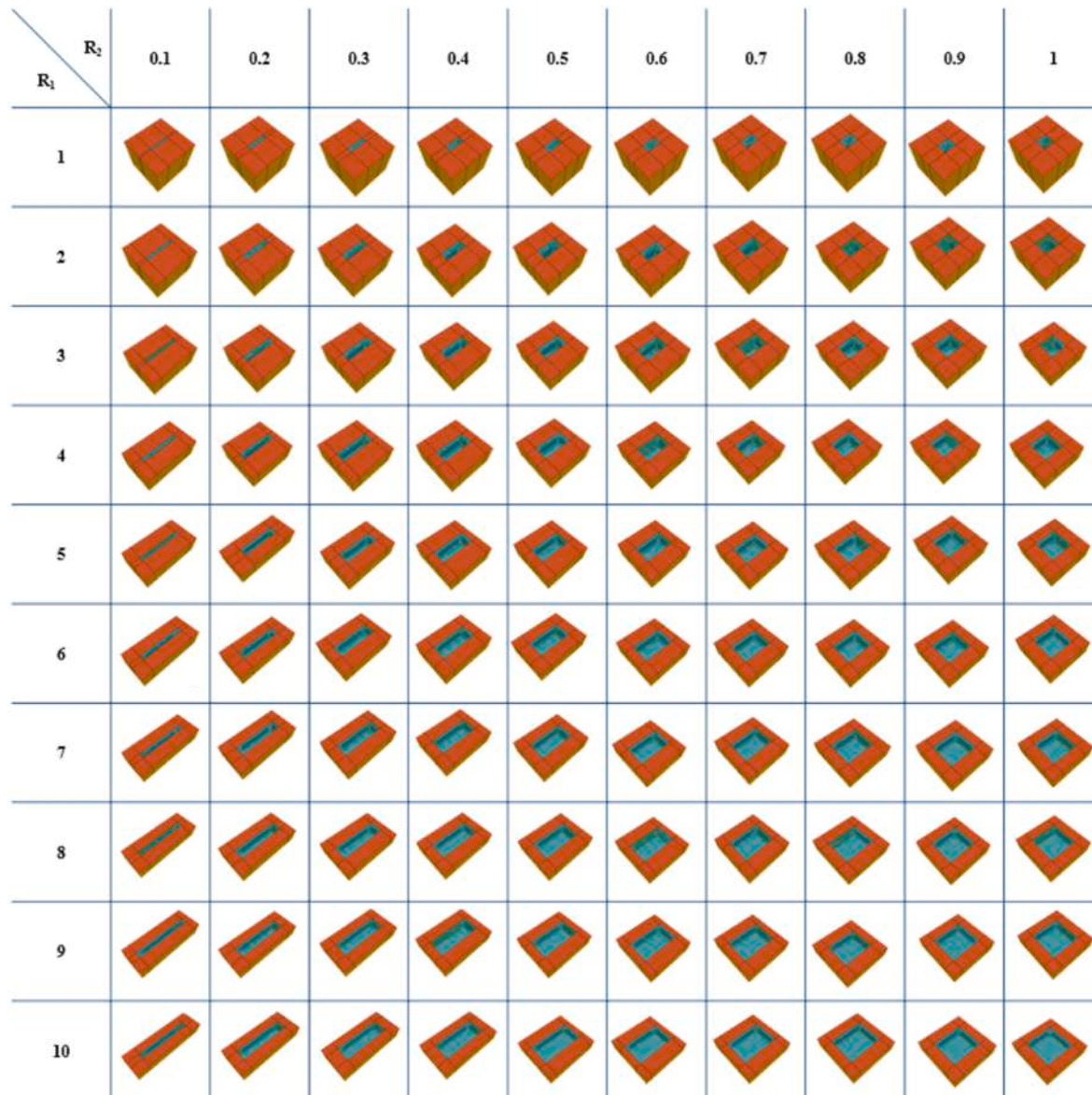


Fig. 11. Presentation of the different courtyard morphologies studied.

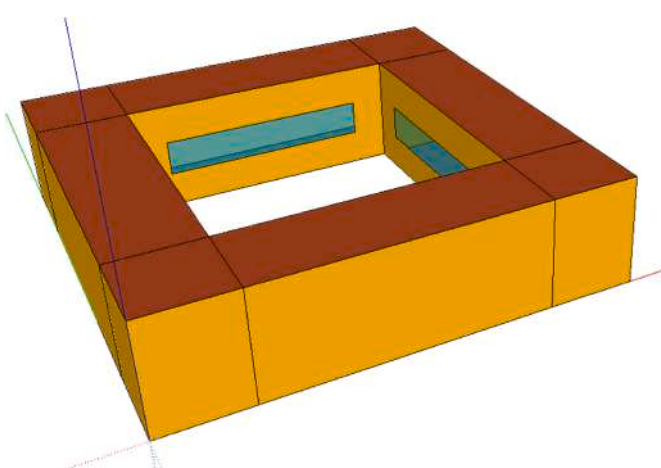


Fig. 12. Overview 3 d of the courtyard building with $R_1 = 10$ and $R_2 = 1$.

5.1.1.1. Heating energy needs

$$Y = \beta_1 + \frac{\beta_2}{R_1} + \frac{\beta_3}{R_2} + \frac{\beta_4}{R_1^2} + \frac{\beta_5}{R_2^2} + \frac{\beta_6}{R_1 R_2} + \frac{\beta_7}{R_1^3} + \frac{\beta_8}{R_2^3} + \frac{\beta_9}{R_1 R_2^2} + \frac{\beta_{10}}{R_1^2 R_2} \quad (16)$$

5.1.1.2. Cooling energy needs

$$Y = \beta_1 + \frac{\beta_2}{R_1} + \frac{\beta_3}{\ln R_2} + \frac{\beta_4}{R_1^2} + \frac{\beta_5}{(\ln R_2)^2} + \frac{\beta_6}{R_1 \ln R_2} + \frac{\beta_7}{R_1^3} + \frac{\beta_8}{(\ln R_2)^3} + \frac{\beta_9}{R_1 (\ln R_2)^2} + \frac{\beta_{10}}{R_1^2 (\ln R_2)} \quad (17)$$

For cold climate:

5.1.1.3. Heating energy needs

$$Y = \beta_1 + \frac{\beta_2}{R_1} + \frac{\beta_3}{R_2} + \frac{\beta_4}{R_1^2} + \frac{\beta_5}{R_2^2} + \frac{\beta_6}{R_1 R_2} + \frac{\beta_7}{R_1^3} + \frac{\beta_8}{R_2^3} + \frac{\beta_9}{R_1 R_2^2} + \frac{\beta_{10}}{R_1^2 R_2} \quad (18)$$

5.1.1.4. Cooling energy needs

Table 4
Thermophysical properties of construction envelope elements.

Envelope element	Materials	Thickness [cm]	λ [W/m ² .K]	C_p [J/Kg.K]	ρ [Kg/m ³]
Outside Wall	Cement	1.5	1.15	1000	1700
	Brick	7	0.3	741	1200
	Air gap	10	*	1000	1.25
	Brick	7	0.3	741	1200
Adjacent Wall	Cement	1.5	1.15	1000	1700
	Cement	1.5	1.15	1000	1700
	Brick	7	0.3	741	1200
Roof and ceiling	Cement	1.5	1.15	1000	1700
	Tile	0.7	1.4	1000	2500
	Screed	5	0.42	1000	1800
	Concrete	4	2.36	1000	2350
	hollow block	16	0.6	880	1000
Ground floor	Cement	1.5	1.15	1000	1700
	Tile	0.7	1.4	1000	2500
	Screed	5	0.42	1000	1800
Pavement	Concrete	20	2.5	1000	2350
	Ceramics	0.7	1.4	1000	2500
	Concrete	10	2.36	1000	2350

*: The air gap thermal resistance is equal to 0.15 m² K/W.

Table 5
Windows characteristics.

Envelope element	Material	U-value [W/m ² .K]	g-value	ϵ
Windows	Glass	1.4	0.6	0.84

Table 6
Specific values of internal gains.

Appliance	Persons [W/m ²]	Appliances [W/m ²]	Lights [W/m ²]
Convective	3.01	1.05	1.5
Radiative	1.51	0.35	3.5

Concerning the solar absorption coefficient, we have adopted 0.6 for walls and for roofs pavements. The envelope infiltration rate is assumed to be 0.2 ACH while the ventilation flow rate is taken equal to 0.5 vol/h. The cooling and heating temperature set point are respectively 26 °C in summer and 20 °C in winter.

$$Y = \beta_1 + \beta_2 R_1 + \beta_3 R_1^2 + \beta_4 R_1^3 + \beta_5 R_1^4 + \beta_6 R_1^5 + \beta_7 R_1 + \beta_8 R_2^2 + \beta_9 R_2^3 + \beta_{10} R_2^4 + \beta_{11} R_2^5 \quad (19)$$

In this work, to determine the regression coefficients for the heating and cooling energy needs for each climate studied, the TableCurve 3D software was used [51]. Regression coefficients (β) are presented in Table 7.

5.1.2. Model accuracy

A detailed analysis of residuals, i.e., the differences between simulations and predictions, was carried out in order to give an idea about the adequacy of the model used to fit the data. A fitted model's residuals represent the differences between the observed responses for each combination of values of the explanatory variables and the corresponding prediction of the response calculated using the regression function. To examine the distribution of the residuals, scatter plots were presented in Figs 23, 24 and 25.

The residuals were found to be globally scattered around zero and show the absence of any specific pattern or relationship with the value of the independent variable. This is confirmation that the prediction of the models developed for the different climates considered in this study are not significantly drifted, i. e. the model does not lack any significant phenomenon that would generate such a global drift in the prediction.

Obviously, the plots are considered almost too simple for the advanced statistical applications, nevertheless they give a clear idea about the error distribution and the relevance of the mathematical models.

Moreover, the mean absolute error (MAE), the mean square error (MSE), and finally the multiple determination coefficient (R^2) were calculated and analyzed. These coefficients were calculated using the following equations:

$$MAE = \frac{1}{n} \sum_{i=1}^n |y_i - \hat{y}_i| \quad (20)$$

$$MSE = \frac{1}{n} \sum_{i=1}^n (\hat{y}_i - y_i)^2 \quad (21)$$

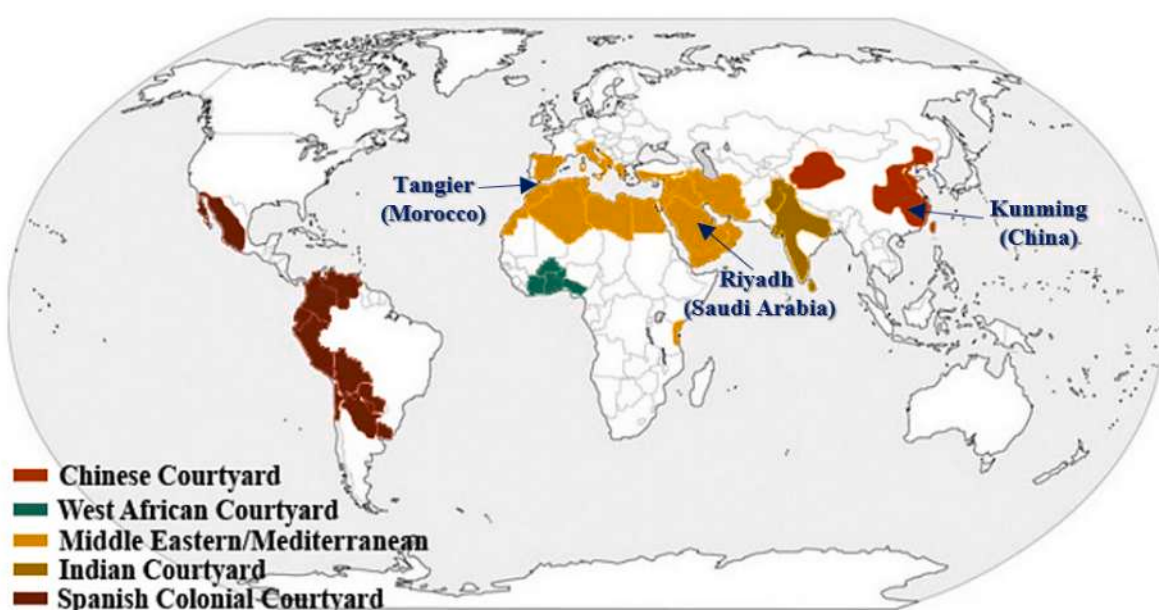


Fig. 13. Distribution of Courtyards in the World [7].

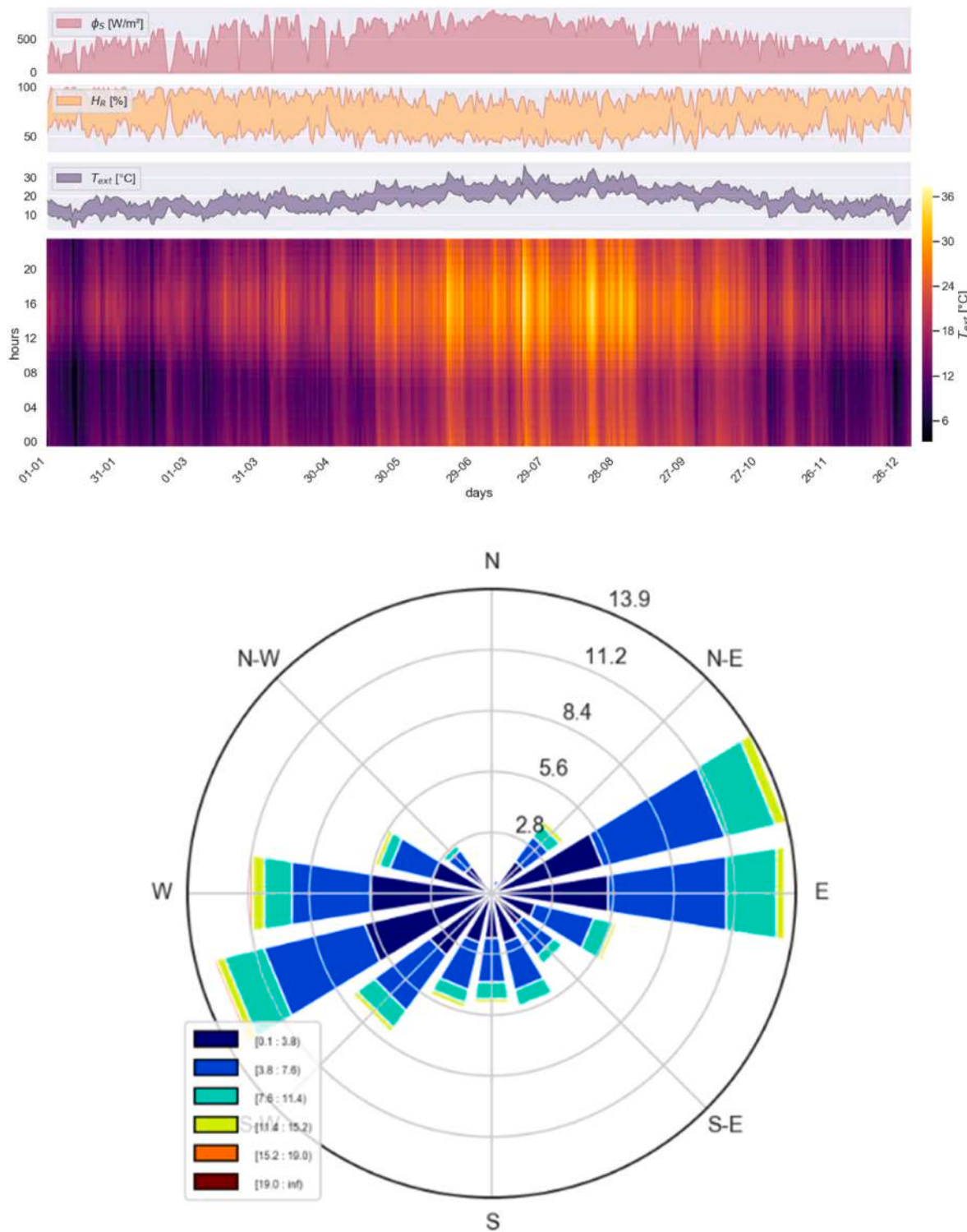


Fig. 14. Meteorological data of the city of Tangier (Morocco).

$$R^2 = \sum_{i=1}^n \frac{(\hat{y}_i - MAE)^2}{(y_i - MAE)^2} \quad (22)$$

Where y_i is the random sample simulation output, \hat{y}_i is the response value predicted by the metamodels.

Table 8 below contains the different error statistics calculated for the different regression models that we have developed in this study.

Based on the obtained results, the accuracy of the developed regression models appears to be acceptable to predict heating and

cooling energy needs for different proportions of courtyard. Finally, the optimization procedure will be performed using those regression models.

5.2. Optimal design of courtyards using pareto-optimal front

The objective in this section is to look for the trade-off solutions using the Pareto-optimal front [52,53]. As such, Pareto-optimal solutions represents a measure of efficiency in the multi-objective context where

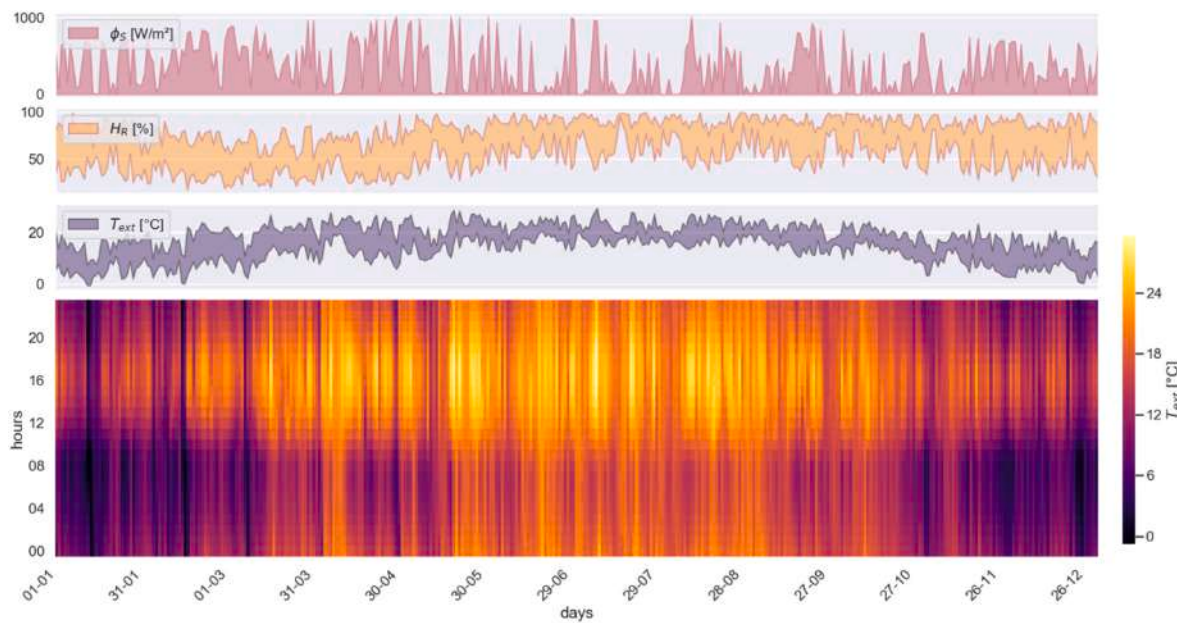


Fig. 15. Meteorological data of the city of Kunming (China).

several conflicting objectives must be considered in an optimization process [54]. Pareto-optimal solutions are based on the concept of dominance among vectors in the objective space [52].

The so-called optimal solutions are those which pass through the front Pareto $P(Y)$. The definition of dominance between two solutions can be expressed as A dominates B by the following equation:

$$P(Y) = \{(A \in Y, B \in Y : B > A, B \neq A) = \emptyset\} \quad (23)$$

As described in the previous section, the alteration to the lower level of R_1 ratio helps to decrease cooling load, whereas it increases the heating load. The higher R_2 ratio decreases the heating load, while it increases the cooling load. The impact of each ratio varies with the alteration of the other, i.e., the interaction effect that makes it even more difficult to select appropriate sets of optimal courtyard proportions to minimize total energy needs. The main and interaction effects of the R_1 and R_2 ratios on heating and cooling energy needs must be considered

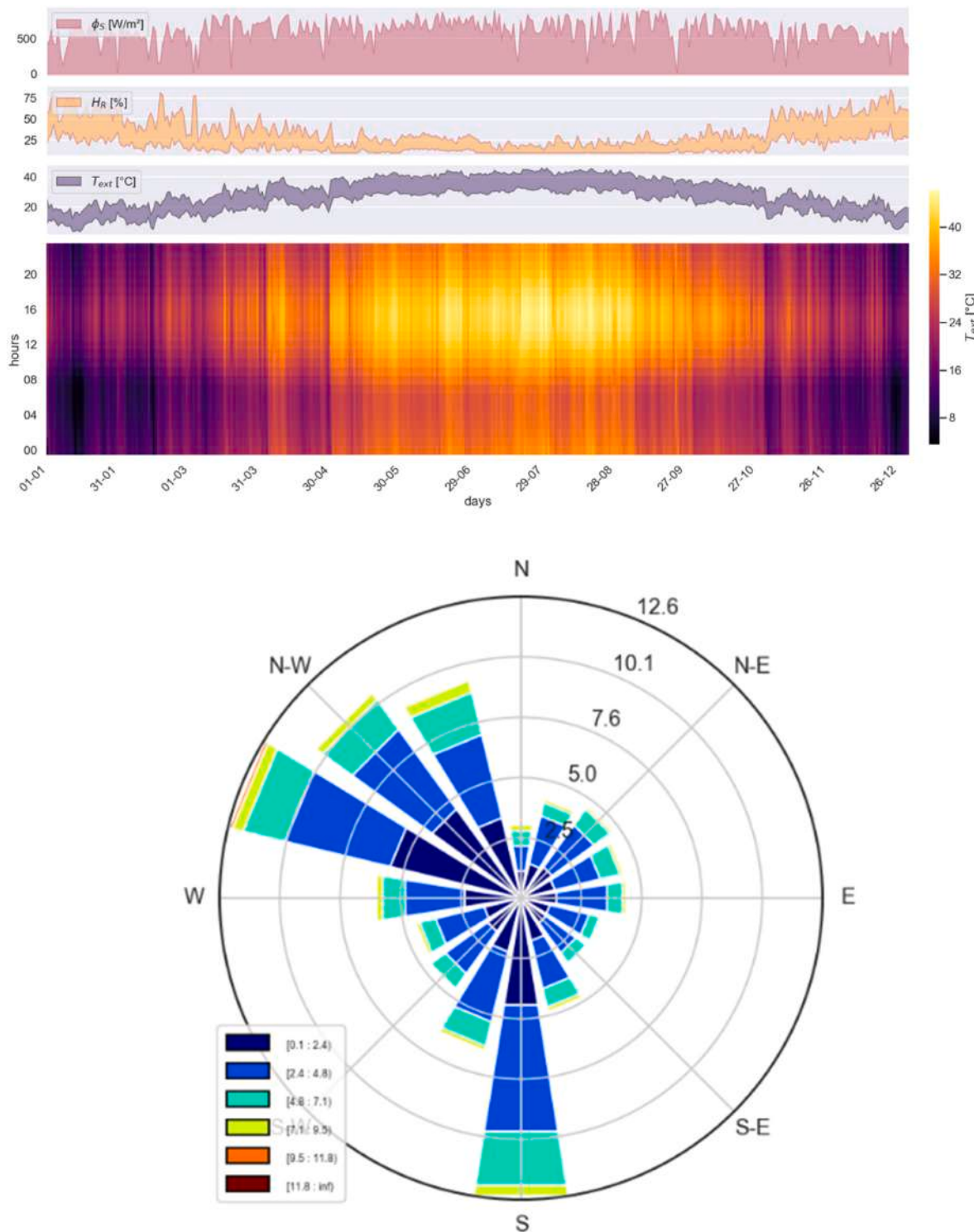


Fig. 16. Meteorological data of the city of Riyadh (Saudi Arabia).

together at once to determine the appropriate courtyard building design.

In this part, for fast prediction of energy needs, the previously developed regression models are used to perform an optimization study to get the optimal proportions (R_1 and R_2 ratios) of courtyard for each climate studied while minimizing the energy needs of cooling and heating. As such, the Pareto Front solving approach is used.

The Figures 25 and 26, 26, 27 and 28 show heating and cooling energy needs of 500,000 iterations performed to optimize the courtyard proportions for each climate considered in this study. The Pareto fronts,

the red lines in these Figures, to minimize both heating and cooling loads of the buildings simultaneously were determined. From this, 1345 sets of Pareto optimal solutions were identified in the design problem space for the temperate climate case, 6980 for the cold climate case and 4958 for the hot arid climate case; where a trade-off conflict between the heating and cooling energy needs was illustrated. The variation of the changing design criteria along the Pareto front line is as follows:

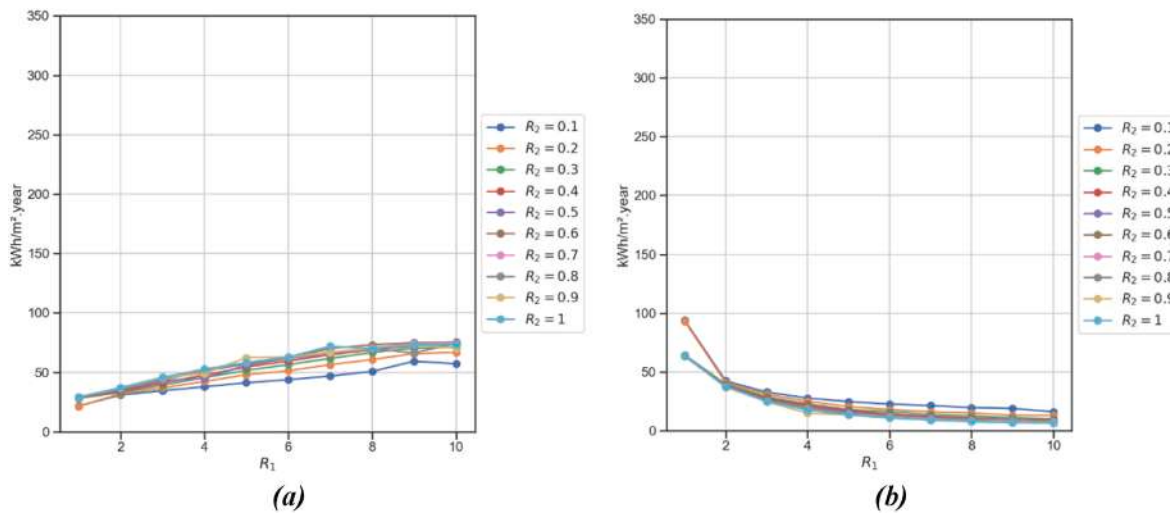


Fig. 17. Impact of varying courtyard proportions R_1 and R_2 on energy needs for a) cooling and b) heating in temperate climate.

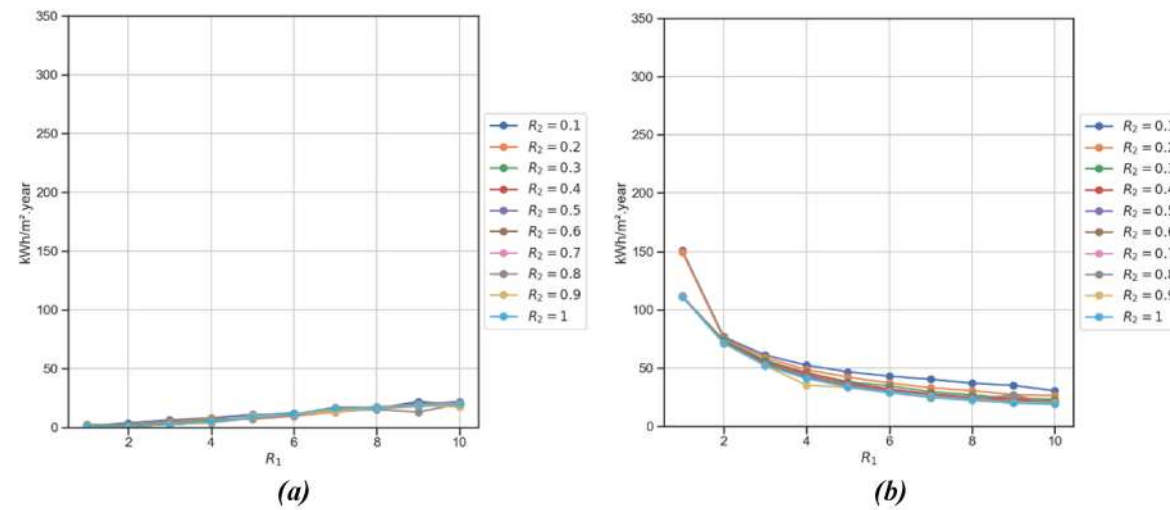


Fig. 18. Impact of varying courtyard proportions R_1 and R_2 on energy needs for a) cooling and b) heating in cold climate.

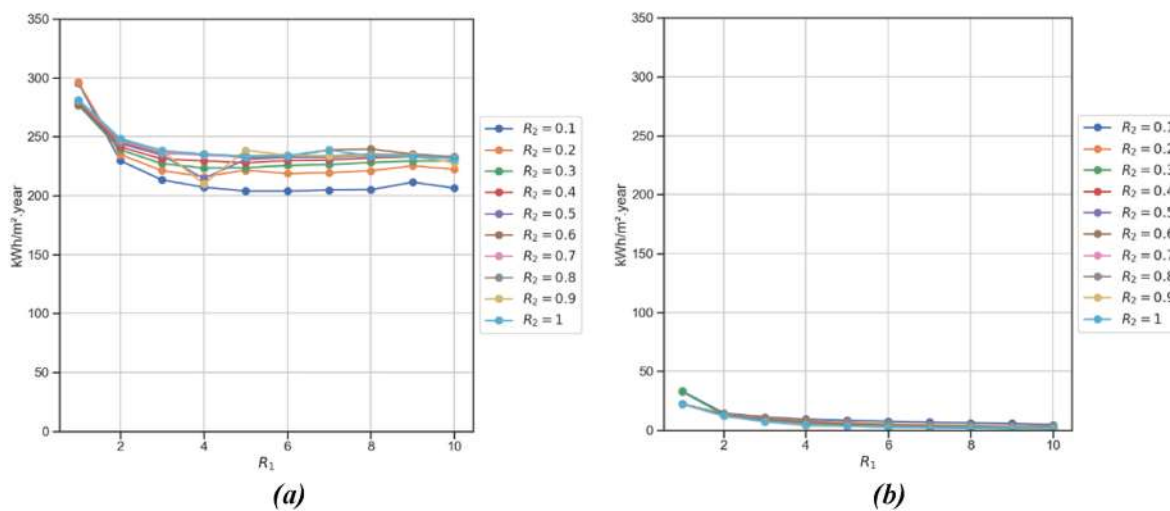


Fig. 19. Impact of varying courtyard proportions R_1 and R_2 on energy needs for a) cooling and b) heating in hot arid climate.

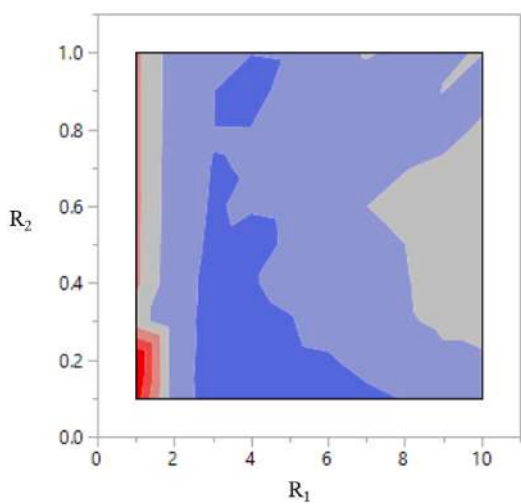


Fig. 20. Abacus of total energy needs for courtyard buildings in temperate climate.

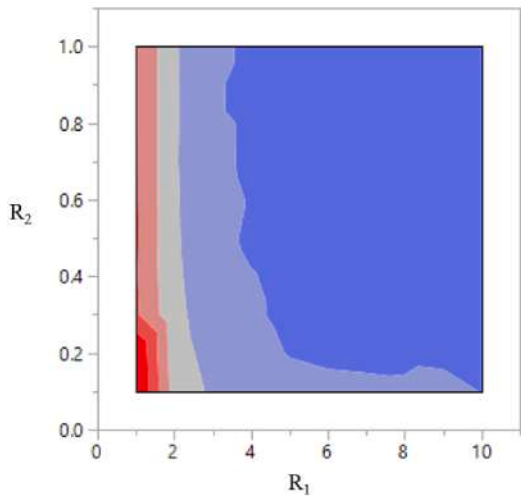


Fig. 21. Abacus of total energy needs for courtyard buildings in cold climate.

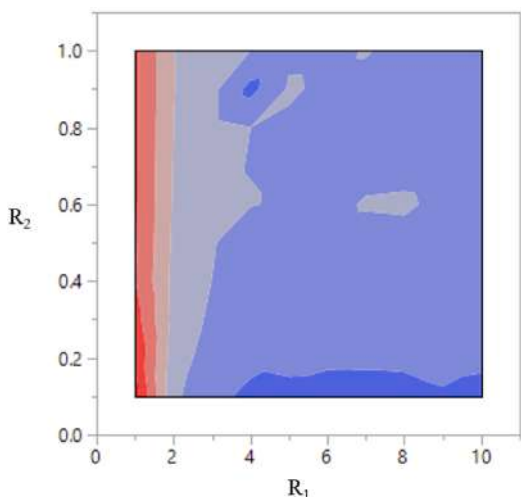


Fig. 22. Abacus of total energy needs for courtyard buildings in hot arid climate.

Table 7

Regression coefficients for the metamodel specific to each locality.

	Temperate climate		Cold climate		Hot arid climate	
	Heating	Cooling	Heating	Cooling	Heating	Cooling
β_1	-8.688	20.196	1.106	8.700	-3.613	242.401
β_2	96.44	9.179	203.106	-5.897	28.669	-112.446
β_3	5.867	-0.106	-1.569	2.981	1.854	-9.976
β_4	-27.825	-0.214	-154.292	-0.512	1.627	349.326
β_5	-0.827	-2.108	1.101	0.044	-0.260	-10.540
β_6	-6.112	1.129	-4.807	-0.001	-1.344	44.313
β_7	-2.615	-0.018	52.604	-41.390	-6.699	-197.807
β_8	0.046	-1.101	-0.073	141.341	0.014	-0.667
β_9	0.095	-0.7181	-0.322	-199.336	0.011	14.472
β_{10}	6.415	-0.207	10.910	106.040	1.720	-29.303
β_{11}	-	-	-	-10.687	-	-

The regression models obtained are very flexible and can be adapted to a wide range of courtyard shapes. However, the major inconvenience is that they are not valid for other building materials.

- For the temperate climate, the heating energy needs run from 5.4 kWh/m².year to 85 kWh/m².year, while the cooling energy needs run from 24.9 kWh/m².year to 72 kWh/m².year;
- For Cold climate, the heating energy needs vary from 19 kWh/m².year to 86.4 kWh/m².year, while the cooling energy needs vary from 0.2 kWh/m².year to 19.7 kWh/m².year;
- For the hot arid climate, the heating energy needs range from 0.7 kWh/m².year to 7.5 kWh/m².year, while the cooling energy needs range from 205.1 kWh/m².year to 234.4 kWh/m².year;

As the Pareto optimization only imposed a partial order on solution candidates, the weighted sum method was then adopted to transform the bi-objective problem to a mono-objective one. The optimal courtyard proportions, which achieves a simultaneous low heating and cooling energy needs for each climate studied, are listed in the Table 9.

Based on these results, we can see that the square shape is more advantageous in cold climates due to the solar gain in winter reducing heating energy needs by approximately 48%, while the deep and less wide shape is more advantageous for hot and arid climates reduces the cooling energy needs by about 10%, which allows for maximum shade in summer and obviously provides better comfort. For temperate climate, we can see that the shape guaranteeing minimum energy needs and, in all seasons, is the one with less width and medium depth allowing a reduction in energy needs of about 58%.

6. Discussion and limitations

By analyzing the existing literature, an alternative approach to building design is needed to improve building environmental performance as well as to minimize energy consumption. To this end, many researchers, architects and urban planners are interested in sustainable building design [55–57]. Effectively, sustainable design strategies can reduce building energy consumption as well as their environmental impact. Consequently, courtyard design can be an effective sustainable strategy to improve the thermal and microclimatic conditions of buildings and urban spaces [20]. Hence, this study is in line with this objective.

Indeed, by combining the results of this study with those of the literature we can summarize that, solar radiation must be considered by architects and engineers when designing the courtyard to provide comfortable thermal conditions for the occupants [22]. Passive cooling through shading is an important principle of thermal comfort in summer [7]. Furthermore, the proportion and the orientation of the courtyard have a significant impact on the received solar radiation and the shading areas created on the courtyard facades, thus strongly contributing to influence the building heating and cooling energy needs.

Geometric parameters (especially proportions and orientation),

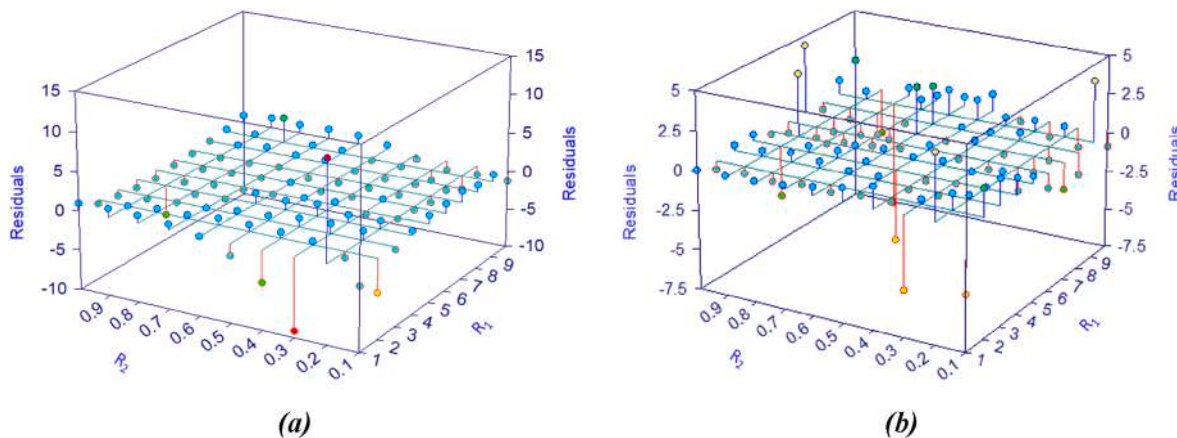


Fig. 23. Residual plot of model predicting courtyard (a) heating and (b) cooling energy needs in temperate climate.

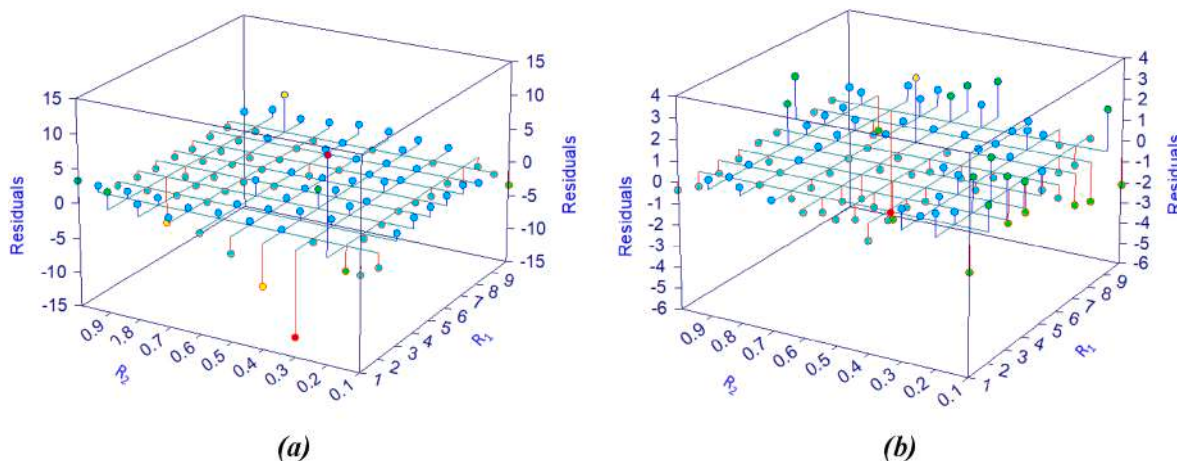


Fig. 24. Residual plot of model predicting courtyard (a) heating and (b) cooling energy needs in cold climate.

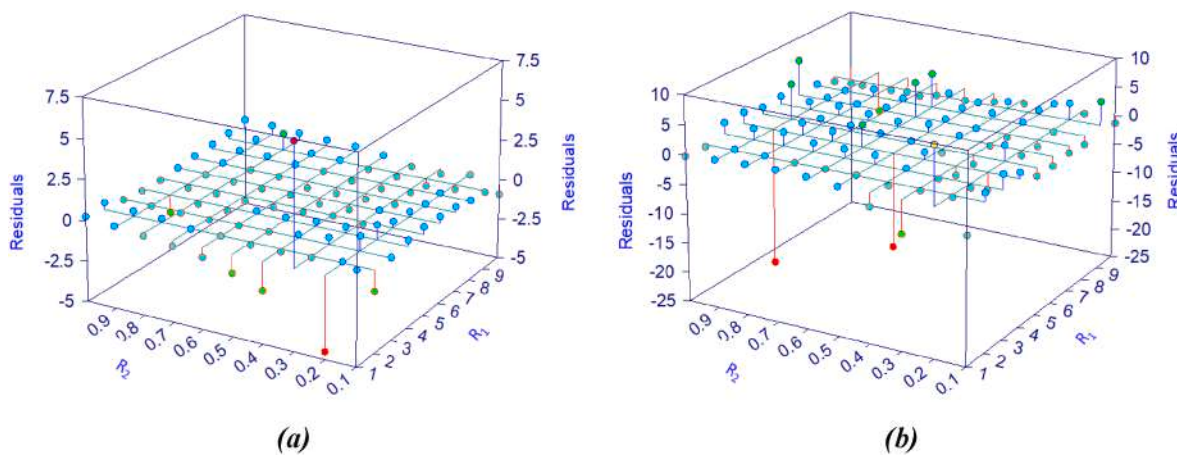


Fig. 25. Residual plot of model predicting courtyard (a) heating and (b) cooling energy needs in the hot arid climate.

climatic conditions, as well as the season and sun's path all affect how a courtyard functions. Generally, a courtyard building with inappropriate proportions or orientation will either receive too much solar radiation when it needs to be shaded, or will create too much shade when solar radiation is needed for its energy needs [9].

On the other hand, the research work carried out in this study has some limitations which can be pursued by many perspectives at the level of improvement of developed models, at the level of applications in the

energy study of buildings and urban microclimates as well as at the level of validations.

To validate the courtyard model, an experimental measurement campaign of a building with a courtyard specifically designed for the purpose must be carried out. At the same time, improvements can be made to the developed models, to optimize the energy performance of the buildings and to improve the local microclimatic conditions, through the integration of numerous energy and environmental models, among

Table 8
Regression models error statistics for each location.

Error statistics	Temperate climate		Cold climate		Hot arid climate	
	Heating	Cooling	Heating	Cooling	Heating	Cooling
MAE [kWh/m ² .year]	2.01	1.66	2.56	1.13	1.01	3.79
MSE [(kWh/m ² .year) ²]	4.04	2.77	6.55	1.27	1.03	14.39
R ²	0.9892	0.98947	0.99309	0.97572	0.97998	0.96258

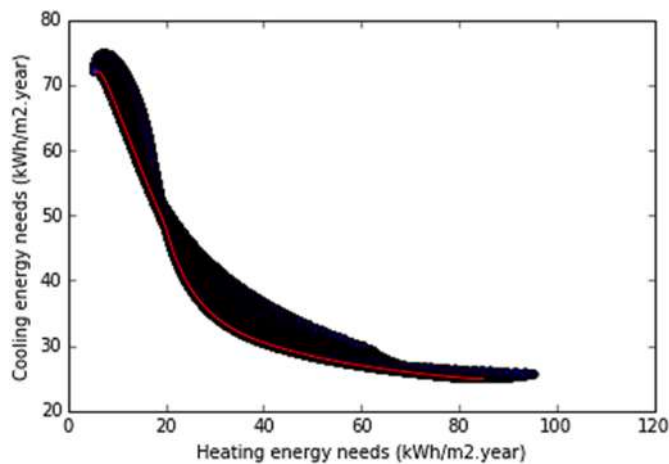


Fig. 26. Pareto front and optimum solution between the heating and cooling energy needs in Temperate climate (Red points are the dominant solutions and blue points are the non-dominant solutions).

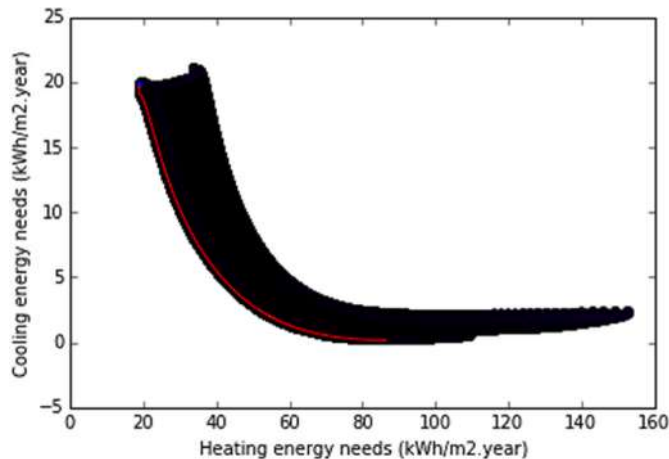


Fig. 27. Pareto front and optimum solution between the heating and cooling energy needs in Cold climate (Red points are the dominant solutions and blue points are the non-dominant solutions).

which we mention:

- Heat and mass transfer modeling;
- Water modeling to study cooling devices, such as fountains for example;
- Modeling of natural ventilation and passive air conditioning operating scenarios;
- Modeling of trees and vegetated walls.

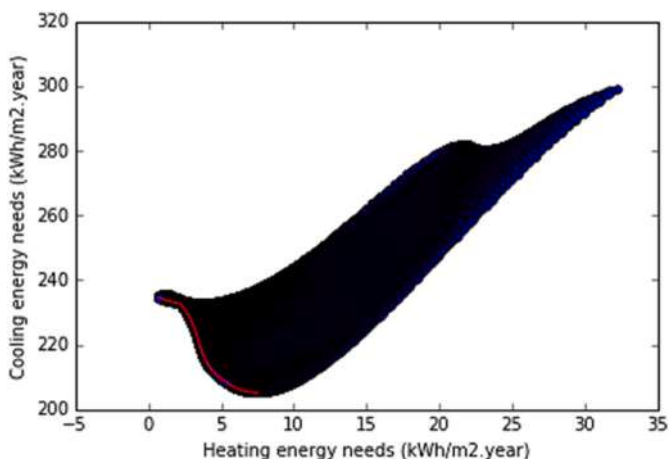


Fig. 28. Pareto front and optimum solution between the heating and cooling energy needs in Hot arid climate (Red points are the dominant solutions and blue points are the non-dominant solutions).

Tableau 9
Optimal courtyard proportions for the three climates studied.

climate	R ₁	R ₂	Heating loads	Cooling loads	courtyard form
Temperate	3.32	0.1	30	34	
Cold	3.81	0.86	43	4	
Hot arid	10	0.11	4	210	

- Consideration of other parameters in the optimization (windows on the external surfaces, thermal insulation ...)

7. Conclusion

In architectural design, the courtyard represents one of the two major building models known in history whose characteristics depend on the surroundings and a region's culture. It had several spiritual, organizational, climate and social roles, as it had to sort of illuminate and ventilate the building. However, the courtyard's characteristics depended on various contextual, morphological and physical factors, as well as the interactions of the courtyard's microclimatic and thermal functions, which remain complex and difficult to model.

In the present study, a zonal approach with the BES software TRNSYS was developed in order to assess the impact of courtyard microclimate on the building energy needs. It considers the effects of dominant winds, radiative trapping, hygrothermal exchange and heat transfer in the soil along the three directions. To evaluate the consistency of this modelling approach, a comparative study between the CFD results and our numerical results, obtained with the model we have developed, is performed. In this way, the numerical results obtained for the courtyard air temperature are very close to the CFD results with a mean absolute error of 0.61 °C, a mean relative error of about 3.37% and regression coefficient R² of 0.99. The advantage of using this method is its fast

calculation time compared to CFD calculations combined with a satisfactory accuracy for the thermal and energy evaluation purposes.

Based on the developed approach, an evaluation of the effect of courtyard morphology on heating and cooling energy needs was performed for three different climates. The obtained results allowed to determine a range of courtyard proportions that minimize the total energy need for each studied climate.

In order to find the optimal courtyard proportions (R_1 and R_2 ratios) for each climate studied while minimizing the cooling and heating energy needs, we have developed regression models based on the developed approach for fast prediction energy needs. As well, the Pareto Front solving approach was used. The results showed that the square shape for cold climates and the deep shape for hot and arid climates are the optimal solutions to be preferred for a better trade-off between heating and cooling energy, where the energy needs have been optimized by 50%. Finally, the proposed method can be used as a decision-making tool for engineers, architects and designers.

Credit author statement

Adnane M'Saouri El Bat: Conceptualization, Methodology, Software, Formal analysis, Writing - original draft. Zaid Romani: Conceptualization, Methodology, Writing - review & editing. Emmanuel Bozonnet: Supervision, Writing - review & editing. Abdeslam Draoui: Supervision, Writing - review & editing. Francis Allard: Supervision, Writing - review & editing.

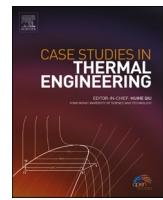
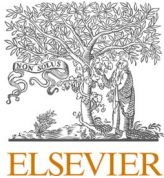
Declaration of competing interest

The authors declare that they have no known competing financial interests or personal relationships that could have appeared to influence the work reported in this paper.

References

- [1] United Nations. World urbanization prospects - population division. United Nations; 2019.
- [2] Reckien D, Salvia M, Heidrich O, Church JM, Pietrapertosa F, De Gregorio-Hurtado S, et al. How are cities planning to respond to climate change? Assessment of local climate plans from 885 cities in the EU-28. *J Clean Prod* 2018;191:207–19. <https://doi.org/10.1016/j.jclepro.2018.03.220>.
- [3] Edwards B, Sibley M, Land P, Hakmi M. Courtyard housing: past, present and future. 2006.
- [4] Nelson R. The courtyard inside and out: a brief history of an architectural ambiguity. *Enq A J Archit Res* 2014;11. <https://doi.org/10.17831/enq:arcc.v11i1.206>.
- [5] Xu X, Luo F, Wang W, Hong T, Fu X. Performance-based evaluation of courtyard design in China's cold-winter hot-summer climate regions. *Sustainability* 2018;10: 3950. <https://doi.org/10.3390/su10113950>.
- [6] Saxon R. Atrium buildings: development and design. LONDON Archit Press; 1983. 182 PP ISBN 0-85139-849-9 182 ILLUS BIBLOG(General).
- [7] Taleghani M, Tenpierik M, van den Dobbelaer A. Environmental impact of courtyards—a review and comparison of residential courtyard buildings in different climates. *J Green Build* 2012;7:113–36.
- [8] Chi F, Xu L, Peng C. Integration of completely passive cooling and heating systems with daylighting function into courtyard building towards energy saving. *Appl Energy* 2020;266:114865. <https://doi.org/10.1016/j.apenergy.2020.114865>.
- [9] Muhaisen AS, Gadi MB. Effect of courtyard proportions on solar heat gain and energy requirement in the temperate climate of Rome. *Build Environ* 2006;41: 245–53.
- [10] Muhaisen AS, Gadi MB. Mathematical model for calculating the shaded and sunlit areas in a circular courtyard geometry. *Build Environ* 2005;40:1619–25. <https://doi.org/10.1016/j.buildenv.2004.12.018>.
- [11] Muhaisen AS. Shading simulation of the courtyard form in different climatic regions. *Build Environ* 2006;41:1731–41.
- [12] Taleghani M, Tenpierik M, van den Dobbelaer A, Sailor DJ. Heat in courtyards: a validated and calibrated parametric study of heat mitigation strategies for urban courtyards in The Netherlands. *Sol Energy* 2014;103:108–24. <https://doi.org/10.1016/j.solener.2014.01.033>.
- [13] Taleghani M, Tenpierik M, van den Dobbelaer A. Indoor thermal comfort in urban courtyard block dwellings in The Netherlands. *Build Environ* 2014;82: 566–79. <https://doi.org/10.1016/j.buildenv.2014.09.028>.
- [14] Taleghani M, Kleerekoper L, Tenpierik M, van den Dobbelaer A. Outdoor thermal comfort within five different urban forms in The Netherlands. *Build Environ* 2015; 83:65–78. <https://doi.org/10.1016/j.buildenv.2014.03.014>.
- [15] López-Cabeza VP, Galán-Marín C, Rivera-Gómez C, Roa-Fernández J. Courtyard microclimate ENVI-met outputs deviation from the experimental data. *Build Environ* 2018;144:129–41. <https://doi.org/10.1016/j.buildenv.2018.08.013>.
- [16] López-Cabeza VP, Carmona-Molero FJ, Rubino S, Rivera-Gómez C, Fernández-Nieto ED, Galán-Marín C, et al. Modelling of surface and inner wall temperatures in the analysis of courtyard thermal performances in Mediterranean climates. *J Build Perform Simul* 2021;14:181–202. <https://doi.org/10.1080/19401493.2020.1870561>.
- [17] Martinelli L, Matzarakis A. Influence of height/width proportions on the thermal comfort of courtyard typology for Italian climate zones. *Sustain Cities Soc* 2017;29: 97–106. <https://doi.org/10.1016/j.scs.2016.12.004>.
- [18] Chatzidimitriou A, Yannas S. Microclimate design for open spaces: ranking urban design effects on pedestrian thermal comfort in summer. *Sustain Cities Soc* 2016; 26:27–47. <https://doi.org/10.1016/j.scs.2016.05.004>.
- [19] Yang X, Li Y, Yang L. Predicting and understanding temporal 3D exterior surface temperature distribution in an ideal courtyard. *Build Environ* 2012;57:38–48. <https://doi.org/10.1016/j.buildenv.2012.03.022>.
- [20] Zamani Z, Heidari S, Hanachi P. Reviewing the thermal and microclimatic function of courtyards. *Renew Sustain Energy Rev* 2018;93:580–95. <https://doi.org/10.1016/j.rser.2018.05.055>.
- [21] Bagheri Sabzevar H, Masoomi M, Tarzafan S. Dormitory courtyard proportion and orientation in yazd/Iran on energy consumption. *Iran Univ Sci Technol* 2017;27: 75–81.
- [22] Sabzevar HB, Ahmad MH, Gharakhani A. Courtyard geometry on solar heat gain in hot-dry region. *Adv Mater Res* 2014;935:76–9. Trans Tech Publ.
- [23] Gebhart B. Surface temperature calculations in radiant surroundings of arbitrary complexity –for gray, diffuse radiation. *Int J Heat Mass Tran* 1961;3:341–6.
- [24] M'Saouri El Bat A, Romani Z, Bozonnet E, Draoui A. Impact of urban microclimate on the energy performance of riad-type buildings. *Proc. Build. Simul.* 2020;16: 3771–8. <https://doi.org/10.26868/25222708.2019.211272>. 2019 16th Conf. IBPSA.
- [25] M'Saouri El Bat A, Romani Z, Bozonnet E, Draoui A. Integration of a practical model to assess the local urban interactions in building energy simulation with a street canyon. *J Build Perform Simul* 2020;13:720–39. <https://doi.org/10.1080/19401493.2020.1818829>.
- [26] M'Saouri El Bat A, Romani Z, Bozonnet E, Draoui A. Thermal impact of street canyon microclimate on building energy needs using TRNSYS: a case study of the city of Tangier in Morocco. *Case Stud Therm Eng* 2021;24:100834. <https://doi.org/10.1016/j.csite.2020.100834>.
- [27] Bruse M. Development of a microscale model for the calculation of surface temperatures in structured terrain. 1995.
- [28] Stephenson DG, Mitalas G. Calculation of heat conduction transfer functions for multi-layers slabs. *Air Cond Engrs Trans*; (United States); 1970.
- [29] Rodler A, Guernouti S, Musy M, Bouyer J. Energy & Buildings Thermal behaviour of a building in its environment : modelling , experimentation , and comparison. *Energy Build* 2018;168:19–34. <https://doi.org/10.1016/j.enbuild.2018.03.008>.
- [30] Haghishima A, Tanimoto J. Field measurements for estimating the convective heat transfer coefficient at building. *Surfaces* 2003;38:873–81. [https://doi.org/10.1016/S0360-1323\(03\)00033-7](https://doi.org/10.1016/S0360-1323(03)00033-7).
- [31] Zhou Z, Rees SW, Thomas HR. A numerical and experimental investigation of ground heat transfer including edge insulation effects. *Build Environ* 2002;37: 67–78. [https://doi.org/10.1016/S0360-1323\(00\)00089-5](https://doi.org/10.1016/S0360-1323(00)00089-5).
- [32] McDowell T, Thornton J, Duffy M. Comparison of a ground-coupling reference standard modelto simplified approaches. International IBPSA Conference 2009;11: 591–8.
- [33] Kusuda T, Achenbach PR. Earth temperatures and thermal diffusivity at selected stations in the United States. *Build Eng* 1965;61–74.
- [34] Haghishat F. Air infiltration and indoor air quality models—a review. *Int J Ambiat Energy* 1989;10:115–22.
- [35] Inard C, Bouia H, Dalicieux P. Prediction of air temperature distribution in buildings with a zonal model. *Energy Build* 1996;24:125–32. [https://doi.org/10.1016/0378-7789\(95\)00969-8](https://doi.org/10.1016/0378-7789(95)00969-8).
- [36] Musy M, Wurtz E, Winkelmann F, Allard F. Generation of a zonal model to simulate natural convection in a room with a radiative/convective heater. *Build Environ* 2001;36:589–96. [https://doi.org/10.1016/S0360-1323\(00\)00043-3](https://doi.org/10.1016/S0360-1323(00)00043-3).
- [37] Megri A, Haghishat F. Zonal modeling for simulating indoor environment of buildings: review, recent developments, and applications. *HVAC R Res* 2007;13: 887–905. <https://doi.org/10.1080/10789669.2007.10391461>.
- [38] Ai ZT, Mak CM. CFD simulation of flow in a long street canyon under a perpendicular wind direction: evaluation of three computational settings. *Build Environ* 2017;114:293–306.
- [39] Li Y, Delsante A, Symons J. Prediction of natural ventilation in buildings with large openings. *Build Environ* 2000;35:191–206.
- [40] Chu CR, Chiu Y-H, Chen Y-J, Wang Y-W, Chou C-P. Turbulence effects on the discharge coefficient and mean flow rate of wind-driven cross-ventilation. *Build Environ* 2009;44:2064–72.
- [41] Nicholson SE. A pollution model for street-level air. *Atmos Environ* 1975;9:19–31.
- [42] Bruse M, Fleer H. Simulating surface-plant-air interactions inside urban environments with a three dimensional numerical model. *Environ Model Software* 1998;13:373–84. [https://doi.org/10.1016/S1364-8152\(98\)00042-5](https://doi.org/10.1016/S1364-8152(98)00042-5).
- [43] ENVI-met - decode urban nature with ENVI-met software n.d.. <https://www.envi-met.com/>. [Accessed 22 April 2021]. accessed.
- [44] Yamada T, Mellor G. A simulation of the Wangara atmospheric boundary layer data. *J Atmos Sci* 1975;32:2309–29.

- [45] Yang X, Zhao L, Bruse M, Meng Q. Evaluation of a microclimate model for predicting the thermal behavior of different ground surfaces. *Build Environ* 2013; 60:93–104. <https://doi.org/10.1016/j.buildenv.2012.11.008>.
- [46] M'Saouri El Bat A. Développement d'un modèle pour l'étude de l'impact du microclimat urbain sur les performances énergétiques des bâtiments : cas des rues canyons et des cours intérieures. Theses. Université Abdelmalek Essaadi; 2020.
- [47] 11300-1 Uni TS. Energy performance of buildings—Part 1. first ed. Milano: Calc Energy Use Sp Heat Cool; 2008. UNI.
- [48] Meteonorm. Meteonorm - global meteorological database. Meteotest; 2012.
- [49] Di Leo S, Caramuta P, Curci P, Cosmi C. Regression analysis for energy demand projection: an application to TIMES-Basilicata and TIMES-Italy energy models. *Energy* 2020;196:117058. <https://doi.org/10.1016/j.energy.2020.117058>.
- [50] Catalina T, Iordache V, Caracaleanu B. Multiple regression model for fast prediction of the heating energy demand. *Energy Build* 2013;57:302–12. <https://doi.org/10.1016/j.enbuild.2012.11.010>.
- [51] TableCurve 3D v4.0 – Systat Software n.d. <https://systatsoftware.com/product/tablecurve-3d-v4-0/>. [Accessed 25 August 2021]. accessed.
- [52] Sánchez MS, Ortiz MC, Sarabia LA. A useful tool for computation and interpretation of trading-off solutions through pareto-optimal front in the field of experimental designs for mixtures. *Chemometr Intell Lab Syst* 2016;158:210–7. <https://doi.org/10.1016/j.chemolab.2016.09.007>.
- [53] Ortiz MC, Sarabia L, Herrero A, Sánchez MS. Vectorial optimization as a methodological alternative to desirability function. *Chemometr Intell Lab Syst* 2006; 83:157–68. <https://doi.org/10.1016/j.chemolab.2005.11.005>.
- [54] Brisset S, Gillon F. 4 - approaches for multi-objective optimization in the ecodesign of electric systems. In: Bessède J-LBT-E-FI in ET and DN. Woodhead Publishing; 2015. p. 83–97. <https://doi.org/10.1016/B978-1-78242-010-1.00004-5>. Oxford.
- [55] Wang N, Adeli H. Sustainable building design. *J Civ Eng Manag* 2014;20:1–10. <https://doi.org/10.3846/13923730.2013.871330>.
- [56] Evins R. A review of computational optimisation methods applied to sustainable building design. *Renew Sustain Energy Rev* 2013;22:230–45. <https://doi.org/10.1016/j.rser.2013.02.004>.
- [57] Sahlol DG, Elbeltagi E, Elzoughiby M, Abd Elrahman M. Sustainable building materials assessment and selection using system dynamics. *J Build Eng* 2021;35: 101978. <https://doi.org/10.1016/j.jobe.2020.101978>.



Thermal impact of street canyon microclimate on building energy needs using TRNSYS: A case study of the city of Tangier in Morocco

Adnane M'Saouri El Bat^a, Zaid Romani^{b,*}, Emmanuel Bozonnet^c, Abdeslam Draoui^a

^a Team of Heat Transfer & Energetic, Faculty of Sciences and Techniques of Tangier (UAE/U10FST), Abdelmalek Essaïdi University, Morocco

^b National School of Architecture Tetouan, Morocco

^c LaSIE, Université de La Rochelle, France



ARTICLE INFO

Keywords:

Street canyon microclimate

Aspect ratio

Building energy needs

TRNSYS

ABSTRACT

The aim of this study is to demonstrate the requirement to integrate the urban microclimate to predict the energy needs of buildings. To do this, an integrated approach in TRNSYS software was developed and compared with existing experimental results of a street canyon. Afterwards, a case study was carried out in the case of a street canyon located in the city of Tangier in Morocco. The impact of the aspect ratio on the temperature of the building surfaces and the radiation absorbed by them was examined. The results show that there is greater radiation absorption on the building facades in street canyons than on those of stand-alone buildings. These effects lead to higher surface temperatures in street canyons, resulting in increased cooling energy needs in summer and reduced heating energy needs in winter.

1. Introduction

The constructions and human activities in cities generate the climatic phenomena which scientists give a particular attention. In fact, urban parameters such as building density, aspect ratio of street canyons, thermal transmittance and albedo of urban materials have a direct influence on the climate around and in the vicinity of buildings. This microclimate influences the thermal stress of buildings and thus affects indoor comfort as well as energy needs for heating and cooling. In this respect, several studies have shown the impact of urban microclimate on the surface energy balance in urban areas [1–4], as well as on the building energy consumption [5–9]. It is therefore necessary to model and analyse this phenomenon and its interaction with buildings in order to take adequate solutions to reduce energy needs and thus contribute to the sustainable development of our societies.

The lack of consideration for the urban microclimate has led several researchers to study its interaction with buildings. However, the difficulty of studying this interaction is apparent in modelling, given the important number of parameters that need to be taken into account and the results precision required. Within this context, several models have been developed in the literature, such as the simplified models [4,10,11], the SOLENE model coupled with a CFD model [12] and the zonal models [5,13]. These models are generally detailed, but their use is complex due to the high computation time and the difficulties for the coupling between several software. Moreover, these tools are unable to model the thermal behaviour of buildings with precision as building energy simulation tools.

* Corresponding author.

E-mail addresses: a.msaourielbat@gmail.com (A. M'Saouri El Bat), romani.zaid@gmail.com (Z. Romani).

In Morocco, building energy simulations are usually carried out for stand-alone buildings, using averaged weather data files generated from measurements collected by weather stations sited in rural areas [14–19]. These simulations therefore reflect where our cities are located rather than how they are built, neglecting the effects of the urban microclimate. Moreover, several studies can be found in the literature concerning the urban microclimate in Morocco [20–22]. These studies are limited only to the influences of the urban microclimate on outdoor thermal comfort, without providing information on the impact of the local microclimate on the energy performance of buildings.

The main aim of this study is to quantify the influence of the street canyon microclimate with three different aspect ratio (Height/Width = H/W = 0.5, 1 and 2) on the thermal behaviour of building, considering the case of the city of Tangier in Morocco. A detailed study on radiative fluxes on the building facades and the opaque surface temperatures of the envelopes was carried out. For that a simplified approach integrated in the TRNSYS 18 software is used [23]. This approach allows the description of thermal as well as aeraulic and radiative phenomena not only in the buildings, but also at the microclimatic scale of the near environment or the neighbourhood.

2. Methodology

2.1. Numerical model

In this research work, the TRNSYS 18 software was used for the energy simulation knowing that this software does not include urban modelling. Indeed, we developed a model adapted to this software to be able to integrate the microclimatic simulation. With TRNSYS software, the transfer function method of Mitalas and Stephenson [24] is used to express heat conduction through the walls. However, there are two possibilities to model the heat transfer by convection. The first is to set a constant value of the convective heat transfer coefficient and the second one is to use specific correlations. In this study, the heat transfer coefficient value of building facades is assumed to be constant on the inside surfaces of the building (6.1 W/m²K for the ceiling, 1.6 W/m²K for the floor and 4.1 W/m²K for the vertical walls [25]). For the outside surfaces, the heat transfer coefficient by convection was evaluated using the Hagishima and Tanimoto correlation [26] given by formulas (1) and (2) below.

For horizontal surfaces:

$$h_{c,ext} = 2.28V_R + 8.18 \quad (1)$$

For vertical surfaces:

$$h_{c,ext} = 10.21V_{loc} + 4.47 \quad (2)$$

where:

V_R is the wind speed measured at height H' from the roof surface (Fig. 1) and V_{loc} is the wind speed measured at a certain distance d from the building facade and at a certain height (H) from the ground (Fig. 1).

The mean wind speed $u(z)$ at a height z , above a surface can be estimated using Tennekes' formula (3) [27].

$$u(z) = \frac{u_*}{k} \ln\left(\frac{z-d}{Z_0}\right) \quad (3)$$

where u_* is the friction velocity, $k = 0.4$ [28] is von Karman's constant, d is the displacement length and Z_0 is the roughness length of the urban canopy considered.

It should be noted that V_{10} is the wind speed measured at 10 m above ground level in the upstream undisturbed wind flow (Fig. 1).

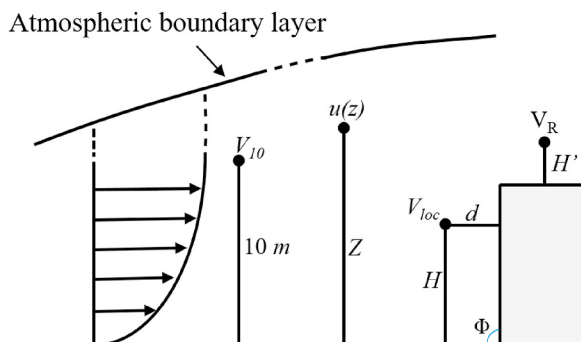


Fig. 1. Different definitions of wind speed for the built environment [29].

This is the only type of wind speed data available in standard building energy simulations tools weather files [29]. This implies that for use in building energy simulations tools, V_R and V_{loc} must be estimated based on V_{10} .

The modelling of ground heat transfers is based on NF EN ISO 13370 standard and Type 77 of TRNSYS [30]. This represents the sinusoidal evolution of the temperature over the year. This model permits the calculation of the temperature profile for flat terrain at different depths based on the Kusuda model [31]. The cyclic evolution of the ground temperature T_{sz} , at a depth z , is expressed as a function of the mean surface temperature $T_{su,avg}$ for the period studied using the Kusuda's formula:

$$T_{sz}(t) = T_{su,avg} + \Delta T_{su} e^{-z\sqrt{\frac{\pi}{a_{sol}\Delta t}}} \cos\left(\frac{2\pi t}{\Delta t} - z \cdot \sqrt{\frac{\pi}{a_{sol}\Delta t}}\right) \quad (4)$$

where ΔT_{su} is the amplitude of the variation of the surface temperature over the period considered, Δt is the period considered and a_{sol} is the thermal diffusivity of the soil.

For radiative exchanges, TRNSYS distinguishes between short wavelength and long wavelength exchanges. These are modelled differently for indoor and outdoor surfaces. More specifically, solar irradiation on outdoor surfaces is considered as a gain while the longwave radiation is treated as a heat loss to the cold sky. A 3D radiation model that takes into account of multiple reflections is provided only on interior zones. However, TRNSYS software cannot model the urban microclimate. Thus, the street canyon building is modelled as an outdoor environment, whereas the radiative model does not consider either the shortwave or the longwave inter-reflections between the facades of street canyon buildings.

The principal aim of this research work is to investigate the influence of microclimatic phenomena generated by the street canyon on the thermal behaviour of a building. The street canyon is modelled by a simplified approach developed in previous studies [23]. In this approach, the radiative model is based on the Gebhart factor [32] to calculate radiative exchanges and inter-reflections as well as the solar radiation distribution coefficients. So to apply this approach, the street canyon is modelled by a single zone (an atrium with an open ceiling and virtual borders). However, the virtual layer must not interfere with the heat transfer between the canyon and the outside environment. Typically, TRNSYS software does not allow to model such openings and some artefacts are used for this virtual wall [33]:

- 1) The thermal resistance of the virtual layer is defined with a very low value (massless layer with very low resistance);
- 2) The convective heat transfer coefficient should be negligible because the heat transfer by convection between the street canyon zone and the ambient air is considered in the specific wind model. This coefficient is therefore set at a very low value (0.001 W/m²K);
- 3) The solar radiation is correctly transmitted to the canyon surfaces because this layer is transparent. However, the TRNSYS software does not consider surface transparency for longwave balance. Therefore, the virtual layer temperature has to be set to the sky temperature.

This latter condition is obtained through an additional heat loss for the virtual surface (4) presented in Fig. 2, see Equations (5) and (6). The sum of longwave radiation to the sky through the virtual surface are represented in Fig. 2.

$$Q_{g,1} + Q_{g,2} + Q_{g,3} = Q_{g,4} \quad (5)$$

$$Q_{g,4} = A_4 \sigma (T_4^4 - T_{sky}^4) \quad (6)$$

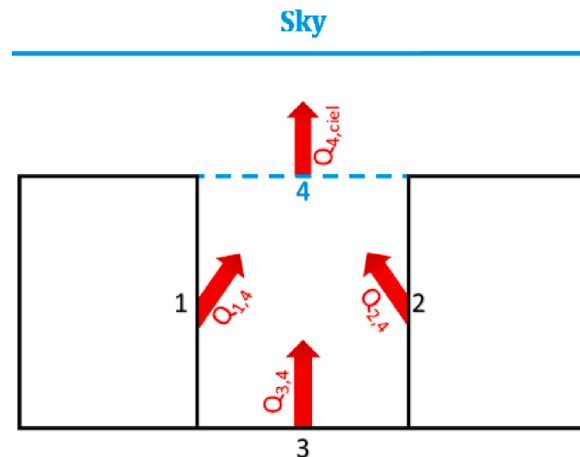


Fig. 2. Schematization of thermal radiation exchange.

$$T_{skyf} = (1 - f_{sky})T_a + f_{sky}T_{sky} \quad (7)$$

where f_{sky} is the sky-view factor seen by surface k, T_a is the ambient temperature and T_{sky} is the fictive sky temperature.

Longwave irradiance from other construction surfaces ($Q_{g,1}$, $Q_{g,2}$ and $Q_{g,3}$) is also based on Gebhart's factors [32]:

$$Q_{g,k} = A_k \varepsilon_k \sigma T_k^4 - \sum_{i=1}^n A_i \varepsilon_i \sigma T_i^4 G_{i,k} \quad (8)$$

$$G_{i,k} = (I - F_{i,k} \rho_k)^{-1} F_{i,k} \varepsilon_k \quad (9)$$

where Q_g is the longwave radiation flux, ε is the thermal emissivity, σ is the Stefan–Boltzmann constant and T is the surface temperature.

The aeraulic model, in this simplified approach, is based on the Soulhac model [34] to calculate the longitudinal wind velocity component U_{canyon} (equation (10)). The transverse wind velocity component u_i is calculated based on the Harman model [35] (equation (16)).

- Longitudinal wind velocity component:

$$U_{canyon} = U_H \cos(\phi) \frac{\delta_i^2}{HW} \left[\frac{2\sqrt{2}}{C} (1 - \beta) \left(1 - \frac{C^2}{3} + \frac{C^4}{45} \right) + \beta \frac{2\alpha - 3}{\alpha} + \left(\frac{W}{\delta_i} - 2 \right) \frac{\alpha - 1}{\alpha} \right] \quad (10)$$

with:

$$\alpha = \ln \left(\frac{\delta_i}{Z_{0,build}} \right) \quad (11)$$

$$\beta = e^{\frac{C}{\sqrt{2}} \left(1 - \frac{H}{\delta_i} \right)} \quad (12)$$

$$U_H = u_* \sqrt{\frac{\pi}{\sqrt{2}k^2 C} \left[Y_0(C) - \frac{J_0(C)Y_1(C)}{J_1(C)} \right]} \quad (13)$$

C is the solution for

$$\frac{Z_{0,build}}{\delta_i} = \frac{2}{C} \exp \left[\frac{\pi}{2} \frac{Y_1(C)}{J_1(C)} - \gamma \right] \quad (14)$$

$$\delta_i = \min \left(H; \frac{W}{2} \right) \quad (15)$$

where J_0 , J_1 , Y_0 and Y_1 are Bessel functions [36], ϕ is the direction of the external wind with respect to the axis of the street, $\gamma = 0.57$ is the Euler constant, H and W are the street height and width, respectively, and $z_{0,build}$ is the roughness length of the canyon walls.

- Transverse wind velocity component:

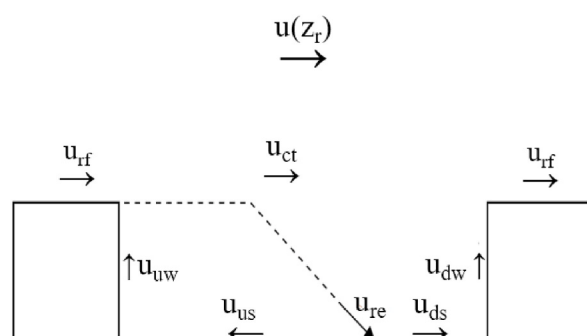


Fig. 3. Schematic of the transverse wind velocities in a street canyon [35].

$$u_i(x) = \frac{u(z_r) \sin(\phi)}{b} e^{-\alpha_1 \frac{L_{se}}{H}} \int_a^{a+b} e^{-\alpha_2 \frac{x}{H}} dx \quad (16)$$

$$u_{re} = u_{ct} e^{\frac{-\alpha_1 L_{se}}{H}} \quad (17)$$

with $u(z_r)$ the velocity at a reference height z_r , $\alpha_1 = 0.9$, $\alpha_2 = 0.15 \times \max(1, 1.5H/W)$, $u_i(x)$ represents the upstream wall (u_{uw}), upstream street (u_{us}), downstream street (u_{ds}) and downstream wall (u_{dw}) velocities (Fig. 3), while a and b are the integration limits related to the length of the canyon surface which the velocity calculation is performed, and $L_{se} = \sqrt{\frac{L_r^2}{4} + H^2}$ is the inclined edge length of the recirculation zone.

The roof (u_{rf}) and center (u_{ct}) velocities are calculated as a function of the wind velocity at a reference height z_r by extending the logarithmic profile of the inertial zone (equation (18) and equation (19)) [35].

$$\frac{u_{rf}}{u(z_r)} = \frac{\ln\left(\frac{H+\delta_{rf}-d}{Z_0}\right)}{\ln\left(\frac{z_r-d}{Z_0}\right)} \quad (18)$$

$$\frac{u_{ct}}{u(z_r)} = \frac{\ln\left(\frac{H-d}{Z_0}\right)}{\ln\left(\frac{z_r-d}{Z_0}\right)} \quad (19)$$

where. $\delta_{rf} = \min[0.1(R - W), (z_r - H)]$

To take into account the variations of the building type (high, medium or low), the orientation of the surface, the shelter effects by other buildings as well as the roughness of the surfaces on the convective heat transfer (equations (1) and (2)), the calculation of V_R and V_{loc} speeds [m/s], can be calculated based on the following formulas [23]:

$$V_R = u_{rf} \quad (20)$$

$$V_{loc} = \sqrt{U_{canyon}^2 + U_{re}^2} \quad (21)$$

The originality of the method used lies in its capacity to model the microclimatic phenomena generated by the neighbourhood, in order to take them into account in a dynamic thermal simulation software for buildings. More details of the simplified approach are reported in a previous study where a reduced scale validation process has been performed [23].

2.2. Comparison of the numerical model and experimental results

In order to validate the developed model on a larger scale, the results were compared with the experimental measurements of the EM2PAU campaign [37,38]. The EM2PAU system represents a street canyon on a scale of 1/2, consisting of two rows: 24 m long, 3.6 m wide and 5.2 m high, giving an aspect ratio H/W (with H: height of the building, W: street canyon width) of 1.4. Each building row was L = 24 m in length, H = 5.2 m in height, and B = 2.45 m in width (Fig. 4-a). The street is oriented 43° to North direction. For the determination of soil roughness, the decomposition method [37,38] is used and the roughness length of the containers is 0.01 m [39] (Fig. 4-b).

Table 1 below presents the thermophysical properties of materials used in the measurement campaign EM2PAU. Where: α is the albedo, ϵ is the emissivity, λ is the conductivity, ρ is the density and C_p is the heat capacity.

Concerning meteorological data (Fig. 5), a TMY2 file was created from experimental measurements of the EM2PAU campaign during the period from April 06, 2011 to April 09, 2011. The results analysed below correspond to the temporal temperature variation

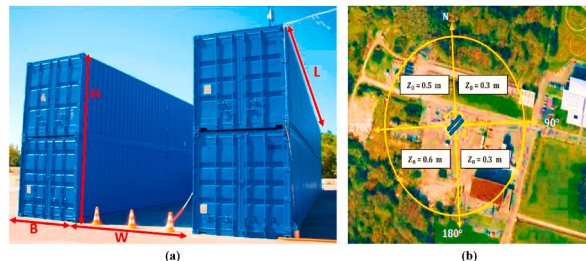
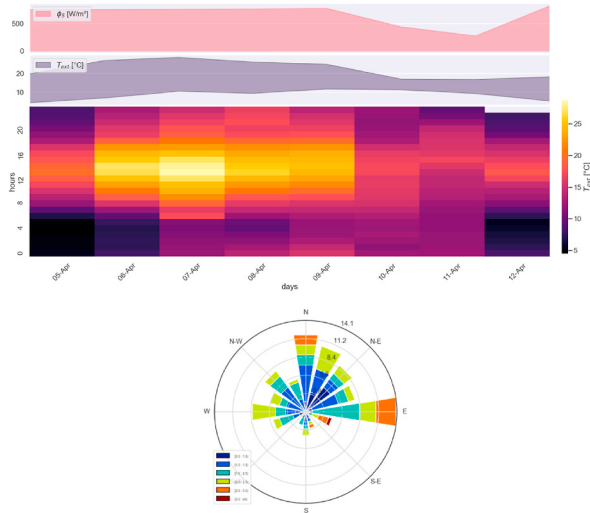


Fig. 4. (a) Dimensions of EM2PAU buildings [38], (b) Ground roughness around the EM2PAU containers [37,38].

Table 1

Thermophysical properties of building and soil materials [37,38].

Materials	Thickness [cm]	α	ϵ	λ [W/m ² .K]	ρ [Kg/m ³]	C_p [J/Kg.K]
Steel	0.25	0.2	0.8	52	7830	500
Air layer	15	–	–	0.04	1.25	1000
Extruded Polystyrene	45	–	–	0.032	35	1450
Asphalt	5	0.17	0.91	2.4	1600	950
Soil	50	–	–	1.3	1600	1100

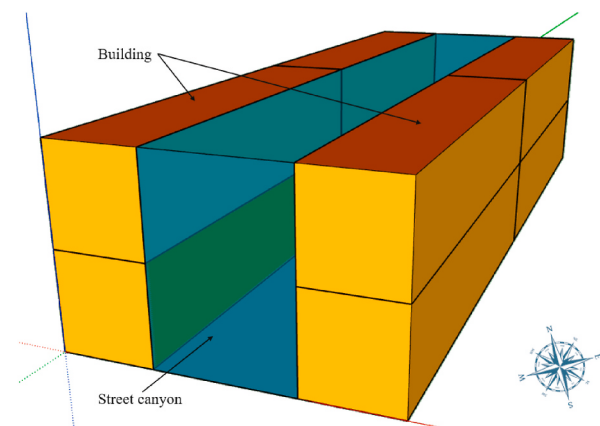
**Fig. 5.** Meteorological data recorded at the experimental site and the local wind rose on the EM2PAU experiment [37,38].

of the East and West external surfaces. It should be noted that TMY2 are databases containing hourly values of solar radiation and meteorological elements such as air temperature, humidity and wind velocity.

The experimental mockup was modelled in the TRNSYS software with the specific models of street canyon presented in previous sections (Fig. 6).

2.2.1. Calculation of the surface temperature for the South-Western facade of the canyon

This comparative study shows a very good consistency between the results obtained using the numerical model for the South-Western surface and those of the EM2PAU measurement campaign [37,38] (Fig. 7-a) with a regression coefficient equal to 0.96 (Fig. 7-b). In this case, the mean absolute error is 1.46 °C, the mean relative error reaches 7.47% and the standard deviation is about 20.48 °C.

**Fig. 6.** 3D overview of TRNSYS simulation model.

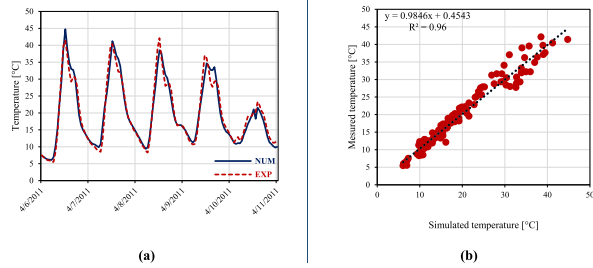


Fig. 7. (a) Temporal temperature variation of South-West surfaces and (b) Comparison of simulated and measured [37,38] temperature values for the South-West surfaces.

2.2.2. Calculation of the surface temperature for the North-Eastern facade of the canyon

As for the South-Western surfaces, a comparative study was conducted between the surface temperatures obtained numerically by the developed model and those of the North-Eastern experimental resulting from EM2PAU [37,38] (Fig. 8-a). In this case, the mean absolute error is 1.33 °C, the mean relative error reaches 6.87% and the standard deviation is about 19.88 °C. Concern at the regression coefficient R^2 is 0.97 (Fig. 8-b). Also, a small underestimation of the midday peaks and an overestimation of the morning minima are noted for both facades. These differences can be explained the hourly time-step chosen as the inlet boundary condition, thus creating smooth results that can explain the superior peaks. The same results have been observed by Athamena et al. [37,38] using the CFD to simulate the EM2PAU experiment.

The comparison between the results obtained using the numerical model and those of the EM2PAU measurement campaign led us to consider that this model can be used as an efficient tool for the energy modelling of buildings and the street canyon microclimate.

2.3. Description of the case study

In order to analyse the microclimatic impact on the energy performance of buildings, an energy modelling was carried out with the developed model for two different cases: a stand-alone building (SAB) in an open field by using only the TRNSYS software (Fig. 9-a) and the same building but located in a street canyon environment (Fig. 9-b). The street canyons have a length of 84 m and aspect ratios of 0.5, 1 and 2 are considered. In the set of simulation only one orientation for the street canyon axes was adopted: W-E. The studied building of the street canyon, has the same thermophysical properties and the same geometry as the stand-alone building.

The studied building consists of three floors with a length of 84 m, a width of 12 m and a height of 9 m (Fig. 9-a). For openings, the window to wall ratio is 25%. Table 2 below gives the thermophysical properties of building and soil materials used for building studied. Where: λ is the conductivity, C_p is the heat capacity and ρ is the density.

The following Table 3 shows the glazing characteristics used:

During the modelling, the internal gains due to the lighting system, electrical appliances, users and occupancy schedules are set according to residential use, as described by UNI [40]. The internal gains shown in Table 4 are related to the total floor area. The presence of occupants is taken into account throughout the day. The usage schedule for the electrical appliances is set "On" from 8:00 a.m. to midnight, while the usage schedule for the lights is set "On" from 5:00 p.m. to midnight.

The ventilation flow rate is taken as equal to 0.5 vol/h while the infiltration flow rate of the envelope is estimated to be equal to 0.2 vol/h. The set point temperatures for cooling and heating are respectively 26 °C and 20 °C. The climatic data used are those of the city of Tangier (Latitude: 35° 46'02" North Longitude: 5° 47'59" West) (Morocco) from Meteonorm software [41], which are illustrated in Fig. 10.

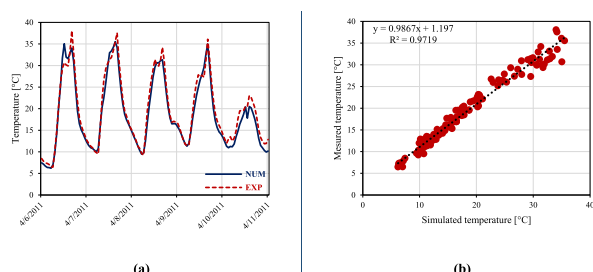


Fig. 8. (a) Temporal temperature variation of North-East surfaces and (b) Comparison of simulated and measured [37,38] temperature values for the North East surfaces.

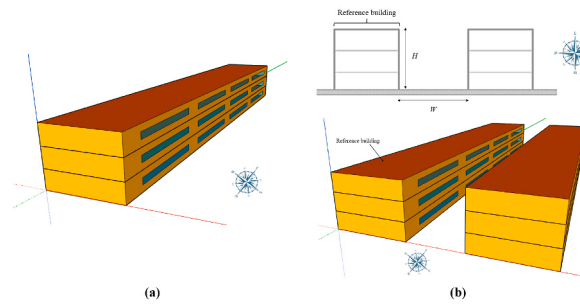


Fig. 9. (a) 3d overview of the stand-alone building, (b) Overview of the street canyon.

Table 2

Thermophysical properties of building and soil materials used [14].

Envelope element	Materials	Thickness [cm]	λ [W/m ² .K]	C_p [J/Kg.K]	ρ [Kg/m ³]
Outside Wall	Cement	1.5	1.15	1000	1700
	Brick	7	0.3	741	1200
	Air	10	—	1000	1.25
	Brick	7	0.3	741	1200
	Cement	1.5	1.15	1000	1700
Adjacent Wall	Cement	1.5	1.15	1000	1700
	Brick	7	0.3	741	1200
	Cement	1.5	1.15	1000	1700
Roof and ceiling	Tile	0.7	1.4	1000	2500
	Screed	5	0.42	1000	1800
	Concrete	4	2.3	1000	2350
	hollow block	16	0.6	880	1000
Ground floor	Cement	1.5	1.15	1000	1700
	Tile	0.7	1.4	1000	2500
	Screed	5	0.42	1000	1800
Sidewalk	Concrete	20	2.5	1000	2350
	Ceramics	0.7	1.4	1000	2500
	Concrete	10	0.04	1000	2350

Table 3

Windows characteristics.

Material	Thickness [mm]	U-value [W/m ² K]	G-value
Single glazing	Ordinary glass	2.5	5.74

Concerning the solar absorption coefficient, we have used 0.6 for walls and roofs and 0.8 for sidewalks of the street.

Table 4

Specific values of internal gains [40].

Appliance	Persons [W/m ²]	Appliances [W/m ²]	Lights [W/m ²]
Convective	3.01	1.05	1.5
Radiative	1.51	0.35	3.5

3. Numerical results and DISCUSSION

3.1. Assessment of the thermal impact of the microclimate at the street canyon scale

3.1.1. Effect of the street canyon on the absorbed solar radiation by building surfaces

The graphs of total absorbed solar radiation (sum of direct, diffuse and reflected radiation) are presented as values normalized to the radiation absorbed of the stand-alone building (Fig. 9-a). The results of the ground floor of the northern building are given for different aspect ratios of the street canyons (Reference building presented in Fig. 9-b). This choice is justified by the fact that it represents the highest influence of the neighbouring buildings on the radiation. In fact, the lower floors are for a longer time period protected from the sun at day-time due to shadowing by neighbouring buildings.

During the summer season (Fig. 11-a), it is observed that the normalized solar radiation absorbed by the South facade follows a

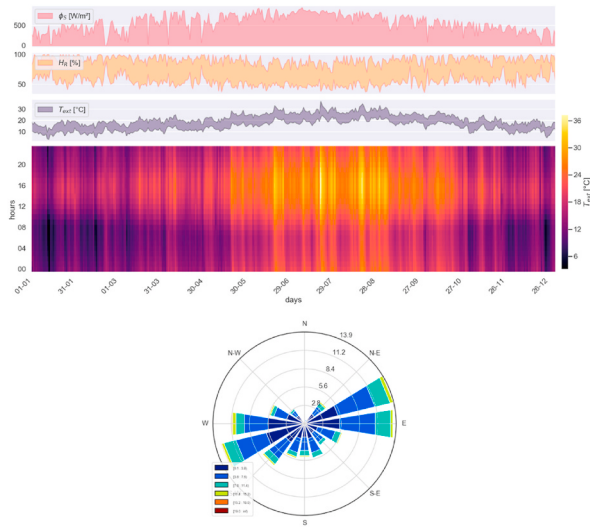


Fig. 10. Meteorological data of the city of Tangier (Morocco).

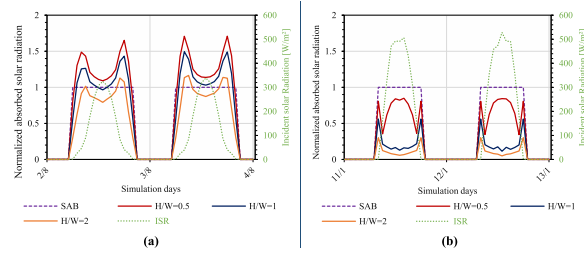


Fig. 11. Absorbed solar radiation on the South facade (a) during the summer season and (b) during the winter season.

classical daily pattern, increasing in the morning, peaking in the afternoon and decreasing in the evening. The direct dependence on the sun position is immediately apparent when comparing the trends of the South facade. In addition, in the case where the aspect ratio is equal to 0.5 ($H/W = 0.5$), i.e. the case of the widest street canyon, the exterior surfaces of the building receives and absorbs more radiation than the stand-alone building (SAB). This can be explained by the fact that more solar radiation can enter the canyon, the more it can be trapped due to the multiple reflections in the wider streets.

By analysing the curve $H/W = 2$ (case of the canyon of the narrow street) of Fig. 11-a below and by comparing it with other configurations, it appears clearly that the radiation is less absorbed, because the facade is more protected from direct sunlight. The solar radiation on a south facade is less sensitive to the aspect ratio (H/W), because direct solar radiation is more important than the contribution of different reflections of the neighbouring building facades. The same conclusions can be deduced for the winter season, as clearly shown in Fig. 11-b, the short duration of the day can be observed.

3.1.2. Analysis of the effect of a street canyon on the global radiation absorbed by building surfaces

In this part, the effect of a street canyon type on the global radiation absorbed by the building surfaces is studied and analysed. In Fig. 12, the global radiation (the sum of solar radiation and long-wave radiation) of the East facade of the building's ground floor. In the summer season (Fig. 12-a), during daytime hours when the facades receive direct solar radiation, starting from the stand-alone building case, net global radiation decreases, as we approach more narrow canyon configurations. This means that the highest peak radiation corresponds to the stand-alone building (SAB) case and the lowest to the $H/W = 2$ case. In the hours when the facade is shaded, the values of the net global radiation absorbed by the stand-alone building shaded facade fall below all the other cases. During the night, negative values of total radiation are observed, which can be explained by the long wave radiation towards the cold sky. In the street canyon configurations, this effect is greatly reduced due to blockage by neighbouring buildings. The blockage effect is greater for narrow street canyons than for wide street canyons. On both facades, the total radiation is much higher for buildings in the street canyon configuration than for those in the stand-alone building configuration, because the stand-alone building does not receive any long-waves radiation reflected from neighbouring buildings and the fraction of sky seen by the stand-alone building facades is greater than in the case of the street canyon building. In fact, when considering the contribution of the long-wave radiation exchange, the skyward heat dispersion of the building is predominant. Also, it can be seen that the total radiation on the facades increases with the width of the street canyons. Wider street canyons receive more total radiation, resulting in higher entrance values and more

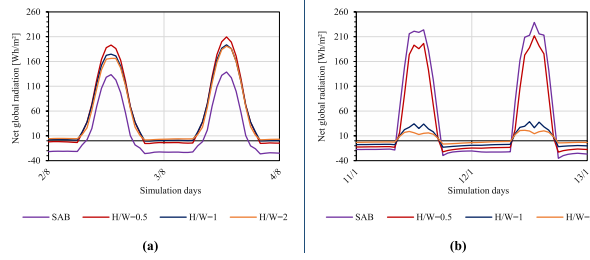


Fig. 12. Global radiation absorbed on the east facades (a) during the summer season and (b) during the winter season.

entrapment of solar radiation. For the winter season, whose graphic is reported in Fig. 12-b, the same conclusions are valid.

3.1.3. Analysis of the effect of street canyon on the building surface temperature

In this section, the influence of a street canyon on the exterior surface temperature of the building is studied numerically by the developed model and the results obtained are analysed. Fig. 13 shows the values of the surface temperature of the facade of the ground floor of the building. In the summer, the values of this temperature of facade follow the global trends of the radiation (Fig. 13-a), since the surface temperature is strongly related to the net radiative heat flux. Another influencing factor is the convective heat transfer at the surface. In the case of winter (Fig. 13-b), a turnaround in the temperature trend is observed on the South facade for the stand-alone building. This is closely related to the increased global radiation which this facade received compared to the same facades of other urban configurations.

3.2. Effect on heating and cooling energy needs

In this part, the building heating and cooling energy needs are analysed. From the results obtained by the developed model for the summer season, presented in Fig. 14-a, the energy needs of the different configurations show that the cooling energy needs of a building located in a large street canyon with an aspect ratio equal to 0.5 ($H/W = 0.5$) is higher than those of a building located in a narrow street canyon ($H/W = 2$) and also they are higher than those of a stand-alone building. Indeed, the wide street canyon can receive more solar radiation than the narrow street canyon and therefore there are more trapped radiation in the case of a wide street canyon. In addition, the shading effect is greater in the case of a narrow street canyon than in the case of a wide street canyon.

For the winter season, the results presented in Fig. 14-b show that the case of aspect ratio of $H/W = 0.5$ is the most advantageous configuration. This is due to the solar radiation being the driving force behind variations in energy needs. Therefore, if more solar radiation reaches the building envelope, heating system requires less energy.

In addition, the comparison between the results obtained by using TRNSYS 18 only and by using the developed approach showed that the estimated demand determined by TRNSYS 18 is overestimated. It is found that the cooling energy needs for SAB configuration, is higher than $H/W = 1$ (+6%) and $H/W = 2$ (+29%) cases, while is lower than the $H/W = 0.5$ (-15%) case. Regarding the heating demands, it is found that of SAB configuration is lower than $H/W = 0.5$ (-16%), $H/W = 1$ (-52%) and $H/W = 2$ (-97%) cases. These results are due to the fact that the TRNSYS 18 does not take into account the microclimate generated by the street canyon, such as the radiative trapping phenomenon that is produced by the multiple inter-reflections between the canyon surfaces.

4. Conclusion

This research aims to study the impact of urban microclimate on building energy needs. To do this, a simplified model developed and integrated in TRNSYS 18 software in a previous work has been validated and used. This new model takes into account the effects of prevailing winds, solar radiation and inter-reflections. With this model, a comparative study was conducted between the energy needs in winter and summer for a stand-alone building and for the same building located in a street canyon in the city of Tangier in Morocco.

First, the results obtained show the importance of taking into account the effect of the street canyon microclimate when forecasting the building energy needs, instead of using only building energy simulation software. Indeed, in the case of buildings located in street

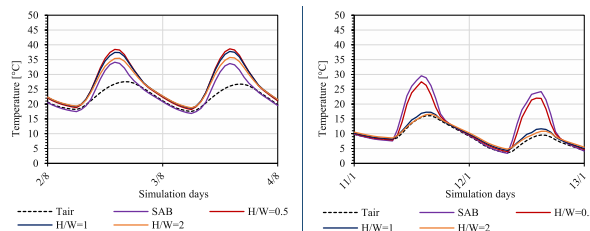


Fig. 13. Surface temperature on the South facades (a) during the summer season and (b) during the winter season.

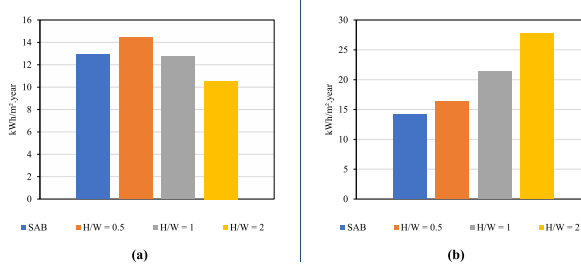


Fig. 14. (a) Cooling energy needs, (b) Heating energy needs.

canyons, the radiation of long wavelengths towards the cold sky is partially blocked. This is the reason why the surface temperatures of the facades of buildings in rural areas are always lower than those of configurations in urban areas. The higher temperatures of the facades then directly lead to an increase in the building's cooling needs in summer and a decrease in heating needs in winter.

Secondly, the aspect ratio of the canyon has a very important role. The results show that during the summer period, the configuration with an aspect ratio equal to 0.5 is the most unfavourable in terms of radiative exchange at long wavelengths. As a result, wider street canyons receive more solar radiation than other configurations, resulting in more radiation trapping, but heat dissipation to the sky is obstructed. This causes an increase in surface temperatures of the facades increasing cooling requirements in summer. In terms of heating energy requirements in winter, the most disadvantageous configuration is the one whose aspect ratio is equal to 2. This is because narrow canyons, radiation input is reduced during the day due to shading, while at night, the blocking of long-wave radiation to the sky increases.

Finally, the results obtained show that the use of the TRNSYS software only without taking into account the microclimate close to the building, leads to an incorrect estimation of the building energy needs. Consequently, this may potentially contribute to correct errors of the dimensioning of heating and cooling systems in buildings.

CRediT authorship contribution statement

Adnane M'Saouri El Bat: Conceptualization, and design of study, Data curation, Formal analysis, Writing - original draft, Approval of the version of the manuscript to be published. **Zaid Romani:** Conceptualization, and design of study, Writing - review & editing, critically for important intellectual content, Approval of the version of the manuscript to be published. **Emmanuel Bozonnet:** Approval of the version of the manuscript to be published. **Abdeslam Draoui:** Writing - review & editing, critically for important intellectual content, Approval of the version of the manuscript to be published.

Declaration of competing interest

No conflict interest.

References

- [1] A. Cantelli, P. Monti, G. Leuzzi, Numerical study of the urban geometrical representation impact in a surface energy budget model, *Environ. Fluid Mech.* 15 (2015) 251–273, <https://doi.org/10.1007/s10652-013-9309-0>.
- [2] N.E. Theeuwes, G.J. Steeneveld, R.J. Ronda, B.G. Heusinkveld, L.W.A. Van Hove, A.A.M. Holtslag, Seasonal dependence of the urban heat island on the street canyon aspect ratio, *Q. J. R. Meteorol. Soc.* 140 (2014) 2197–2210, <https://doi.org/10.1002/qj.2289>.
- [3] E.R. Marciotti, A.P. Oliveira, S.R. Hanna, Modeling study of the aspect ratio influence on urban canopy energy fluxes with a modified wall-canyon energy budget scheme, *Build. Environ.* 45 (2010) 2497–2505, <https://doi.org/10.1016/j.buildenv.2010.05.012>.
- [4] A. Tsiringakis, G. Steeneveld, A.A.M. Holtslag, S. Kotthaus, S. Grimmond, On-and off-line evaluation of the single-layer urban canopy model in London summertime conditions, *Q. J. R. Meteorol. Soc.* 145 (2019) 1474–1489, <https://doi.org/10.1002/qj.3505>.
- [5] E. Bozonnet, R. Belarbi, F. Allard, Thermal Behaviour of buildings: modelling the impact of urban heat island, *J. Harbin Inst. Technol. (New Ser.)* 14 (2007) 19–22.
- [6] J. Allegrini, V. Dorer, J. Carmeliet, Influence of the urban microclimate in street canyons on the energy demand for space cooling and heating of buildings, *Energy Build.* 55 (2012) 823–832, <https://doi.org/10.1016/j.enbuild.2012.10.013>.
- [7] A. Vallati, A. De Lieto Vollaro, I. Golasi, E. Barchiesi, C. Caranese, On the impact of urban micro climate on the energy consumption of buildings, *Energy Procedia* 82 (2015) 506–511, <https://doi.org/10.1016/j.egypro.2015.11.862>.
- [8] A. Salvati, M. Palme, G. Chiesa, M. Kolokotroni, Built form, urban climate and building energy modelling: case-studies in Rome and Antofagasta, *J. Build. Perform. Simul.* 1–17 (2020), <https://doi.org/10.1080/19401493.2019.1707876>.
- [9] G. Pappaccogli, L. Giovannini, F. Cappelletti, D. Zardi, Challenges in the application of a WRF/Urban-TRNSYS model chain for estimating the cooling demand of buildings: a case study in Bolzano (Italy), *Sci. Technol. Built Environ.* 24 (2018) 529–544, <https://doi.org/10.1080/23744731.2018.1447214>.
- [10] D. Robinson, F. Haldi, J. Kämpf, P. Leroux, D. Perez, A. Rasheed, U. Wilke, Citysim: comprehensive micro-simulation of resource flows for sustainable urban planning, *IBPSA 2009 – Int. Build. Perform. Simul. Assoc.* (2009) 1083–1090, 2009.
- [11] V. Masson, A physically-based scheme for the urban energy budget in atmospheric models, *Boundary-Layer Meteorol.* 94 (2000) 357–397, <https://doi.org/10.1023/A:1002463829265>.
- [12] M. Musy, L. Malys, B. Morille, C. Inard, The use of SOLENE-microclimat model to assess adaptation strategies at the district scale, *Urban Clim.* 14 (2015) 213–223, <https://doi.org/10.1016/j.uclim.2015.07.004>.
- [13] A. Gros, E. Bozonnet, C. Inard, Cool materials impact at district scale - coupling building energy and microclimate models, *Sustain. Cities Soc.* 13 (2014) 254–266, <https://doi.org/10.1016/j.scs.2014.02.002>.



Journal of Building Performance Simulation

ISSN: (Print) (Online) Journal homepage: <https://www.tandfonline.com/loi/tbps20>

Integration of a practical model to assess the local urban interactions in building energy simulation with a street canyon

Adnane M'Saouri El Bat , Zaid Romani , Emmanuel Bozonnet & Abdeslam Draoui

To cite this article: Adnane M'Saouri El Bat , Zaid Romani , Emmanuel Bozonnet & Abdeslam Draoui (2020) Integration of a practical model to assess the local urban interactions in building energy simulation with a street canyon, *Journal of Building Performance Simulation*, 13:6, 720-739, DOI: [10.1080/19401493.2020.1818829](https://doi.org/10.1080/19401493.2020.1818829)

To link to this article: <https://doi.org/10.1080/19401493.2020.1818829>



Published online: 14 Sep 2020.



Submit your article to this journal 



View related articles 



View Crossmark data 



Integration of a practical model to assess the local urban interactions in building energy simulation with a street canyon

Adnane M'Saouri El Bat ^a, Zaid Romani ^b, Emmanuel Bozonnet ^c and Abdeslam Draoui^a

^aTeam of Heat Transfer & Energetic, Faculty of Sciences and Techniques of Tangier (UAE/U10FST), Abdelmalek Essaâdi University, Tangier, Morocco; ^bNational School of Architecture Tetouan, Tetouan, Morocco; ^cLaSIE, La Rochelle University, La Rochelle, France

ABSTRACT

To improve the prediction of the building's energy performance, it has become necessary to evaluate their interactions with the urban microclimate. This study aims to propose an integrated model in the TRNSYS software with a simplified approach to assess building energy demand, including microclimate interactions on buildings. This model is based on thermoradiative and aeraulic modelling by considering the moisture transfer through the envelope. To evaluate the validity of this method, an urban canyon was modelled and compared with existing experimental results. The numerical results are close to the experimental observations with a mean absolute error of about 1°C for the outside surface temperature and a mean relative error of approximately 5%. The developed model has shown its potential in reducing an unexpected impact of interoperability when using several tools and to ensure shorter computation time compared to CFD calculations, with an accuracy satisfying the thermal and energy evaluation objectives.

ARTICLE HISTORY

Received 25 June 2020

Accepted 28 August 2020

KEYWORDS

Urban building energy model; urban microclimate; urban canyon; building energy needs

1. Introduction

The building sector remains a key contributor that have an important environmental impact due to its high energy consumption, since the large majority of energy used in buildings is derived from non-renewable fossil such as fuel resources. According to the IEA (IEA 2018), the building sector is responsible for the world's final energy consumption by 30%, the world's electricity consumption by more than 50% and CO₂ emissions by 25%.

It should also be noted that to ensure an adequate indoor climate and thermal comfort, more than 60% of building energy consumption is attributed to heating, ventilation and air conditioning systems (Manzano-Agugliaro et al. 2015; Chan, Riffat, and Zhu 2010; Pérez-Lombard, Ortiz, and Pout 2008). Consequently, they are the major sources of energy use in buildings and of greenhouse gas (GHG) production (IEA 2018). Moreover, building energy consumption is influenced by occupant behaviour (Pantazaras et al. 2018; Gaetani, Hoes, and Hensen 2016; Hong et al. 2017), building facilities (Hepbasli 2012), building envelope (Pacheco, Ordóñez, and Martínez 2012; De Boeck et al. 2015; Van Hooff et al. 2015) and the building design (Bektaş Ekici and Teoman Aksoy 2011). Therefore, estimating the building's energy needs is the key to controlling its energy performance and consequently reduce its environmental impact.

In order to predict energy requirements and thermal comfort, building energy simulation (BES) was first developed with simplified weather conditions. These BES tools are widely used and developed in building design such as TRNSYS, EnergyPlus or ESP-r, etc. Weather data are generally given for a typical year from weather stations located in rural areas. However, this weather data is not representative of the external environment for a building located in an urban area.

Land-site, constructions and human activities generate climatic phenomena, which can have impact on the climatic environment specific to each building. The interaction of heat and mass transfer phenomena in urban fabric, with anthropogenic parameter, contributes to particular microclimatic phenomena. Urban heat island (UHI) is the most representative of these phenomena (Yezioro, Dong, and Leite 2008; Santamouris 2007; Kolokotroni, Giannitsaris, and Watkins 2006; Musco 2016; Gartland 2012; Sun and Augenbroe 2014). In this sense, the knowledge and consideration of urban climate impact is essential for a better building energy modelling (Bouyer, Inard, and Musy 2011; Moonen et al. 2012; Jamei et al. 2016; Mills 2014; Yang et al. 2012).

Numerous studies have investigated urban microclimate and its impact on buildings energy demand (Salvati et al. 2020; Lauzet et al. 2016; Rodler et al. 2018; Vallati,

Mauri, and Colucci 2018; Gros et al. 2016; Asawa, Hoyano, and Nakaohkubo 2008; Malys, Musy, and Inard 2015; Selakov, Milos, and Savic 2014; Sun et al. 2014; Miller et al. 2018). Among the models that have been developed, Bozonnet, Belarbi, and Allard (2007) studied the impact of urban microclimate on building energy demand for street canyon using coupled heat and airflow modelling with zonal model. Bouyer (2009) has developed a dynamic simulation platform based on the coupling of a thermoradiative model (Solene) and a computational fluid dynamic programme (Fluent), in order to assess interactions between buildings and urban microclimate and to define impacts of urban planning on building energy consumption. Then, Robinson et al. (2009) has developed a model called CitySim that permits the determination of building energy needs in a neighbourhood. This model is constituted by a simplified thermal building model, based on the electrical analogy (resistance-capacitor). The radiation model is based on the simplified radiosity algorithm SRA (Simplified Radiosity Algorithm). However, this model shows a lack of water and vegetation modelling. Also, its simplified building energy model may be unsatisfactory for the energy design of buildings.

Athamena (2012) has studied the impact of the specific urban morphological heterogeneity of eco-districts on the thermal comfort of outdoor public spaces. Within this framework, he developed a numerical model based on the coupling of a CFD model (Code_Saturne) and a thermoradiative model (Solene). Yang et al. (2012) have developed a model for evaluating the effects of microclimate on the building's energy performance. In this model, a coupling between the ENVI-met microclimate model and the EnergyPlus building energy simulation software is realised.

Gros et al. (2014) proposed a numerical model coupling building energy simulation to urban microclimate by using the Solene and EnviBatE software. This model was applied to the Pin-Sec district of Nantes city in France for different scenarios. More recently, Daviau-Pellegrin (2016) has coupled a computational fluid dynamics model (Code_Saturne) with the BuildSysPro building model to simulate the energy exchanges between urban atmosphere and buildings. These models are generally detailed and more appropriate for district-scale studies because they allow to accurately take into account local urban environment effects. Nevertheless, their use is complex due to the high computation time and the coupling between several software. Furthermore, these tools are unable to model the thermal behaviour of buildings with precession such as building energy simulation tools.

Bueno et al. (2013) proposed the Urban Weather Generator (UWG) to estimate the air temperature in the urban

canopy layer using meteorological information collected by an operational weather station. This model uses input parameters that describe urban morphology, geometry and surface materials. It is composed of four coupled modules (Lauzet et al. 2019): the rural station model (forcing temperature), the vertical diffusion model, the urban boundary layer model, and the urban cover and Building Energy Modeling (BEM). Based on this chain of models, rural temperatures can be translated into urbanized temperatures for a specific city site (Lauzet et al. 2019). It can be extended for city scale simulations. However, the influence of the position and orientation of the surrounding buildings and the terrain in UWG is unknown. For example, the orientation and inclination of slopes may have seasonal effects. Other limitations of the UWG is that it cannot reproduce the impact of surrounding objects on wind movement.

There are some other studies on urban microclimate modelling using the building energy software TRNSYS (Djedjig, Bozonnet, and Belarbi 2016; Masson 2000; Vallati et al. 2017), including those devoted to urban canopy modelling. These models are used to describe the interaction between mesoscale and urban canopy and generally defined by a simplified urban morphology consisting of street's elementary cell or repeated urban blocks. They can be used to predict with acceptable accuracy the intensity of microclimatic phenomena such as urban heat islands. Among these urban canopy models, the Town Energy Budget model (TEB) (Masson 2000) that evaluates the average airflow, turbulent flows, energy and vapour transfers between the urban canopy and the atmosphere, including anthropogenic heat and humidity sources from buildings and road traffic. TEB is also used with SURFEX modelling platform to simulate different types of urban surfaces, composed of different building materials, water or vegetated surfaces (Lemonsu et al. 2012). Djedjig, Bozonnet, and Belarbi (2016) have proposed a green wall hygrothermal model coupled with the Harman model (Harman, Barlow, and Belcher 2004) to simulate mass flows in street canyons using TRNSYS software. However, this model does not integrate all of the radiative exchanges between the different canyon surfaces. Allegri, Dorer, and Carmeliet (2012) used also the TRNSYS software to simulate a street canyon in order to analyse the impact of its aspect ratio and its orientation on building energy needs considering the longwave radiation exchange. In this study, the street canyon was modelled as an open atrium and only radiation exchanges were considered, so that the indoor radiation model using Gebhart factors was applied to evaluate the multiple reflection effect of solar and thermal radiation in street canyon.

Indeed, there is a lack of a modelling approach for radiative, aeraulic and hygrothermal exchanges allowing the simulation of the urban microclimate impact on building energy performance in a single software without using CFD. In this context, this study proposed a simplified approach with TRNSYS 18 software. This allows the description of airflows and thermoradiative balances coupled at building and street scales. The radiative model is based on the Gebhart factor (Gebhart 1961) to calculate radiative exchanges and inter-reflections as well as the solar radiation distribution coefficients. The airflow model is based on Harman, Barlow, and Belcher (2004) and (Soulhac, Perkins, and Salizzoni 2008) models which allows to take into account the effects of prevailing winds. In addition, a moisture transfer model has been applied for inside and outside building surfaces. It is based on the 'effective moisture penetration depth' (EMPD) model coupled with dynamic heat transfer. To assess the quality of the model developed, the numerical results were compared with 'ClimaBat' experimental measurements (Doya, Bozonnet, and Allard 2012; Djedjig, Bozonnet, and Belarbi 2016; Djedjig, Bozonnet, and Belarbi 2015).

2. Method

2.1. Thermoradiative model

The thermoradiative model proposed for the street was developed using TRNSYS 18 software (Klein et al. 2010). In this BES software, heat transfers through thermal conduction are modelled by transfer functions. Convective heat transfers are modelled either with constant average coefficient or with specific correlations. Radiative balances are computed for both shortwave (wavelengths lower than $2.5 \mu\text{m}$) and longwave (higher than $2.5 \mu\text{m}$). These radiative exchanges are modelled differently for indoor zones between wall surfaces and outdoor surfaces with a simplified environment modelled from sky view factor and the surroundings albedo.

However, TRNSYS is not fit for urban environment and a street canyon is characterized by the phenomenon of radiative trapping which affects the energy balance and is materialized by the multi-reflection's radiation on the different surfaces. In the proposed model, the TRNSYS outdoor conditions are replaced with a street canyon zone which is modelled with an open ceiling and virtual edges, transparent to radiative exchanges (opened windows). The canyon is then considered as a specific thermal zone, in which the effects of radiative inter-reflections are evaluated and also the shading due to neighbouring buildings can be modelled more precisely.

2.1.1. Solar radiation modelling

For interior surfaces of the building, direct and diffuse solar radiation are not processed in the same way by TRNSYS software. The distribution of direct radiation can be specified by the user, in contrast to diffuse radiation. Two options are available to model direct solar radiation: a fast and simplified model or a detailed model with view factors.

Due to limitations of the detailed model, such that the direct radiation entering an area through adjacent windows (external building windows) cannot be modelled, the fast and simplified model was chosen. In our proposed model, for each time step, the solar radiation distribution is computed with specific coefficients, which depend on solar angles and surface orientations. Solar radiation entering the zone is then distributed to all surfaces as diffuse radiation with these weighting coefficients (sum of all values of these coefficients is not allowed to exceed 1 within a zone).

The calculation of the distribution coefficients was carried out over all surfaces with the exception of the opened boundaries (virtual windows). This coefficient represents the fraction of the total entering direct solar radiation that strikes the surface. In the case of a street canyon morphology, these coefficients GS_j are determined by formula (1) which take into account the solar masks. For this purpose, we have developed a calculation code using Python language which is implemented in TRNSYS.

$$GS_j = \frac{A_j - A_{sj}}{\sum_i (A_i - A_{si})} \quad (1)$$

where A_j and A_{sj} are respectively the areas of the considered wall (j) and of the shadow on this same wall. As well, A_i and A_{si} are respectively the areas of the remaining walls and their shadows on the (i) wall.

In order to determine the surface A_{sj} , we propose an analytical method for an urban canyon. This shadow surface depends on azimuth (θ_s) and zenith (φ_s) solar angles. These angles are determined by TRNSYS model. Then Equations (2) and (3) are used to calculate A_{sj} for walls and road respectively.

$$A_{sj} = \frac{1}{2} \left| \sum_{j=0}^{n-1} (z_j y_{j+1} - z_{j+1} y_j) \right| \quad (2)$$

$$A_{sj} = \frac{1}{2} \left| \sum_{j=0}^{n-1} (x_j y_{j+1} - x_{j+1} y_j) \right| \quad (3)$$

where x_j , y_j , z_j are the coordinates of the projected shadow, and I_j is the projection of this shadow on the xy, yz or xz plane.

$$x_j = I_j \sin \theta_s \quad (4)$$

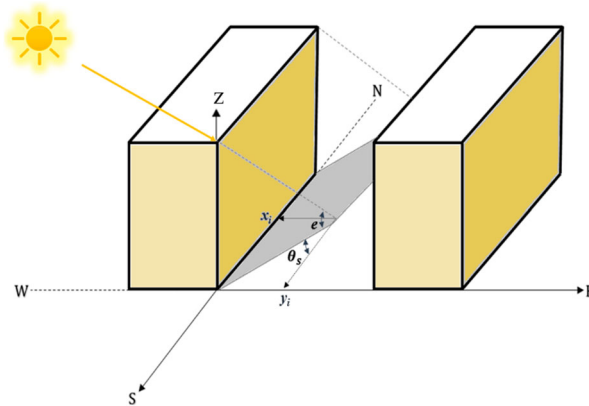


Figure 1. Schematization of the shadow projection on the ground.

$$y_j = l_j \cos \theta_s \quad (5)$$

$$l_j = \frac{H}{\tan e} \quad (6)$$

$$e = 90^\circ - \varphi_s \quad (7)$$

z_j is determined as a function of x_j .

Figure 1 illustrates the projection of shadow on the ground.

For the distribution of direct solar radiation through the adjacent openings (windows) of the street canyon we have adopted the method proposed by Chatzigeorgiou and Bouris (2009). The total quantity of solar radiation entering through an opening i ($Q_{dir,i}$) is distributed among the other five internal surfaces according to the view factors ($F_{i \rightarrow j}$) given by the formula (8).

$$Q_{dir,i} = \sum_j^n F_{i \rightarrow j} Q_{dir,i} \quad (8)$$

The total direct radiation entering a zone of the building is then defined as follows:

$$Q_{dir,tot} = \sum_{j=1}^n GS_j \sum_{i=1}^n Q_{dir,i} \quad (9)$$

where: GS_j is the distribution coefficient.

As the total direct solar radiation entering a zone the building is then given by the following formula:

$$Q_{dir,tot} = \sum_{i=1}^n Q_{dir,i} = \sum_j^n \sum_i^n F_{i \rightarrow j} Q_{dir,i} \quad (10)$$

Distribution coefficient GS_j of the building's interior surfaces are finally given as follows:

$$GS_j = \frac{\sum_i^n F_{i \rightarrow j} Q_{dir,i}}{\sum_i^n Q_{dir,i}} \quad (11)$$

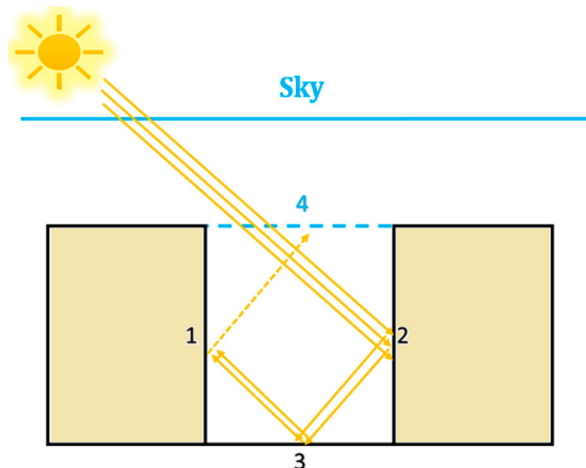


Figure 2. Scheme of the solar radiation trapping model.

The absorbed solar energy is then computed with the solar absorption coefficient α_s (Based on thermal properties of materials and their effective area relative to the solar access). The reflected radiation is taken into account with a detailed model of the diffuse radiation of TRNSYS based on Gebhart's factors (Gebhart 1961; Klein et al. 2010) which allows to include the multi-reflections of solar radiation (Figure 2). These factors are calculated by Equation (12).

$$\mathbf{G}_{i,k} = (\mathbf{I} - [F_{i,k}\rho_k])^{-1} \mathbf{F}_{i,k} (\mathbf{I} - [F_{i,k}\rho_k]) \quad (12)$$

where $\mathbf{G}_{i,k}$ is the Gebhart factor matrix; given the indexes i of one surface exchanging with other surfaces indexed k ; \mathbf{I} is the identity matrix; $\mathbf{F}_{i,k}$ is the view factor matrix and ρ_k is the reflectivity of the surface indexed k .

The solar radiation fluxes in the semi-closed volume of the street is calculated as follows:

$$Q_{s,k} = A_k (1 - \alpha_k) I_{s,k} + \sum_{i=1}^n A_i G_{i,k} \alpha_i I_{s,i} \quad (13)$$

With n is the surface number, i is one of the surfaces that exchanges shortwaves radiation with the considered surface k , Q_s is the shortwave radiation flux, A is the area, α is the surface albedo and I_s is the solar irradiance.

2.1.2. Longwave radiation modelling

Longwave irradiance from other construction surfaces is also based on Gebhart's factors (Gebhart 1961):

$$Q_{g,k} = A_k \varepsilon_k T_k^4 - \sum_{i=1}^n A_i \varepsilon_i T_i^4 G_{i,k} \quad (14)$$

$$G_{i,k} = (\mathbf{I} - F_{i,k}\rho_k)^{-1} F_{i,k} \varepsilon_k \quad (15)$$

where Q_g is the longwave radiation flux, ε is the thermal emissivity, σ is the Stefan–Boltzmann constant and T is the surface temperature.

The net longwave radiation to the sky (heat loss) is calculated by the following formula:

$$Q_{g,k} = A_k \varepsilon_k (T_k^4 - T_{fsky}^4) \quad (16)$$

$$T_{fsky} = (1 - f_{sky}) T_a + f_{sky} T_{sky} \quad (17)$$

where f_{sky} is the sky fraction seen by surface k , T_a is the ambient temperature and T_{sky} is the sky temperature.

As previously mentioned, the canyon is modelled by a single zone in the BES with an opened ceiling and virtual borders (noting that the street canyon between the buildings is modelled as an atrium within the building). However, the virtual layer must not interfere with the heat transfer between the canyon and the outside environment. Typically, BES software such as TRNSYS does not allow to model such openings and some artefacts are used for this virtual wall:

- The virtual layer thermal resistance is defined with a very low resistance (massless layer with very low resistance);
- The convective heat transfer coefficient should be negligible as convection between the street canyon zone and ambient air is considered in the specific wind model. So this coefficient is set to a very low value ($0.001 \text{ W/m}^2\text{K}$);
- The solar radiation is correctly transmitted to the canyon surfaces because this layer is transparent. However, the BES model does not consider surface transparency for longwave balance. Therefore, the virtual layer temperature has to be set to the sky temperature.

This latter condition is obtained through an additional heat loss for the virtual surface (4), see Equations (19) and (18). The sum of longwave radiation to the sky through the virtual surface are represented in Figure 3.

$$Q_{g,1} + Q_{g,2} + Q_{g,3} = Q_{g,4} \quad (18)$$

$$Q_{g,4} = A_4 (T_4^4 - T_{fsky}^4) \quad (19)$$

2.1.3. Heat and moisture transfer model of walls

In the multizone building model of TRNSYS (TRNBuild), the transient conduction heat transfer through the walls is modelled by using the transfer function method of Mitalas and Stephenson (Stephenson and Mitalas 1970). This method consists in determining transfer functions for 1-D conduction heat transfer through walls by solving the conduction equation with Laplace and Z-transform theory. The calculation of the transfer function coefficients depends on the properties of each layer constituting the wall (density, heat capacity, conductivity and thickness) (Klein et al. 2010).

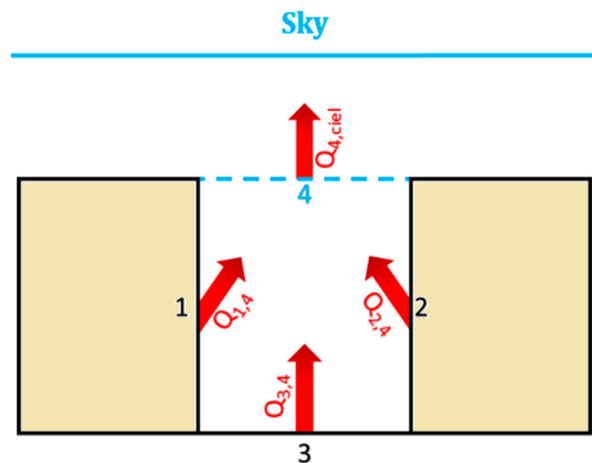


Figure 3. Schematization of thermal radiation exchange.

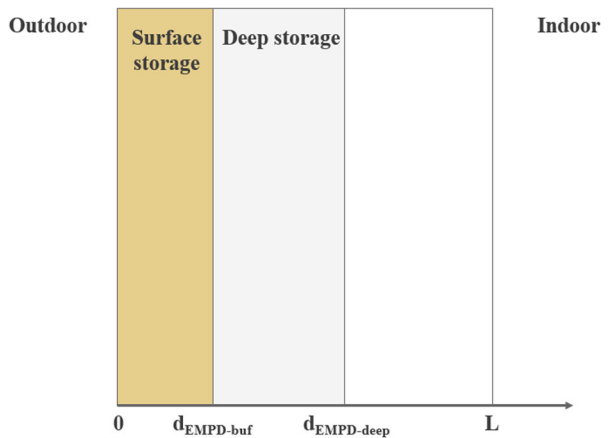


Figure 4. EMPD-model including surface buffer and deep buffer.

Modelling moisture transfer through the walls was performed using the effective moisture penetration depth (EMPD) model (M J Cunningham 1988; Kerestecioglu and Gu 1989; Malcolm J Cunningham 1992). The wall behaviour is represented by two layers; a surface storage layer, having a d_{EMPD} thickness, that reacts with the humidity of the zone and a deep storage layer that exchanges the humidity with the surface storage layer (Figure 4). The d_{EMPD} thickness depends on the period of the moisture variation cycle and the moisture storage and sorption properties of the material.

The effective penetration depth d_{EMPD} is calculated by Equation (20), in which $\delta(\phi)$ is the vapour permeability of the materials [$\text{kg/s}\cdot\text{m}\cdot\text{Pa}$], ϕ is the relative humidity [%], P_{sat} is the saturated vapour pressure [Pa] at temperature T [$^\circ\text{C}$], t_p is the humidity cycle period [s], ρ the density of the material [kg/m^3], $\xi(\phi)$ is the moisture capacity in terms of humidity derived from the material sorption

isotherm [kg/kg].

$$d_{EMPD} = \sqrt{\frac{\delta(\phi)P_{sat}(T)t_p}{\rho\xi(\phi)\pi}} \quad (20)$$

The saturated vapour pressure P_{sat} can be calculated as a function of the temperature according to the following empirical expression (Lin et al. 2006):

$$P_{sat} = 610.5e^{(17.269T/237.3+T)} \quad (21)$$

The following differential equations describe the dynamics of the water content of the surface and the deep storage.

$$\begin{aligned} A\rho\xi(\phi_{buf})d_{EMPD,buf}\frac{d}{dt}\left(\frac{P_{buf}}{P_{sat}(T_{buf})}\right) \\ = A\frac{P_i - P_{buf}}{(1/h_m) + (d_{EMPD,buf}/2\delta(\phi_{buf}))} \\ + A\frac{P_{deep} - P_{buf}}{(d_{EMPD,buf}/2\delta(\phi_{buf})) + (d_{EMPD,deep} \\ - d_{EMPD,buf}/2\delta(\phi_{deep}))} \end{aligned} \quad (22)$$

$$\begin{aligned} A\rho\xi(\phi_{deep})d_{EMPD,deep}\frac{d}{dt}\left(\frac{P_{deep}}{P_{sat}(T_{deep})}\right) \\ = A\frac{P_{deep} - P_{buf}}{(d_{EMPD,buf}/2\delta(\phi_{buf})) + (d_{EMPD,deep} \\ - d_{EMPD,buf}/2\delta(\phi_{deep}))} \end{aligned} \quad (23)$$

where: A is the surface of layer [m^2]; P is the vapour pressure [Pa]; h_m is the mass transfer coefficient [$\text{kg}/\text{Pa.m}^2.\text{s}$]; $d_{EMPD,buf}$ and $d_{EMPD,deep}$ are the effective penetration depths for the surface and deep layers, respectively.

As previously noted, the street canyons were modelled by interior zones in the BES. This choice permitted us to apply the EMPD model for the different canyon surfaces. However, for an external wall, the both faces of this wall are exposed to two different environments, the outdoor climatic environment and the indoor living environment (Figure 4). To take into account the heat and moisture transfer through an external surface, the heat balance of the surface will be constituted by convective and radiative heat transfers, sensible heat transfers due to precipitation as well as latent and sensible heat transfers due to vapour exchange. While the moisture balance will be constituted by precipitation and vapour exchange. However, the EMPD model used in TRNSYS has some limitations. It is an isothermal moisture model, which excludes the temperature effects, with constant material properties and is not coupled with heat transfer in the wall and does not consider the liquid transport mechanism. In addition, the EMPD model does not take account the moisture flow between the outside and inside surfaces. These can affect the surface temperatures and the sensible heat transfer

through the wall, as well as affect the inside surface conditions and the heat and mass transfer with the indoor air.

In this respect, since the liquid transport does not have much effect on the inside sensible and latent heat fluxes (Kim 2017), we have decided to programme another Type of EMPD model. This choice consists primarily to improve the heat and moisture transfer through the building envelope by applying the EMPD model to the outside and the inside surfaces of the building.

In this Type, the Equations (24) and (25) are used to couple the EMPD model (Equations (22) and (23)) to the heat transfer in the wall where the material properties are updated at each time step (Janssen and Roels 2009). As in TRNSYS, it is made up of two buffer layers, one for the short term (daily variation) and the other one for the long term (yearly variation).

$$\begin{aligned} A\rho_{surf}C_{p,surf}\frac{dT_{buf}}{dt} = \frac{A(T_{Surf,i} - T_{buf})}{(1/h_c) + (d_{EMPD,buf}/\lambda_{surf})} \\ + \frac{A(T_{deep} - T_{buf})}{(d_{EMPD,deep}/\lambda_{deep})} \end{aligned} \quad (24)$$

$$A\rho_{deep}C_{p,deep}\frac{dT_{deep}}{dt} = \frac{A(T_{deep} - T_{buf})}{(d_{EMPD,deep}/\lambda_{deep})} \quad (25)$$

where: C_p is the heat capacity [$\text{J}/\text{kg.K}$], h_c is the convective heat transfer coefficient [$\text{W}/\text{m}^2\text{K}$] and λ is the thermal conductivity [$\text{W}/\text{m}^2.\text{K}$].

The calculation method for the thermal conductivity in function of the moisture content is expressed as (Kumaran 1996):

$$\lambda(\omega) = a + b\cdot\omega \quad (26)$$

$$\omega = a\left(1 - \frac{\ln(\phi)}{b}\right)^{(-1/c)} \quad (27)$$

with ω is the sorption isotherm and a , b and c are the coefficients given by material catalogues (Kumaran 1996).

2.1.4. Soil model

The modelling of ground heat transfers is based on TRNSYS Type 49. This component takes into account the heat transfers in the ground along the three directions (Figure 5). The heat transfer is assumed to be conductive only. This Type is based on a three-dimensional finite difference model and requires a mesh of the ground covered by the building or district (near-field) as well as the surrounding area of the building or district (far-field) in order to calculate the heat transfer between the ground floor or the road pavement areas (slab) and the ground (Figure 5). A more detailed description of the model is presented in (Zhou, Rees, and Thomas 2002) and (McDowell, Thornton, and Duffy 2009).

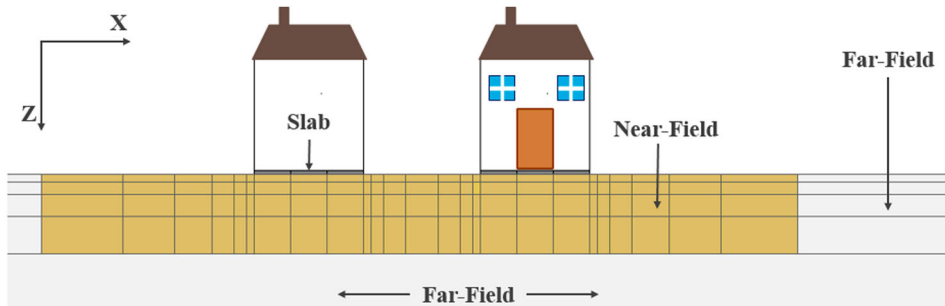


Figure 5. Ground mesh under a building and field designations: Near-Field and Far-Field.

Concerning the far-field temperature of the soil, at a depth of 10 m, is calculated by the Kusuda model (Kusuda and Achenbach 1965) (Equation 28). This temperature changes only as a function of depth and period of the year. In contrast, the near-field temperature calculation takes into account the heat exchanges (conduction heat transfer) between the ground and the building or the district.

The evolution of the ground temperature T_{sz} , at a depth z , is expressed as a function of the mean surface temperature $T_{su,avg}$ for the period studied using the following formula:

$$T_{sz}(t) = T_{su,avg} + \Delta T_{su} \cdot e^{(-z\sqrt{\pi/a_{sol}\cdot\Delta t})} \times \cos\left(\frac{2\pi t}{\Delta t} - z \cdot \sqrt{\frac{\pi}{a_{sol}\cdot\Delta t}}\right) \quad (28)$$

with ΔT_{su} is the amplitude of surface temperature variation over the period considered, Δt is the period considered and a_{sol} is the thermal diffusivity of the ground.

2.2. Aeraulic model of an urban district

The airflow in an urban environment depends, amongst others, on the urban canopy geometry. The computational fluid dynamics models are often used to simulate the flow field in urban areas. These models are very precise, but the computing time and the memory required were not suitable for our purpose, which was to calculate the coupled effects over an annual period. In this study, the street canyon was particularly studied. For this purpose, an aeraulic model was programmed in the python programming language and then integrated into a new Type in the TRNSYS software as presented in the following sections. During the simulation, the weather data file, which includes both wind direction and wind velocity measured at 10 m (dominant wind), is linked to the developed aeraulic model and then used to compute the wind velocity components in the canyon (longitudinal and transverse). For each time step, the multizone

building model of TRNSYS (TRNBuild) takes the velocities computed by the developed model to calculate the thermo-aeraulic exchanges in the canyon.

2.2.1. Longitudinal flow modelling

In street canyons, the longitudinal airflow is generated by wind component relative to the street axis. Then, the total airflow consists of a recirculation in the plane transverse to the street and a longitudinal flow along the street.

The longitudinal wind velocity component U_{canyon} is modelled by the Soulhac model (Soulhac, Perkins, and Salizzoni 2008). The main hypothesis of this model is that longitudinal flow results from a balance between entrainment by the external flow and friction on the sides of the street. Following these assumptions, the U_{canyon} velocity can be calculated as follows (Soulhac, Perkins, and Salizzoni 2008):

$$U_{canyon} = U_H \cos(\varphi) \frac{\delta_i^2}{HW} \left[\frac{2\sqrt{2}}{C} (1 - \beta) \left(1 - \frac{C^2}{3} + \frac{C^4}{45} \right) + \beta \frac{2\alpha - 3}{\alpha} + \left(\frac{W}{\delta_i} - 2 \right) \frac{\alpha - 1}{\alpha} \right] \quad (29)$$

With:

$$\alpha = \ln\left(\frac{\delta_i}{Z_{0,build}}\right) \quad (30)$$

$$\beta = e^{\frac{C}{\sqrt{2}}\left(1 - \frac{H}{\delta_i}\right)} \quad (31)$$

$$U_H = u_* \sqrt{\frac{\pi}{\sqrt{2}k^2C}} \left[Y_0(C) - \frac{J_0(C)Y_1(C)}{J_1(C)} \right] \quad (32)$$

$$C \text{ is the solution for } \frac{Z_{0,build}}{\delta_i} = \frac{2}{C} \exp\left[\frac{\pi}{2} \frac{Y_1(C)}{J_1(C)} - \gamma\right] \quad (33)$$

$$\delta_i = \min\left(H; \frac{W}{2}\right) \quad (34)$$

where J_0 , J_1 , Y_0 and Y_1 are Bessel functions (Arfken, Weber, and Harris 2013), u_* is the friction velocity, φ is the external wind direction with respect to the street axis, $\gamma = 0.57$ is the Euler constant, H and W are the street

height and width, respectively, and $z_{0,\text{build}}$ is the roughness length of canyon walls.

The mean wind speed $u(z)$ at a height z , above a surface can be estimated using Tennekes' formula (35) (Tennekes 1973).

$$u(z) = \frac{u_*}{k} \ln \left(\frac{z - d}{Z_0} \right) \quad (35)$$

where u^* is the friction velocity, $k = 0.4$ (Högström 1996) is von Karman's constant, d is the displacement length and Z_0 is the roughness length of the urban canopy considered. For the calculation of these coefficients, the parametric relationships derived by Kastner-Klein and Rotach (2004) are used:

$$d = 0,4H \frac{A_p}{A_T} e^{-2,2((A_p/A_T)-1)} + 0,6 \frac{A_p}{A_T} \quad (36)$$

$$z_0 = 0,072H \frac{A_p}{A_T} (e^{-2,2((A_p/A_T)-1)} - 1) \quad (37)$$

with A_p/A_T represents the ratio between the average plan area of roughness elements and total surface area.

2.2.2. Transverse flow modelling

In the case of a transverse flow in a street canyon, a distinction between the different types of flow is necessary. Oke (1987) has distinguished three types of flow as a function of the H/W aspect ratio (Figure 6):

- (a) Isolated roughness flow regime for wide street canyons ($H/W < 1/3$);
- (b) Interference flow regime for intermediate street canyons ($1/3 < H/W < 2/3$);
- (c) Skimming flow regime for narrow street canyons ($H/W > 2/3$).

In this study, we modelled the transverse flow using the model developed by Harman, Barlow, and Belcher (2004). This model decomposes the street canyon into two separate regions according to its geometry: a recirculation region and a ventilated region (Figure 7).

The recirculation region is approximated by a trapezoidal cross-section (Malet 1983) of a length (L_r) that depends on the turbulence of the boundary layer and the geometric shape of the buildings and that varies between $2H$ and $3.5H$ according to the authors. In this model, the length L_r has been fixed at $3H$.

The airflows in the ventilated and recirculation region are due to the air jet generated by the air detachment behind the upstream roof. According to Harman, Barlow, and Belcher (2004), these air flows develop boundary layers along the street canyon facets as a function of the size recirculation region.

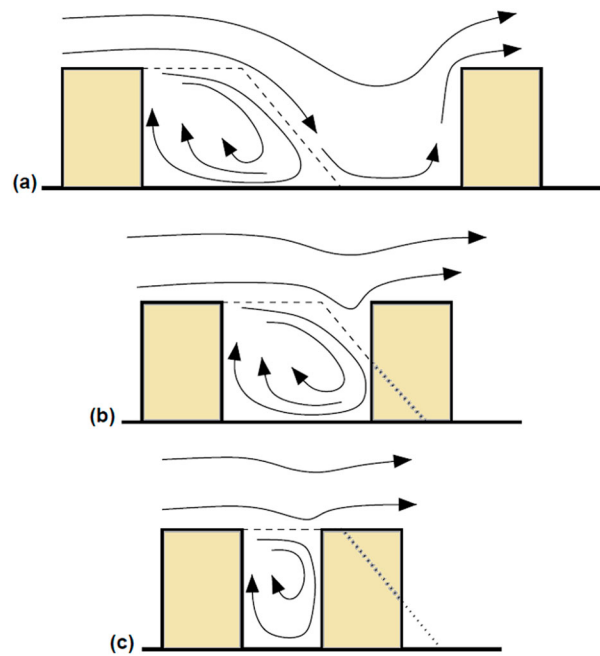


Figure 6. Schematic of the streamlines in the three flow regimes (Oke 1987; Harman, Barlow, and Belcher 2004).

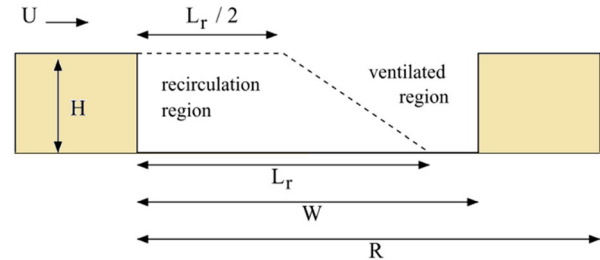


Figure 7. Schematic of the circulation region and the ventilated region in a street canyon (Harman, Barlow, and Belcher 2004).

For determining the jet velocity profile, Harman, Barlow, and Belcher (2004) proposed a logarithmic profile that describes the effect of the aerodynamic resistance exerted by the surfaces on the jet (Figure 8) using the formula (38):

$$u_i(x) = \frac{u(z_r) \sin(\varphi)}{b} e^{-\alpha_1(L_{se}/H)} \int_a^{a+b} e^{-\alpha_2(x/H)} dx \quad (38)$$

with $u(z_r)$ the velocity at a reference height z_r , $\alpha_1 = 0.9$, $\alpha_2 = 0.15 \times \max(1, 1.5H/W)$, a is the total distance of the jet from the edge of the four canyon facets indexed i for uw (upstream wall), us (upstream street), ds (downstream street) or dw (downstream wall), b is the length of the facet and φ is the external wind direction with respect to the street axis.

In the recirculation zone (index uw or us), the total distance of the jet from the start of the considered facet is a , and b is the length of this facet. For example, considering

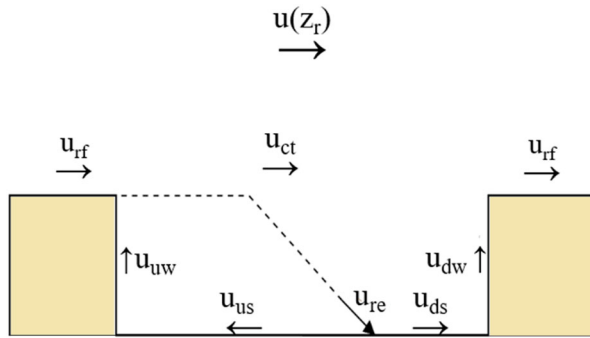


Figure 8. Schematic of the transverse wind velocities in a street canyon (Harman, Barlow, and Belcher 2004).

the upstream wall (u_{uw}) and isolated roughness regime (Figure 6a), $a = L_r$ and $b = H$. For skimming flow regime (Figure 6c), $a = W + H$ and $b = H$.

In the ventilated region (index ds or dw), for the downstream street (ds) $a = 0$ and $b = W - L_r$, and for the downstream wall $a = W - L_r$ and $b = W - L_r + H$.

The average velocity u_{re} on the recirculation boundary facet is calculated as follows:

$$u_{re} = u_{ct} e^{(-\alpha_1 L_{se}/H)} \quad (39)$$

Where $L_{se} = \sqrt{(L_r^2/4) + H^2}$ is the inclined edge length of the recirculation zone.

The roof (u_{rf}) and centre (u_{ct}) velocities are calculated as a function of the wind velocity at a reference height z_r , by extending the logarithmic profile of the inertial zone (formula 40 and formula 41).

$$\frac{u_{rf}}{u(z_r)} = \frac{\ln(H + \delta_{rf} - d/Z_0)}{\ln(z_r - d/Z_0)} \quad (40)$$

$$\frac{u_{ct}}{u(z_r)} = \frac{\ln(H - d/Z_0)}{\ln(z_r - d/Z_0)} \quad (41)$$

where $\delta_{rf} = \min[0.1(R - W), (z_r - H)]$

2.2.3. Determination of the convective heat transfer coefficient

The convection heat transfer coefficients for the building external surfaces are essential to calculate the convection heat gains and losses of façades and roofs with the exterior environment. However, these coefficients are complex functions, with respect to several factors such as the building geometry, the building environment, the roughness of the building facades, the air flows around the building and the temperature gradient. In this context, several correlations have been proposed in the literature in order to estimate the value of these exchange coefficients as a function of the configuration studied (Mirsadeghi et al. 2013).

In this study, we calculated the heat transfer coefficient for the external surfaces using the Hagishima and

Tanimoto (2003) correlation given by formulae (42) and (43).

For Horizontal surfaces:

$$h_{c,ext} = 2.28V_R + 8.18 \quad (42)$$

For vertical surfaces:

$$h_{c,ext} = 10.21V_{loc} + 4.47 \quad (43)$$

where V_R is the roof air velocity and V_{loc} is the air velocity measured at a certain distance from the walls. About the calculation of V_R and V_{loc} , we propose to take into account the building height variations (high, medium or low), the orientation of the surface, the shelter effects by other buildings as well as the roughness of the surfaces. Indeed, these velocities can be calculated based on the following formulas:

$$V_{loc} = \sqrt{U_{canyon}^2 + u_{re}^2} \quad (44)$$

$$V_R = u_{rf} \quad (45)$$

It has to be noted that the velocities U_{canyon} , u_{re} and u_{rf} are calculated respectively from Equations (29), (39) and (40).

3. Validation with experimental results

To evaluate the validity of developed model integrated in TRNSYS, a comparative study was carried out between the developed model results and existing experimental results, specifically the 'ClimaBat' experimental measurements (Doya, Bozonnet, and Allard 2012; Djedjig, Bozonnet, and Belarbi 2016; Djedjig, Bozonnet, and Belarbi 2015).

3.1. The ClimaBat experiment

The experimental model 'ClimaBat' represents an urban scene on a scale of 1:10 composed of five parallel and identical rectangular buildings with facades facing East and West (Figure 9) (Doya, Bozonnet, and Allard 2012; Djedjig, Bozonnet, and Belarbi 2016; Djedjig, Bozonnet, and Belarbi 2015). Each building is formed by the juxtaposition of 3 rainwater collection tanks. The tanks, made of concrete, are 1.26 m high, 1.13 m wide and 1.68 m long. The regular spacing of the building's forms four street canyons with an aspect ratio of Width/Height equal to 0.8. The roadway is equivalent to a light pedestrian area. It consists of 4 cm thick gravel concrete slabs placed on a bed of sand and 80 cm gravel.

The Table 1 summarizes the thermophysical properties of the materials used in the ClimaBat model.

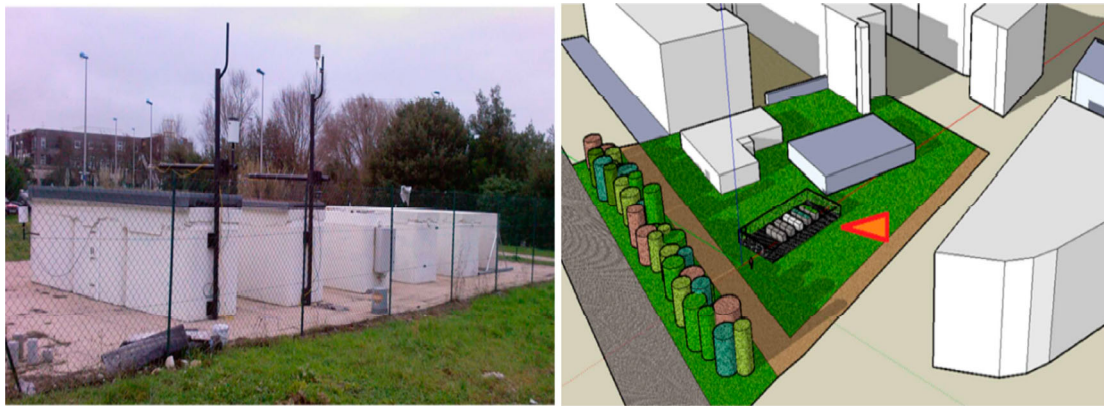


Figure 9. Experimental platform for the ClimaBat model (Djedjig 2013).

Table 1. Thermophysical properties of building and soil materials (Doya, Bozonnet, and Allard 2012; Djedjig, Bozonnet, and Belarbi 2016; Djedjig, Bozonnet, and Belarbi 2015).

Materials	Thickness [m]	α_s	ϵ	λ [W/m ² .K]	ρ [Kg/m ³]	C_p [J/Kg.K]
Concrete	0.045	0.36	0.9	2.36	2150	915
Roadway	0.1	0.64	0.9	0.04	1.25	1000

Note: α_s is the solar absorption coefficient, ϵ is the emissivity, λ is the conductivity, ρ is the density and C_p is the heat capacity.

Concerning the ClimaBat model instrumentation, it allows several measurements collection of great utility. The choice of the used instruments and their locations in the model is dictated by the objectives of the experimental campaign. The distribution of sensors on the experimental platform is outlined in Figure 10. Surface temperatures are measured with a distribution of thermocouples: 3 along the outdoor vertical profile on facades (16, 43 and 70 cm), 1 in the middle of the roof, and 2 on the pavement (25 cm from each facade). The air temperatures are measured with thermocouples protected from irradiations (2 concentric tubes with high solar reflectivity and low thermal emittance) and arranged according to the following distribution (Doya, Bozonnet, and Allard 2012):

- A vertical row of 3 thermocouples close to the facade (about 5 cm from the facade) and 1 in the middle of the west facade.
- One thermocouple above the roof.
- Two thermocouples above the pavement north and south side of the street.

The pyranometers (solar radiative flux sensors) and the pyrgoimeters (longwave radiative flux sensors) are placed in the middle of the streets at 10 cm above the roofs top. They are oriented downwards in order to measure street short and longwave radiances in relation to their specific locations. The sonic anemometer is placed

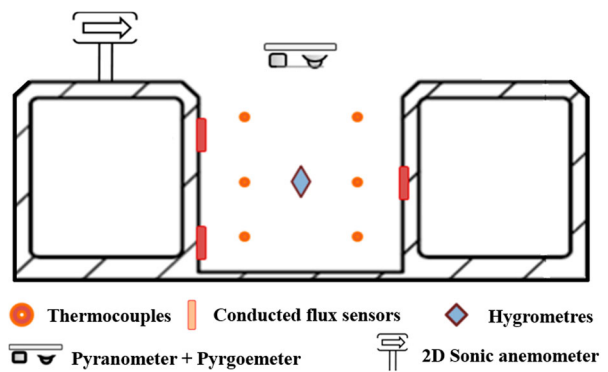


Figure 10. Schematic description of ClimaBat mockup.

28 cm above the central block building's roof. It measures the instantaneous wind speed and direction at this location. Also, hygrometers are used to measure relative humidity and air temperature simultaneously.

For meteorological data including air temperature and humidity, wind speed and direction, short and long-wave horizontal irradiance and rainfall, are measured from 17/08/2012–04/09/2012 using sensors installed in the experimental platform and a meteorological station installed on the roof of a proximity university building (Figure 11).

3.2. Description of the BES model developed

As already mentioned, to evaluate the validity of our model, we have performed comparative studies between our results and the ClimaBat experimental measurements (Doya, Bozonnet, and Allard 2012; Djedjig, Bozonnet, and Belarbi 2016; Djedjig, Bozonnet, and Belarbi 2015). To evaluate the accuracy of the developed model, the mean absolute error (MAE), the mean relative error (MRE), the mean squared error (MSE) and finally the determination coefficient (R^2) were calculated and analysed.

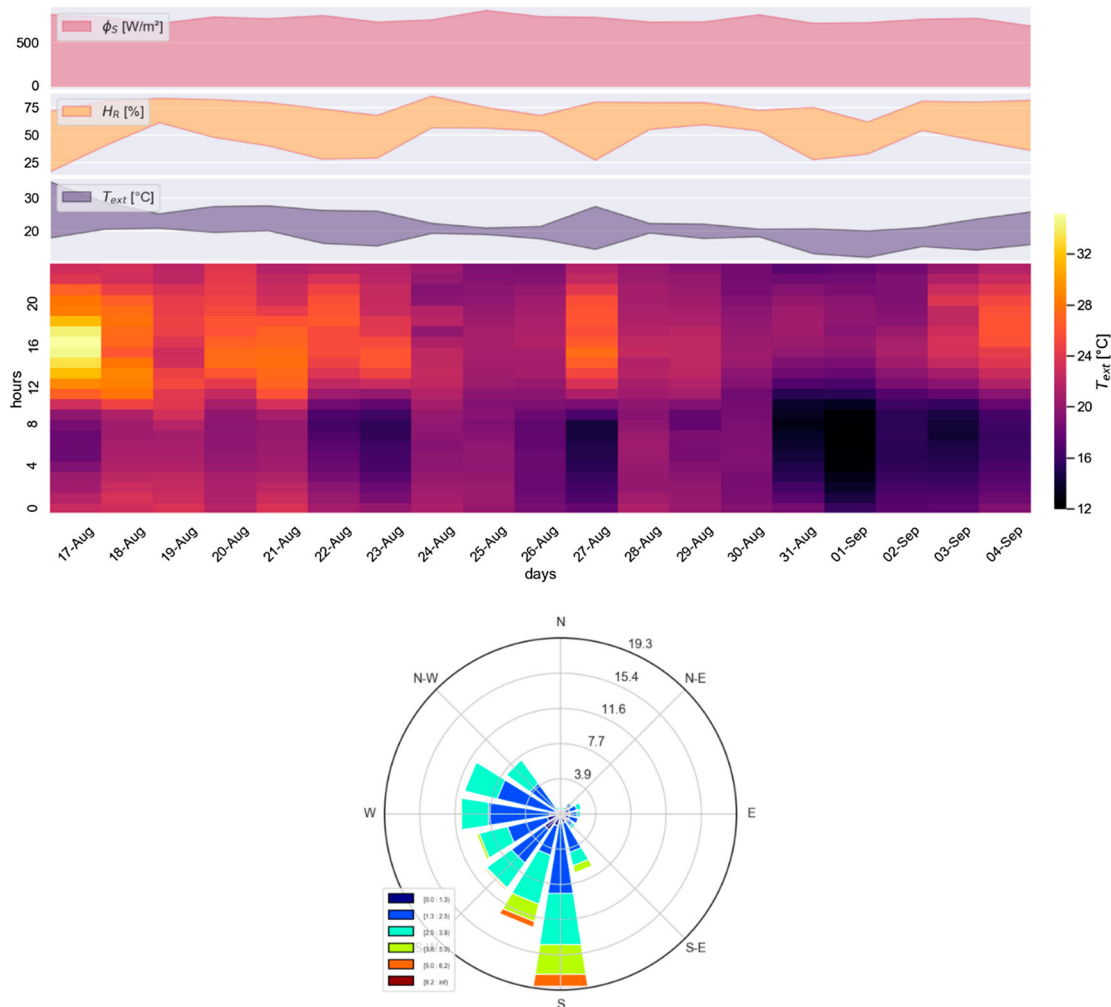


Figure 11. Meteorological data recorded at the experimental site and the local wind rose on ClimaBat bench.

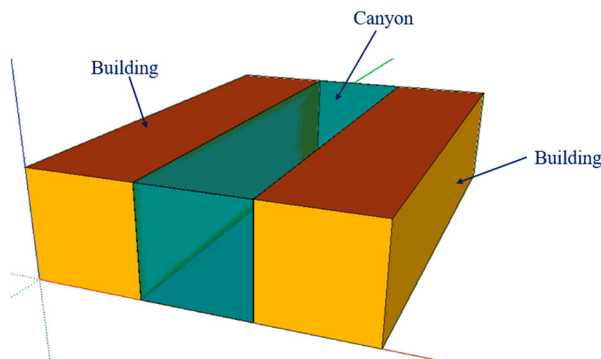


Figure 12. 3D overview of TRNSYS simulation model.

The experimental mockup was modelled in the TRNSYS software with the specific street canyon models presented in previous sections (Figure 12).

In this model, the airflow in the canyon is skimming flow regime (Figure 6c) where $\alpha_1 = 0.9$, $\alpha_2 = 0.225$ and $z_{0,build} = 0.005$ m are the parameters used in the airflow model. The heat transfer coefficient for façades is

assumed to be constant inside the building ($6.1 \text{ W/m}^2\text{K}$ for the ceiling, $1.6 \text{ W/m}^2\text{K}$ for the floor and $4.1 \text{ W/m}^2\text{K}$ for the walls). The external thermal convection coefficient was calculated according to the approach presented in section 2.2.3. The weather conditions are given through an hourly weather data file created for the specific period of experimental measurements from 17/08/2012 to 04/09/2012 (Figure 11).

3.3. Comparison of the canyons' façades surface temperatures

The comparison of the results obtained using the model developed and those of the ClimaBat (Doya, Bozonnet, and Allard 2012; Djedjig, Bozonnet, and Belarbi 2016; Djedjig, Bozonnet, and Belarbi 2015) experimental study for the estimation of eastern surfaces temperatures of the canyon shows a good agreement (Figure 13). The mean absolute and the relative errors are respectively 0.75°C and 3.83%. Also, the mean squared error is about

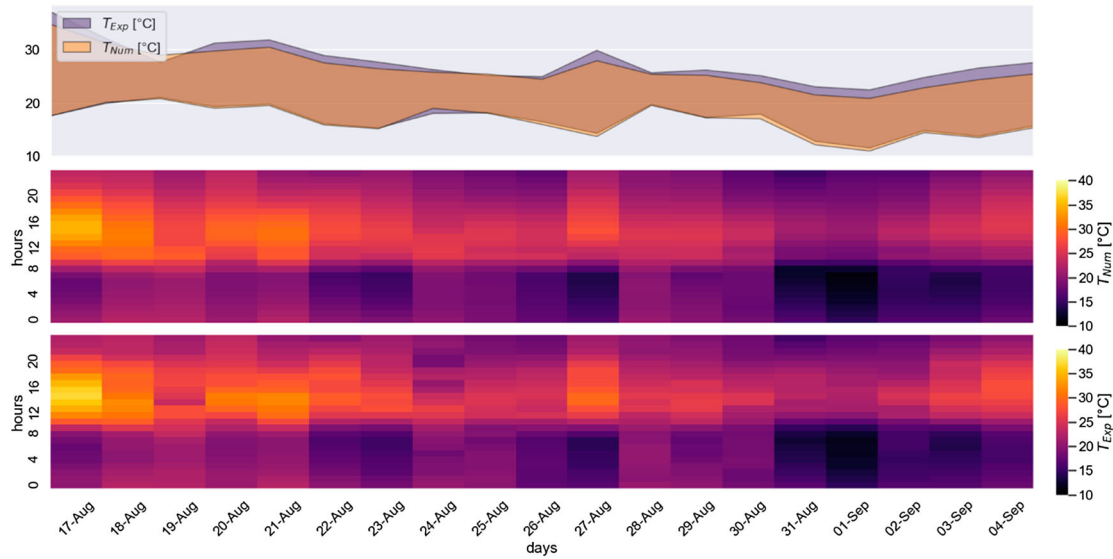


Figure 13. Temporal variation of the East façade temperature.

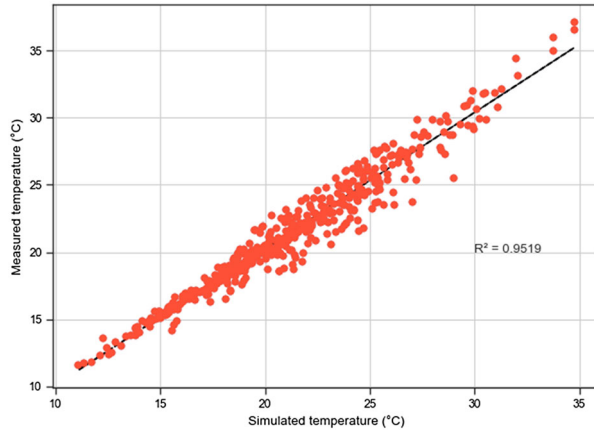


Figure 14. Comparison of simulated and measured temperature values for the East surfaces.

1°C and the regression coefficient is greater than 0.95 (Figure 14).

Similarly, to the East surface temperatures, a comparative study was conducted between the numerical and experimental West surface temperatures (Figure 15). In this case, the mean squared error is about 1°C, the mean absolute error is 0.88°C and the mean relative error reaches 3.87%. The regression coefficient R^2 is 0.97 (Figure 16).

A statistical method has been recommended by Chang and Hanna (2004) to assess the validity of numerical models against the experiments. The fractional bias (FB), the geometric mean bias (GM), the normalized mean square error (NMSE), the geometric variance (GV) and the fraction of predictions within a factor of two of observations (FAC2) have been calculated according to the following

equations:

$$FB = \frac{(\bar{C}_o - \bar{C}_m)}{0.5(\bar{C}_o + \bar{C}_m)} \quad (46)$$

$$GM = \exp(\bar{\ln C}_o - \bar{\ln C}_m) \quad (47)$$

$$NMSE = \frac{(C_o - C_m)^2}{\bar{C}_o \bar{C}_m} \quad (48)$$

$$GV = \exp[(\bar{\ln C}_o - \bar{\ln C}_m)^2] \quad (49)$$

$$FAC2 = 0.5 \leq \frac{C_m}{C_o} \leq 2.0 \quad (50)$$

where C_m is the model value, C_o is the observed value and (\bar{C}) is the average over the data set.

The statistical parameters calculated for eastern and western surface temperatures from the average of the simulated and measured results are presented in Table 2.

The results show a very good performance of the model with FB and NMSE practically equal to zero, GM and GV practically equal to 1 and FAC2 de 0.98. Based on this comparative study, the microclimatic model developed is able to estimate outdoor surface temperatures and can subsequently be used in the building's energy modelling and the urban microclimate.

To evaluate the microclimate impact generated by the canyon on surface temperatures, we compared the temperature of the canyon surfaces with the external surface's temperature having the same orientation. Figures 17 and 18 show clearly the difference between the canyon surfaces temperature and the outside surfaces temperature. During the day, this difference can be explained by the confinement in relation to solar gains in the canyon space, as the radiative fluxes on the vertical surface at street level are lower because of the shadows

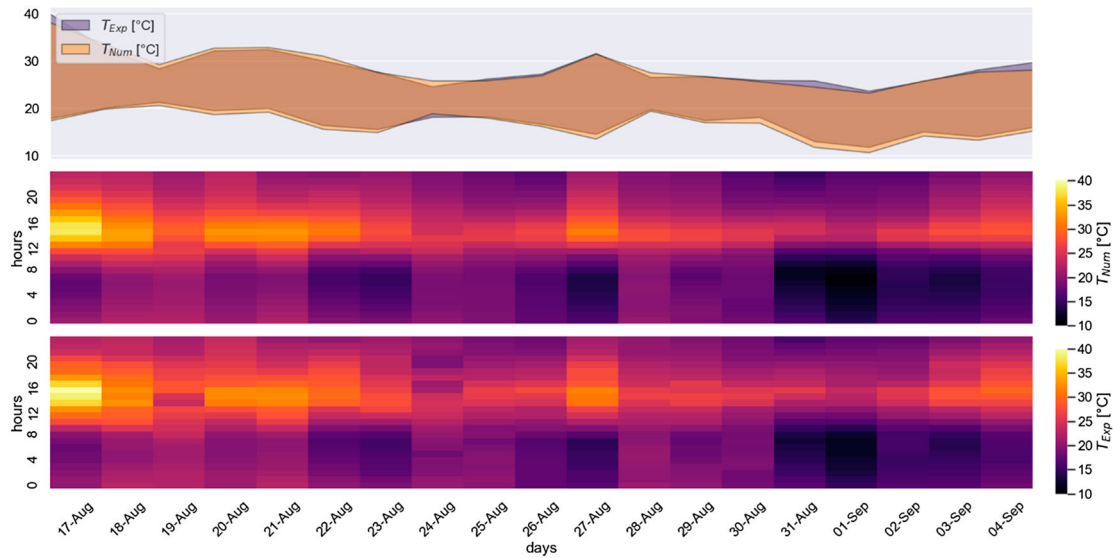


Figure 15. Temporal variation of the West façade temperature.

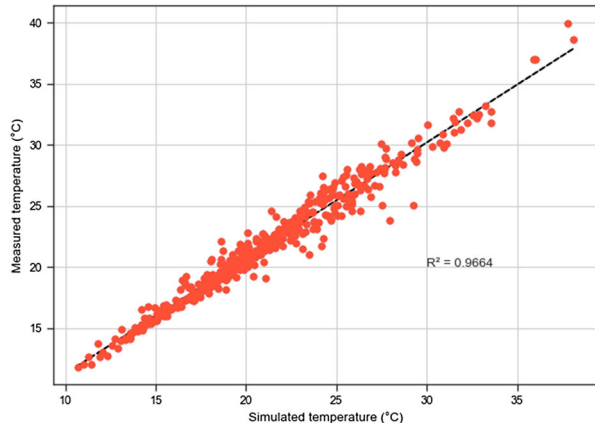


Figure 16. Comparison of simulated and measured temperature values for the West surfaces.

cast. While at night the canyon surfaces have less visibility to the sky, which impedes their longwave radiation exchange with the sky.

3.4. Comparison of canyon simulated and measured air temperature results

Figure 20 shows the comparison between simulated and measured air temperature in the canyon. It can be seen

that the simulated air temperature in the street canyon shows the same variation trend as the measured air temperature (Figure 19). The comparison of the temperature measured in the monitored canyon with the reference meteorological temperature shows that the air temperature in the street is attains values higher than the temperature measured by the meteorological station. These differences are mostly due to the radiative trapping effect where the street floor and walls warm up; the large temperature differences between these surfaces and the air generate an overheating on the street. It could increase by 3.5°C at noon (Figure 20). The fresh air flow from the vicinity of the experimental platform is responsible for the negative temperature differences recorded during the night. Indeed, the experimental platform is surrounded by green spaces that are less warm than the street canyon.

According to the correlation analysis, the simulated temperatures were in agreement with the measured data. In this case, the mean absolute error is 0.96°C, the mean relative error is 4.21% and the mean squared error is about 1.5°C. The regression coefficient R^2 is 0.94 (Figure 21). In addition, the statistical parameter results of the canyon air temperature are satisfactory with good performance as shown in Table 3.

Table 2. Statistical parameters calculated for surface temperatures.

Statistical factors	FB	GM	NMSE	GV	FAC2
Ideal target	0	1	0	1	1
"Good" (Chang and Hanna 2004)	$-0.3 \leq FB \leq 0.3$ 0.0128	$0.7 \leq GM \leq 1.3$ 0.9664	$NMSE \leq 4$ 0.025	$GV < 1.6$ 1.001	$FAC2 \geq 0.5$ 0.9873
East façade temperature	0.0238	1.0237	0.0024	1.0259	0.9765
West façade temperature					

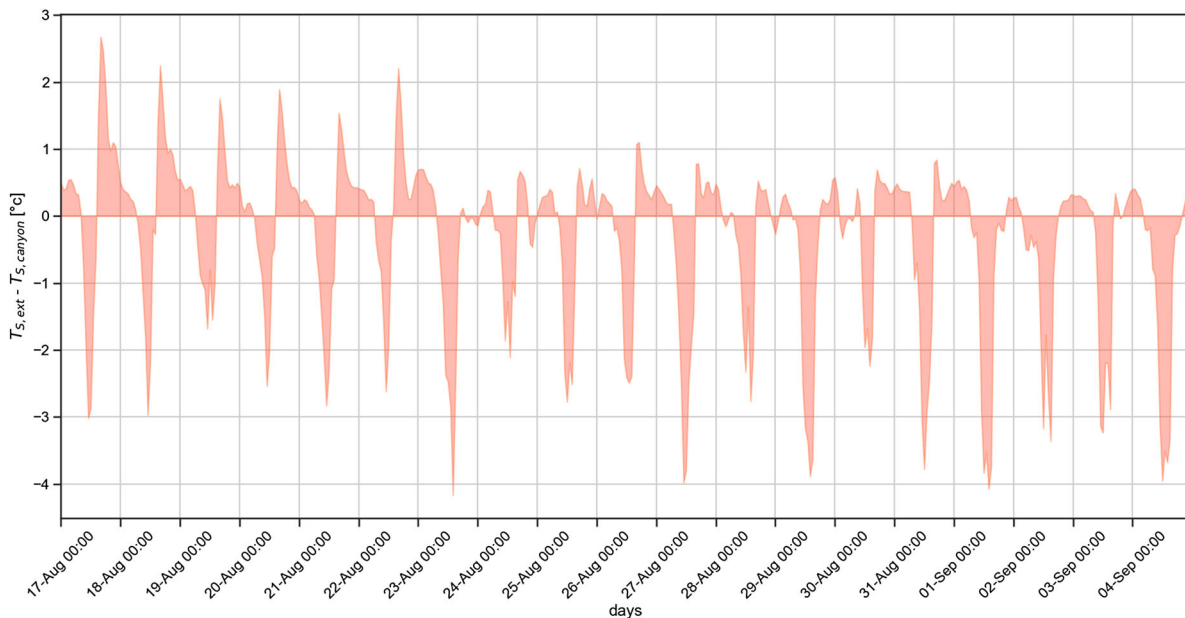


Figure 17. Evolution of the canyon's effect on the West surface.

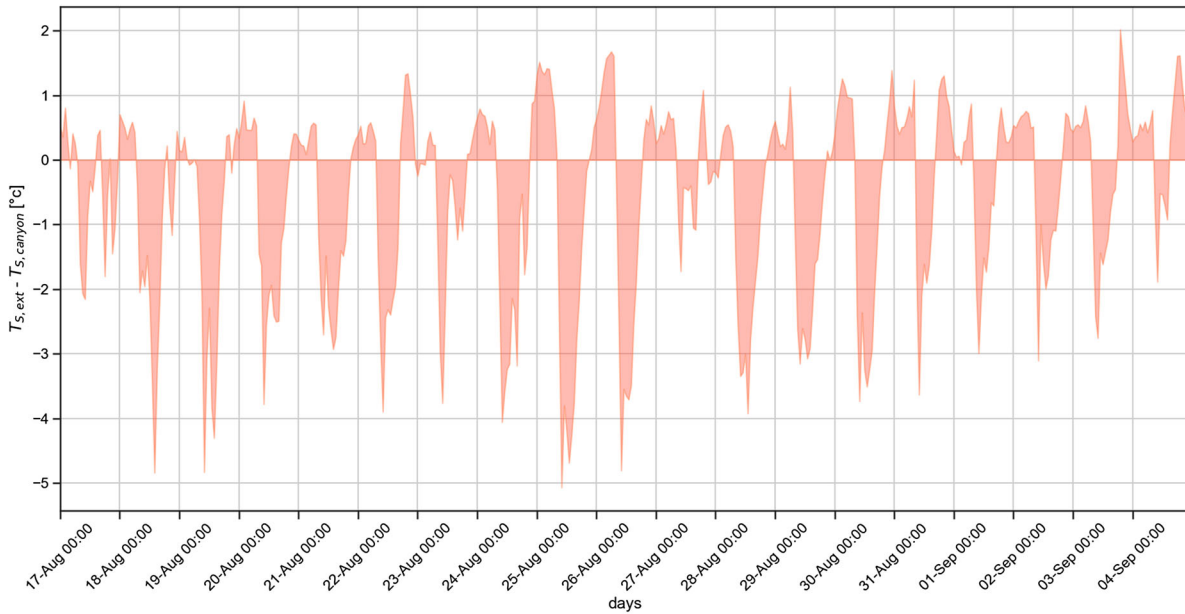


Figure 18. Evolution of the canyon's effect on the East surface.

4. Application of the developed model to a test case

4.1. Building energy simulation model

This section will compare the building heating and cooling energy needs with taking into account or not of the microclimatic model developed in this study. Two cases were studied: a stand-alone building by using only TRNSYS software (Figure 22) and the same building with a street canyon modelled by using the developed approach (Figure 23).

The simulated urban scene consists of a street canyon with aspect ratio of 0.8, comparable to the experimental reduced scale mockup. In the set of simulation only one orientation for the street canyon axe was adopted: N-S (Figure 23).

The studied building is a three-story building with a length 84, 12 m width and 9 m height (Figure 23), since one of the purposes was to represent a long building with similar adjacent apartments but also to minimize the effects of the boundary conditions on the short sides of the building. Concerning the openings, the percentage

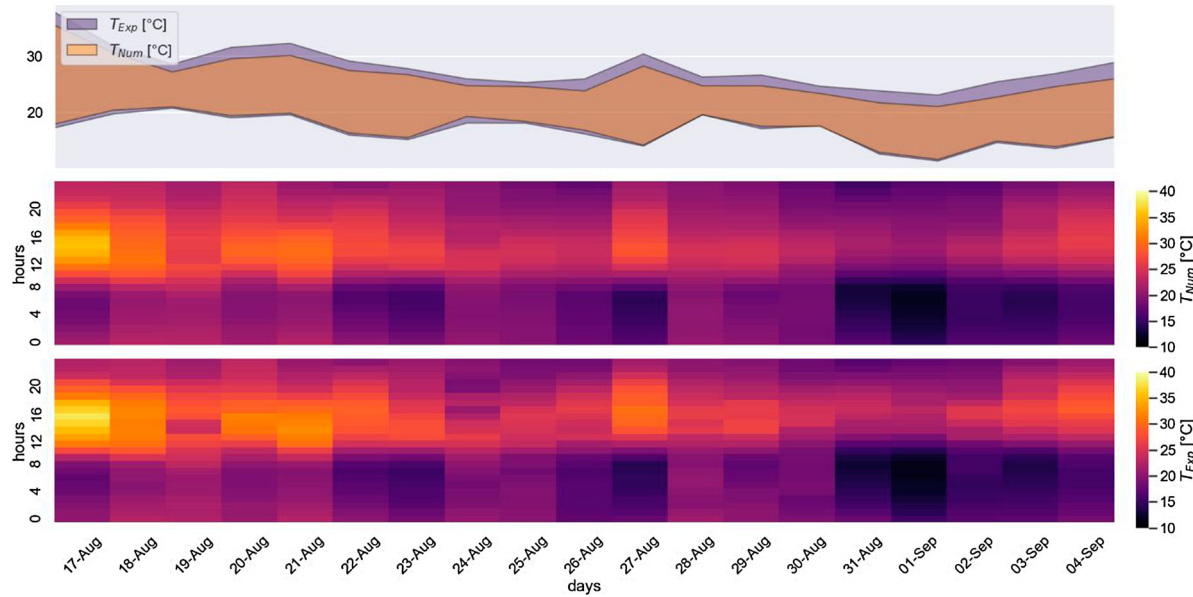


Figure 19. Temporal variation of the canyon air temperature.

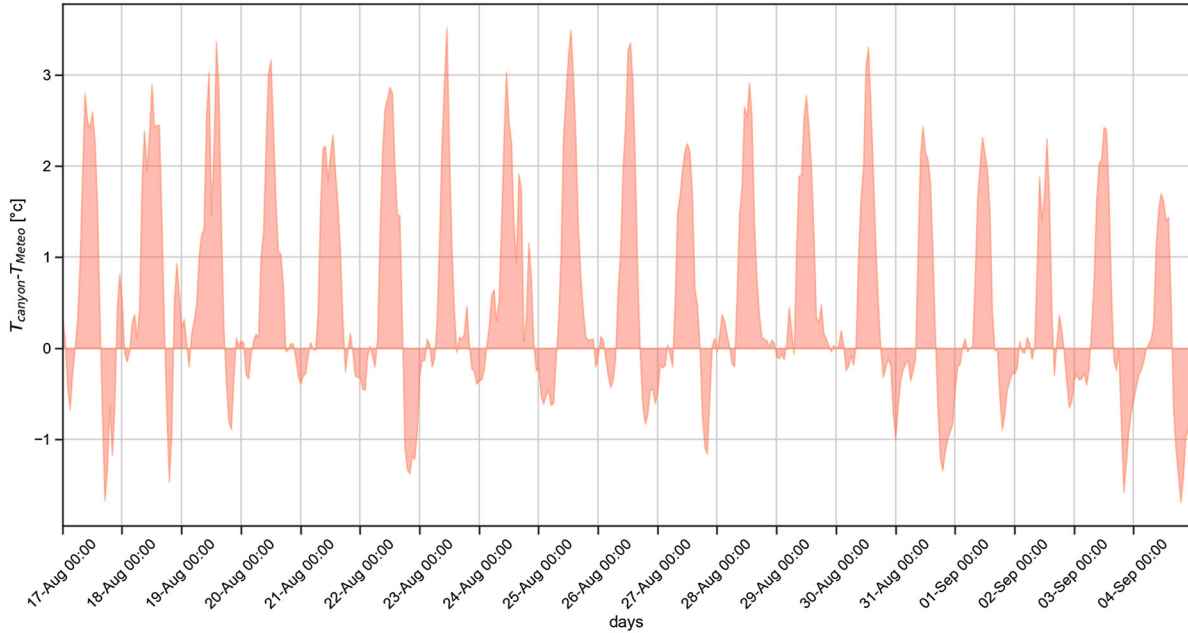


Figure 20. Overheating in the street compared with local weather.

of glazed surface in the façade is about 25%. Table 4 gives the thermophysical properties of building and soil materials used as a case study.

The following Table 5 shows the glazing characteristics used:

Concerning the solar absorption coefficient, we have adopted 0.6 for walls and roofs and 0.8 for pavements. The envelope infiltration rate is assumed to be 0.6 vol/h according to French thermal regulation (Ministère de l'Egalité des Territoires et du Logement 2013). The cooling and heating temperature set point are respectively 26 °C and 19°C (Ministère de l'Egalité des Territoires et du

Logement 2013). The climatic data taken into account are those of the city of La Rochelle (France) and they are used as input for the building energy simulation.

During the modelling, the internal gains due to the lighting system, electrical appliances, users and occupancy schedules are set according to residential use, as described in (UNI 2008). The gains shown in Table 6 are related to the total floor area. The presence of users is taken into account for 24 h per day. The usage schedule for the electrical appliances is set 'on' from 8:00 am to 12:00 pm, while the usage schedule for the lights is set 'on' from 5:00 pm to 12:00 am

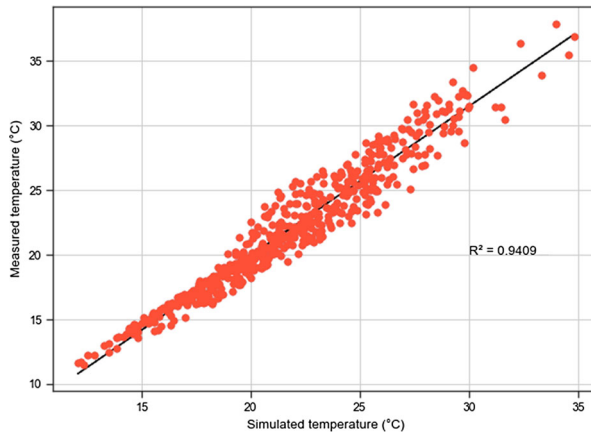


Figure 21. Comparison of simulated and measured air temperature values for the canyon.

Table 3. Statistical parameters calculated for canyon air temperature.

Statistical factors	FB	GM	NMSE	GV	FAC2
Canyon temperature	0.02	0.96	0.04	1.001	0.98

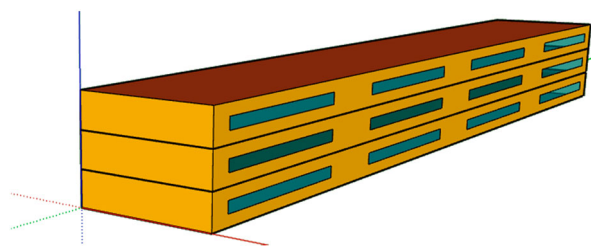


Figure 22. Overview 3d of the reference building.

4.2. Numerical results

The comparison of the results from TRNSYS and developed approach shows that stand-alone building cooling demands is 46% lower than that of building located in an urban environment with a street canyon (Figure 24a). As well, the heating demands of the stand-alone building is 48% higher than that of building located in street canyon (Figure 24b). These results are due to that the TRNSYS does not take into account the microclimate generated by the street canyon, such as the radiative trapping phenomenon that is materialized by the multiple inter-reflections between the canyon surfaces.

These results are consistent with those obtained in the experimental study by Matheos Santamouris et al. (2001). It was estimated that for a building located in an urban canyon in Athens the cooling demands may be doubled compared to a building located in a suburban area. While in winter the urban climate effect on the energy consumption of buildings can be positive, and therefore an overestimation of heating energy needs about 30–50%.

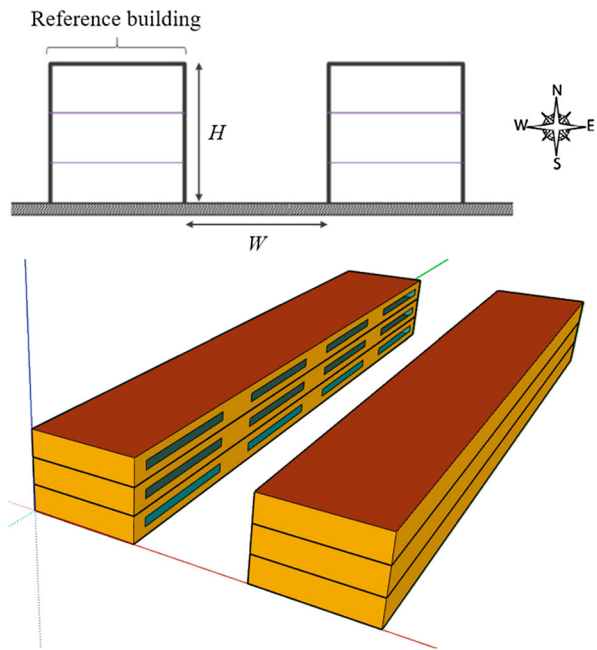


Figure 23. Overview of the street canyon.

Table 4. Thermophysical properties of building and soil materials.

Envelope element	Materials	Thickness [cm]	λ [W/m².K]	C_p [J/Kg.K]	ρ [Kg/m³]
Wall	Cinder block	20	1.04	1000	2300
Roof and ceiling	Concrete	12	2.36	915	2150
Pavement	Ceramics	0.7	1.4	1000	2500
	Concrete	10	0.04	1000	2350

Note: λ is the conductivity, C_p is the heat capacity and ρ is the density.

Table 5. Windows characteristics.

Envelope element	Material	U-value [W/m².K]	g-value	ϵ
Windows	Glass	1.4	0.6	0.84

Table 6. Specific values of internal gains.

Appliance	Persons [W/m²]	Appliances [W/m²]	Lights [W/m²]
Convective	3.01	1.05	1.5
Radiative	1.51	0.35	3.5

It is therefore necessary to confirm the drastic effect of considering the urban microclimate in the building energy simulations. This leads to a significant error to dimensioning the HVAC systems. In addition, any underestimation of cooling demand can lead to indirect impacts of heat islands, which can result in heat dissipation from buildings, playing an important role in amplifying urban warming. This phenomenon is therefore part of a sort of auto-amplification circle: as having higher outdoor temperatures, building gets heated and in turn requires forced cooling to bring the indoor temperatures

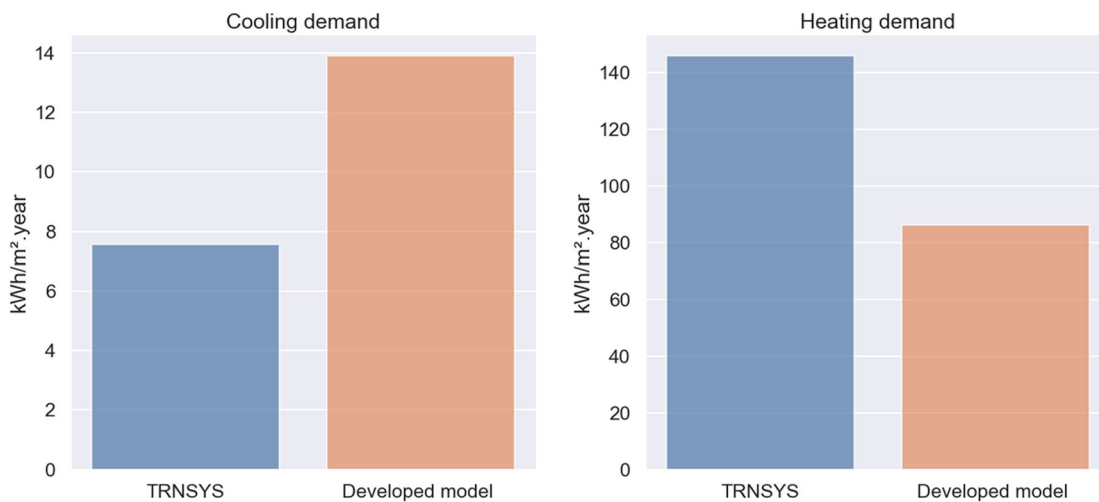


Figure 24. (a) Cooling energy demands, (b) Heating energy demands.

down, which results in higher emissions and more waste heat redirected towards the outdoors (Bozonnet 2005). Which makes this unfavourable cycle.

This study showed the efficiency of the developed method for its reduced computation time compared to CFD, approximately 15 min to simulate one year VS 16 days to simulate a week using CFD (Athamena 2012), while maintaining a satisfactory accuracy for thermal and energy evaluation.

5. Conclusion

In this study, a simplified approach with the BES software TRNSYS was developed in order to assess the impact of urban microclimate on the building energy demand. This approach takes into account the effects of dominant winds, radiative trapping, hygrothermal exchange and heat transfer in the ground along the three directions. We have verified the consistency of this modelling approach through a comparative study with the experimental results of the ClimaBat experiment.

In fact, the numerical results obtained are very close to the experimental observations particularly for the external walls. For example, in the external wall surface temperature East side, the mean absolute error is only 0.88°C with a mean relative error as about 3.83%. As well, in the external wall surface temperature West side, the mean absolute error is 0.87°C with a mean relative error approximately 3.87%. Concerning the comparison of simulated and measured air temperature in the canyon, the mean absolute error is about 0.96°C with a mean relative error as about 4.21%.

The advantage of the thermoradiative model is reflected in its ability to model short and longwave radiation exchange between different canyon buildings, as well as the distribution of inside solar radiation. In addition, it

allows the evaluation of the microclimate impact generated by the canyon on surface temperatures.

The contribution of the airflow model makes it possible to take into account the turbulence airflow variations as a function of the geometrical street's characteristics of the building's walls roughness and the wind speed as well as its direction and the angle of incidence.

Furthermore, a comparison between the building heating and cooling energy needs of a street canyon building and a stand-alone building are evaluated. The obtained results show that the use of regional climate data is poorly representative of urban site specificities. In fact, the urban microclimate generated by a street canyon can increase the space cooling around 46% and decrease the space heating demands by around 48%.

Finally, this method is also in practice interesting regarding its reduced calculation time compared to more complex models such as CFD calculations, without resorting to interoperability and the use of several software with a satisfactory accuracy for thermal and energy evaluation purposes. However, this approach is specific to the case of the dominant wind. For this reason, it will be interesting to take into account the different boundary wind directions as an object of future studies. Another perspective of this study is the application of the approach developed at the scale of a district while taking into account the street canyon intersection.

Disclosure statement

No potential conflict of interest was reported by the author(s).

ORCID

Adnane M'Saouri El Bat <http://orcid.org/0000-0003-1609-1405>
 Zaid Romani <http://orcid.org/0000-0002-5284-2862>
 Emmanuel Bozonnet <http://orcid.org/0000-0002-5357-6404>

References

- Allegrini, Jonas, Viktor Dorer, and Jan Carmeliet. 2012. "Influence of the Urban Microclimate in Street Canyons on the Energy Demand for Space Cooling and Heating of Buildings." *Energy and Buildings* 55: 823–832. doi:10.1016/j.enbuild.2012.10.013.
- Arfken, George B, Hans J Weber, and Frank E Harris. 2013. "Chapter 14 - Bessel Functions." In *Mathematical Methods for Physicists*. 7th ed. doi:10.1016/B978-0-12-384654-9.00014-1.
- Asawa, Takashi, Akira Hoyano, and Kazuaki Nakaohkubo. 2008. "Thermal Design Tool for Outdoor Spaces Based on Heat Balance Simulation Using a 3D-CAD System." *Building and Environment* 43 (12): 2112–2123. doi:10.1016/j.buildenv.2007.12.007.
- Athamena, Khaled. 2012. "Modélisation et Simulation Des Microclimats Urbains : Etude de l'impact de La Morphologie Urbaine Sur Le Confort Dans Les Espaces Extérieurs. Cas Des Eco-Quartiers." Ecole Centrale de Nantes. <https://tel.archives-ouvertes.fr/tel-00811583>.
- Bektaş Ekici, Betül, and U. Teoman Aksøy. 2011. "Prediction of Building Energy Needs in Early Stage of Design by Using ANFIS." *Expert Systems with Applications* 38 (5): 5352–5358. doi:10.1016/j.eswa.2010.10.021.
- Bouyer, Julien. 2009. "Modélisation et Simulation Des Microclimats Urbains—Étude de l'impact de l'aménagement Urbain Sur Les Consommations Énergétiques Des Bâtiments." Université de Nantes.
- Bouyer, Julien, Christian Inard, and Marjorie Musy. 2011. "Microclimatic Coupling as a Solution to Improve Building Energy Simulation in an Urban Context." *Energy and Buildings* 43 (7): 1549–1559. doi:10.1016/j.enbuild.2011.02.010.
- Bozonnet, Emmanuel. 2005. "Impact Des Microclimats Urbains Sur La Demande Énergétique Des Bâtiments-Cas de La Rue Canyon." Université de la Rochelle.
- Bozonnet, Emmanuel, Rafik Belarbi, and Francis Allard. 2007. "Thermal Behaviour of Buildings: Modelling the Impact of Urban Heat Island." *Journal of Harbin Institute of Technology (New Series)* 14 (Sup.): 19–22.
- Bueno, Bruno, Leslie Norford, Julia Hidalgo, and Grégoire Pigeon. 2013. "The Urban Weather Generator." *Journal of Building Performance Simulation* 6 (4): 269–281. doi:10.1080/19401493.2012.718797.
- Chan, Hoy Yen, Saffa B. Riffat, and Jie Zhu. 2010. "Review of Passive Solar Heating and Cooling Technologies." *Renewable and Sustainable Energy Reviews* 14 (2): 781–789. doi:10.1016/j.rser.2009.10.030.
- Chang, Joseph C, and Steven R Hanna. 2004. "Air Quality Model Performance Evaluation." *Meteorology and Atmospheric Physics* 87 (1–3): 167–196.
- Chatzangelidis, K., and D. Bouris. 2009. "Calculation of the Distribution of Incoming Solar Radiation in Enclosures." *Applied Thermal Engineering* 29 (5–6): 1096–1105. doi:10.1016/j.applthermaleng.2008.05.026.
- Cunningham, M. J. 1988. "The Moisture Performance of Framed Structures—A Mathematical Model." *Building and Environment* 23 (2): 123–135.
- Cunningham, Malcolm J. 1992. "Effective Penetration Depth and Effective Resistance in Moisture Transfer." *Building and Environment* 27 (3): 379–386.
- Daviau-Pellegrin, Noëlie. 2016. "Modélisation Fine Des Échanges Thermiques Entre Les Bâtiments et l'atmosphère Urbaine." Université PARIS-EST.
- De Boeck, L., S. Verbeke, A. Audenaert, and L. De Mesmaeker. 2015. "Improving the Energy Performance of Residential Buildings: A Literature Review." *Renewable and Sustainable Energy Reviews* 52: 960–975. doi:10.1016/j.rser.2015.07.037.
- Djedjig, Rabah. 2013. "Impacts Des Enveloppes Végétales à l'interface Bâtiment Microclimat Urbain." Université de la Rochelle. <https://tel.archives-ouvertes.fr/tel-01141046>.
- Djedjig, Rabah, Emmanuel Bozonnet, and Rafik Belarbi. 2015. "Analysis of Thermal Effects of Vegetated Envelopes: Integration of a Validated Model in a Building Energy Simulation Program." *Energy & Buildings* 86: 93–103. doi:10.1016/j.enbuild.2014.09.057.
- Djedjig, Rabah, Emmanuel Bozonnet, and Rafik Belarbi. 2016. "Urban Climate Modeling Green Wall Interactions with Street Canyons for Building Energy Simulation in Urban Context." *Urban Climate* 16: 75–85. doi:10.1016/j.uclim.2015.12.003.
- Doya, Maxime, Emmanuel Bozonnet, and Francis Allard. 2012. "Experimental Measurement of Cool Facades' Performance in a Dense Urban Environment." *Energy and Buildings* 55: 42–50. doi:10.1016/j.enbuild.2011.11.001.
- Gaetani, Isabella, Pieter Jan Hoes, and Jan L.M. Hensen. 2016. "Occupant Behavior in Building Energy Simulation: Towards a Fit-for-Purpose Modeling Strategy." *Energy and Buildings* 121: 188–204. doi:10.1016/j.enbuild.2016.03.038.
- Gartland, Lisa. 2012. *Heat Islands: Understanding and Mitigating Heat in Urban Areas*. doi:10.4324/9781849771559.
- Gebhart, B. 1961. "Surface Temperature Calculations in Radiant Surroundings Ofarbitrary Complexity—for Gray, Diffuse Radiation." *International Journal of Heat and Mass Transfer* 3: 341–346.
- Gros, Adrien, Emmanuel Bozonnet, and Christian Inard. 2014. "Cool materials impact at district scale—Coupling building energy and microclimate models." *Sustainable Cities and Society* 13: 254–266. doi:10.1016/j.scs.2014.02.002.
- Gros, Adrien, Emmanuel Bozonnet, Christian Inard, and Marjorie Musy. 2016. "Simulation Tools to Assess Microclimate and Building Energy - A Case Study on the Design of a New District." *Energy and Buildings* 114: 112–122. doi:10.1016/j.enbuild.2015.06.032.
- Hagishima, Aya, and Jun Tanimoto. 2003. "Field Measurements for Estimating the Convective Heat Transfer Coefficient at Building Surfaces" 38: 873–881. doi:10.1016/S0360-1323(03)00033-7.
- Harman, Ian N, Janet F Barlow, and Stephen E Belcher. 2004. "Scalar Fluxes from Urban Street Canyons. Part I: Model." *Boundary-Layer Meteorology* 113 (3): 387–409. doi:10.1023/B:BOUN.0000045526.07270.a3
- Hepbasli, Arif. 2012. "Low Exergy (LowEx) Heating and Cooling Systems for Sustainable Buildings and Societies." *Renewable and Sustainable Energy Reviews* 16 (1): 73–104. doi:10.1016/j.rser.2011.07.138.
- Högström, U. 1996. "Review of Some Basic Characteristics of the Atmospheric Surface Layer." *Boundary-Layer Meteorology* 78 (January): 215–246. doi:10.1007/BF00120937.
- Hong, Tianzhen, Da Yan, Simona D'Oca, and Chien fei Chen. 2017. "Ten Questions Concerning Occupant Behavior in Buildings: The Big Picture." *Building and Environment* 114: 518–530. doi:10.1016/j.buildenv.2016.12.006.
- IEA. 2018. *Market Report Series Energy Efficiency 2018*. IEA Publications. doi:10.1007/978-3-642-41126-7.

- Jamei, Elmira, Priyadarsini Rajagopalan, Mohammadmehdi Seyedmahmoudian, and Yashar Jamei. 2016. "Review on the Impact of Urban Geometry and Pedestrian Level Greening on Outdoor Thermal Comfort." *Renewable and Sustainable Energy Reviews* 54: 1002–1017. doi:10.1016/j.rser.2015.10.104.
- Janssen, Hans, and Staf Roels. 2009. "Qualitative and Quantitative Assessment of Interior Moisture Buffering by Enclosures." *Energy and Buildings* 41 (4): 382–394. doi:10.1016/j.enbuild.2008.11.007.
- Kastner-Klein, P., and M. W. Rotach. 2004. "Mean Flow and Turbulence Characteristics in an Urban Roughness Sublayer." *Boundary Layer Meteorology* 111: 55–84. doi:10.1023/B:BOUN.0000010994.32240.b1.
- Kerestecioglu, A., and L. Gu. 1989. "Incorporation of the Effective Penetration Depth Theory into TRNSYS." *Draft Report, Florida Solar Energy Center, Cape Canaveral, Florida*.
- Kim, Joowook. 2017. "Development of a Simplified Heat and Moisture Transfer Model for Residential Buildings."
- Klein, S. A., W. A. Beckman, J. W. Mitchell, J. A. Duffie, N. A. Duffie, T. L. Freeman, J. C. Mitchell, et al. 2010. *TRNSYS 17: A Transient System Simulation Program*. Madison, USA: Solar Energy Laboratory, University of Wisconsin.
- Kolokotroni, M., I. Giannitsaris, and R. Watkins. 2006. "The Effect of the London Urban Heat Island on Building Summer Cooling Demand and Night Ventilation Strategies." *Solar Energy* 80 (4): 383–392. doi:10.1016/j.solener.2005.03.010.
- Kumaran, M. K. 1996. "Heat, Air and Moisture Transfer in Insulated Envelope Parts. Final Report, Volume 3, Task 3: Material Properties." *International Energy Agency Annex 24*: 135.
- Kusuda, T., and P. R. Achenbach. 1965. "Earth Temperatures and Thermal Diffusivity at Selected Stations in the United States." *ASHRAE Transactions* 71 (1): 61–74. <http://www.dtic.mil/cgi/tr/fulltext/u2/472916.pdf>.
- Lauzet, Nicolas, Benjamin Morille, Thomas Leduc, Marjorie Musy, Nicolas Lauzet, Benjamin Morille, Thomas Leduc, et al. 2016. "What Is the Required Level of Details to Represent the Impact of the Built Environment on Energy Demand??? To Cite This Version : HAL Id : Hal-01409618 International Conference on Sustainable Synergies from Buildings to the Urban Scale, SBE16 What Is The ."
- Lauzet, Nicolas, Auline Rodler, Marjorie Musy, Marie-Hélène Azam, Sihem Guernouti, Dasaraden Mauree, and Thibaut Collinart. 2019. "How Building Energy Models Take the Local Climate Into Account in an Urban Context – A Review." *Renewable and Sustainable Energy Reviews* 116 (December). doi:10.1016/j.rser.2019.109390.
- Lemonsu, A., V. Masson, L. Shashua-Bar, E. Erell, and D. Pearlmuter. 2012. "Inclusion of Vegetation in the Town Energy Balance Model for Modelling Urban Green Areas." *Geoscientific Model Development*, doi:10.5194/gmd-5-1377-2012.
- Lin, Mark W, Justin B Berman, Mehran Khoshbakht, Carl A Feickert, and Ayo O Abatan. 2006. "Modeling of Moisture Migration in an FRP Reinforced Masonry Structure." *Building and Environment* 41 (5): 646–656.
- Malet, M. L. 1983. "Air Pollution Modeling and Its Application." *Eos, Transactions American Geophysical Union* 64 (52): 1008. doi:10.1029/E0064i052p01008.
- Malys, Laurent, Marjorie Musy, and Christian Inard. 2015. "Microclimate and Building Energy Consumption: Study of Different Coupling." July. doi:10.1080/17512549.2015.1043643.
- Manzano-Agugliaro, Francisco, Francisco G. Montoya, Andrés Sabio-Ortega, and Amós García-Cruz. 2015. "Review of Bioclimatic Architecture Strategies for Achieving Thermal Comfort." *Renewable and Sustainable Energy Reviews* 49: 736–755. doi:10.1016/j.rser.2015.04.095.
- Masson, Valéry. 2000. "A Physically-Based Scheme for the Urban Energy Budget in Atmospheric Models." *Boundary-Layer Meteorology* 94 (3): 357–397.
- McDowell, Timothy, Jeff Thornton, and Matthew Duffy. 2009. "Comparison of a Ground-Coupling Reference Standard Model to Simplified Approaches." *IBPSA 2009 - International Building Performance Simulation Association* 2009, January.
- Miller, Clayton, Daren Thomas, Jérôme Kämpf, and Arno Schlueter. 2018. "Urban and Building Multiscale Co-Simulation: Case Study Implementations on Two University Campuses." *Journal of Building Performance Simulation* 11 (3): 309–321. doi:<https://doi.org/10.1080/19401493.2017.1354070>.
- Mills, Gerald. 2014. "Urban Climatology: History, Status and Prospects." *Urban Climate* 10 (P3): 479–489. doi:10.1016/j.uclim.2014.06.004.
- Ministère de l'Egalité des Territoires et du Logement. 2013. "Réglementation Thermique 2012, Version Modifiée Avril 2013." *Journal Officiel de La République Française* 12. <http://www.legifrance.gouv.fr>.
- Mirsadeghi, M., D. Cóstola, B. Blocken, and J. L. M. Hensen. 2013. "Review of External Convective Heat Transfer Coefficient Models in Building Energy Simulation Programs: Implementation and Uncertainty" 31 (March).
- Moonen, Peter, Thijs Defraeye, Viktor Dorer, Bert Blocken, and Jan Carmeliet. 2012. "Urban Physics: Effect of the Micro-Climate on Comfort, Health and Energy Demand." *Frontiers of Architectural Research* 1 (3): 197–228. doi:10.1016/j foar.2012.05.002.
- Musco, Francesco. 2016. *Counteracting Urban Heat Island Effects in a Global Climate Change Scenario*. doi:10.1007/978-3-319-10425-6.
- Oke, T. R. 1987. "Boundary Layer Climates." *Earth-Science Reviews* 27. doi:10.1016/0012-8252(90)90005-G.
- Pacheco, R., J. Ordóñez, and G. Martínez. 2012. "Energy Efficient Design of Building: A Review." *Renewable and Sustainable Energy Reviews* 16 (6): 3559–3573. doi:10.1016/j.rser.2012.03.045.
- Pantazaras, Alexandros, Mattheos Santamouris, Siew Eang Lee, and M. N. Assimakopoulos. 2018. "A Decision Tool to Balance Indoor Air Quality and Energy Consumption: A Case Study." *Energy and Buildings* 165: 246–258. doi:10.1016/j.enbuild.2018.01.045.
- Pérez-Lombard, Luis, José Ortiz, and Christine Pout. 2008. "A Review on Buildings Energy Consumption Information." *Energy and Buildings* 40 (3): 394–398. doi:10.1016/j.enbuild.2007.03.007.
- Robinson, Darren, Frédéric Haldi, J. Kämpf, Philippe Leroux, Diane Perez, Adil Rasheed, and Urs Wilke. 2009. "CitySim: Comprehensive Micro-Simulation of Resource Flows for Sustainable Urban Planning." *Proc. Building Simulation* 11: 1614–1627.
- Rodler, Auline, Sihem Guernouti, Marjorie Musy, and Julien Bouyer. 2018. "Energy & Buildings Thermal Behaviour of a Building in Its Environment : Modelling, Experimentation, and Comparison." *Energy & Buildings* 168: 19–34. doi:10.1016/j.enbuild.2018.03.008.
- Salvati, A., M. Palme, G. Chiesa, and M. Kolokotroni. 2020. "Built Form, Urban Climate and Building Energy Modelling:

- Case-Studies in Rome and Antofagasta." *Journal of Building Performance Simulation*, 1–17. doi:10.1080/19401493.2019.1707876.
- Santamouris, Mattheos. 2007. "Heat Island Research in Europe: The State of the Art." *Advances in Building Energy Research* 1 (1): 123–150. doi:10.1080/17512549.2007.9687272.
- Santamouris, Mattheos, Nikos Papanikolaou, Iro Livada, Ioannis Koronakis, Chrysa Georgakis, Athanasios Argiriou, and D. N. Assimakopoulos. 2001. "On the Impact of Urban Climate on the Energy Consumption of Buildings." *Solar Energy* 70 (3): 201–216.
- Selakov, Aleksandar, Dragan Milos, and Stevan Savic. 2014. "Cold and Warm Air Temperature Spells During the Winter and Summer Seasons and Their Impact on Energy Consumption in Urban Areas." doi:10.1007/s11069-014-1074-y.
- Soulhac, Lionel, Richard J Perkins, and Pietro Salizzoni. 2008. "Flow in a Street Canyon for Any External Wind Direction," 365–388. doi:10.1007/s10546-007-9238-x.
- Stephenson, D. G., and G. P. Mitalas. 1970. "Calculation of Heat Conduction Transfer Functions for Multi-Layers Slabs." *Air Cond. Engrs. Trans; (United States)*.
- Sun, Yuming, and Godfried Augenbroe. 2014. "Urban Heat Island Effect on Energy Application Studies of Office Buildings." *Energy and Buildings* 77: 171–179. doi:10.1016/j.enbuild.2014.03.055.
- Sun, Yuming, Yeonsook Heo, Matthias Tan, Huizhi Xie, C. F. Jeff Wu, and Godfried Augenbroe. 2014. "Uncertainty Quantification of Microclimate Variables in Building Energy Models." *Journal of Building Performance Simulation* 7 (1): 17–32. https://doi.org/10.1080/19401493.2012.757368.
- Tennekes, H. 1973. "The Logarithmic Wind Profile." *Journal of the Atmospheric Sciences*. doi:10.1175/1520-0469(1973)030<0234:TLWP>2.0.CO;2.
- UNI, T S. 2008. "11300-1, Energy Performance of Buildings—Part 1." *Calculation of Energy Use for Space Heating and Cooling*, 1st Ed., UNI, Milano.
- Vallati, A., L. Mauri, and C. Colucci. 2018. "Impact of Shortwave Multiple Reflections in an Urban Street Canyon on Building Thermal Energy Demands." *Energy and Buildings* 174: 77–84.
- Vallati, A., L. Mauri, C. Colucci, and P. Ocioán. 2017. "Effects of Radiative Exchange in an Urban Canyon on Building Surfaces' Loads and Temperatures." *Energy and Buildings* 149: 260–271.
- Van Hooff, T., B. Blocken, J. L. M. Hensen, and H. J. P. Timmermans. 2015. "Reprint of: On the Predicted Effectiveness of Climate Adaptation Measures for Residential Buildings." *Building and Environment* 83: 142–158. doi:10.1016/j.buildenv.2014.10.006.
- Yang, Xiaoshan, Lihua Zhao, Michael Bruse, and Qinglin Meng. 2012. "An Integrated Simulation Method for Building Energy Performance Assessment in Urban Environments." *Energy & Buildings* 54: 243–251. doi:10.1016/j.enbuild.2012.07.042.
- Yezioro, Abraham, Bing Dong, and Fernanda Leite. 2008. "An Applied Artificial Intelligence Approach Towards Assessing Building Performance Simulation Tools." *Energy and Buildings* 40 (4): 612–620. doi:10.1016/j.enbuild.2007.04.014.
- Zhou, Zhaoyu, S. W. Rees, and H. R. Thomas. 2002. "A Numerical and Experimental Investigation of Ground Heat Transfer Including Edge Insulation Effects." *Building and Environment* 37 (January): 67–78. doi:10.1016/S0360-1323(00)00089-5.